

2010

Combined treatment of human tumour cells with adenovirus dl1520 and melphalan as a strategy to enhance cancer therapy

Alexander Sykelyk

Follow this and additional works at: <https://ir.lib.uwo.ca/digitizedtheses>

Recommended Citation

Sykelyk, Alexander, "Combined treatment of human tumour cells with adenovirus dl1520 and melphalan as a strategy to enhance cancer therapy" (2010). *Digitized Theses*. 3733.
<https://ir.lib.uwo.ca/digitizedtheses/3733>

This Thesis is brought to you for free and open access by the Digitized Special Collections at Scholarship@Western. It has been accepted for inclusion in Digitized Theses by an authorized administrator of Scholarship@Western. For more information, please contact wlsadmin@uwo.ca.

**Combined treatment of human tumour cells with adenovirus
dl1520 and melphalan as a strategy to enhance cancer therapy**

(Spine Title: Adenovirus and melphalan cancer therapy)

(Thesis Format: Monograph)

By:

Alexander Sykelyk

Graduate Program in Physiology and Pharmacology

A thesis submitted in partial fulfillment
of the requirements for the degree of
Master of Science

School of Graduate and Postdoctoral Studies

The University of Western Ontario

London, Ontario, Canada

THE UNIVERSITY OF WESTERN ONTARIO

School of Graduate and Postdoctoral Studies

CERTIFICATE OF EXAMINATION

Supervisor

Examiners

Dr. James Koropatnick

Dr. Andrew Watson

Supervisory Committee

Dr. David Freeman

Dr. Peter Ferguson

Dr. Joseph Mymryk

Dr. James Hammond (GSR)

The thesis by

Alexander Sykelyk

entitled:

**Combined treatment of human tumour cells with adenovirus dl1520 and
melphalan as a strategy to enhance cancer therapy**

is accepted in partial fulfillment of the
requirements for the degree of
Master of Science

Date

Chair of the Thesis Examination Board

CO-AUTHOR ABSTRACT

Oncolytic adenoviruses exploit tumour-specific properties to selectively kill tumor cells. Anti-tumour effects of combined treatment with adenovirus dl1520 (selective for p53-deficient cells) and chemotherapy are well documented. It was hypothesized that combined treatment of dl1520 and melphalan would be more effective than established dl1520-chemotherapy combinations. Colourimetric-based cell viability assays and flow cytometric analysis of cell death were used to assess anti-tumour effects of combined treatments. Melphalan-mediated changes in coxsackievirus and adenovirus receptor (CAR) mRNA and protein levels were assessed using RT-PCR and immunoblot, respectively. Melphalan enhanced the anti-proliferative effects of dl1520 better than cisplatin and paclitaxel. Combined dl1520-melphalan treatment resulted in greater-than-additive cell death. Upregulation of CAR mRNA and protein after melphalan treatment was observed, although at concentrations higher than assayed for melphalan-mediated changes in dl1520 sensitivity. Combining dl1520 with melphalan has potential to afford enhanced therapeutic benefit compared to an established chemotherapy-dl1520 combination for treatment of cancer.

Key Words: dl1520, oncolytic, adenovirus, melphalan, cisplatin, paclitaxel, cytotoxicity, head and neck cancer, colon cancer, drug-resistance

CO-AUTHORSHIP STATEMENT

All work presented in this thesis was fully performed by Alex Sykelyk, with the exception of Figures 3.3.3B and 3.4.3B, which were performed by Nelson Andre (summer student) under the direct supervision of Alex Sykelyk.

ACKNOWLEDGEMENTS

First and foremost I would like to thank my supervisor, Dr. James Koropatnick, for providing me this opportunity and for the continued guidance throughout the duration of this project. I would like to sincerely thank Dr. Peter Ferguson for the countless hours spent helping to better my work. Your continued efforts have helped me grow both as a scientist and as a person and for that I am in your debt. I would also like to thank Dr. James Hammond and Dr. Graham Wagner for the advice and mentorship provided as members of my advisory committee.

Thank you to the Koropatnick lab members (past, and present: Rene Figueredo, Alayne Brisson, Christine DiCresce, Katie Calonego, Stephanie Cull, Nelson Andre, Dr. Julio Masabanda, Dr. Reza Mazaheri, Mark Niglas, Dr. Benjamin Navarro, and Dr. Dusan Sajic). It has been an honour and a pleasure to work side-by-side with you throughout my time at the VRL. I will cherish the friendships and the memories we have shared as we grew together over these few years.

Special thanks go to; Dr. Peter Ferguson for helping to plan my experiments, Rene Figueredo and Alayne Brisson for the laboratory training and assistance with troubleshooting my experiments, Dr. Julio Masabanda for his training on the fluorescence microscope, Dr. Ben Hedley and Wendy Brown for the training and assistance in flow cytometry, Jai Ablack and Greg Fonseca for their assistance with working with human adenovirus, Dr. Arnold Berk, Carol Eng, and Onyx Pharmaceuticals for providing us with a working stock of dl1520. I

would also like to thank my department for providing me the opportunity to help mentor the next generation of scientists through my work as a teaching assistant. To Jenny Chu: thank you for everything you have done for me. Your support and motivation throughout my Master's and the long process of compiling this thesis have helped keep me focused and have been vital to my success. I hope that one day I can return the favour. I would also like to sincerely thank all the scientists, students, and technicians working at the LRCP and VRL for providing a supportive and fun environment to both learn and work in. You are truly a group of wonderful people.

Most importantly, I would like to thank my family for everything they have done to help me pursue my passion. Your continued love and support has given me the strength and drive to chase my dream. For that I will always be grateful. I love you all.

This work was supported by grants from the CIHR-STP, NSERC, the Schulich Graduate Scholarship, and Onyx Pharmaceuticals Inc.

TABLE OF CONTENTS

CERTIFICATE OF EXAMINATION	II
ABSTRACT	III
CO-AUTHORSHIP STATEMENT	IV
ACKNOWLEDGEMENTS	V
TABLE OF CONTENTS	VII
LIST OF FIGURES	XI
CHAPTER 1: INTRODUCTION	1
1.1. Cancer	1
1.1.1. The disease	1
1.1.2. Cancer statistics	2
1.2. Head and neck cancer	3
1.2.1. Molecular biology	3
1.2.2. Diagnosis	5
1.2.3. Treatment	5
1.3. Establishment of a novel treatment strategy	8
1.3.1. Human adenovirus	9
1.3.1.1. Rationale for use as a therapeutic agent	9
1.3.1.2. Taxonomy	10
1.3.1.3. Morphology	10
1.3.2. Human adenovirus replication process	13
1.3.2.1. Cellular attachment	13
1.3.2.2. Coxsackievirus and adenovirus receptor	16
1.3.2.3. Internalization	17
1.3.2.4. Gene expression	18
1.4. Oncolytic human adenovirus dl1520 (ONYX-015, CI-1042)	23
1.4.1. In vitro and in vivo studies	24
1.4.2. Phase I & II clinical trials	27
1.4.3. Phase III clinical trials	30
1.5. Limitations of oncolytic human adenoviruses	32
1.5.1. CAR levels in tumour tissues	32
1.6. Thesis rationale, hypothesis, and objectives	34

1.6.1. Rationale	34
1.6.2. Hypotheses	36
1.6.3. Specific objectives.....	36
CHAPTER 2: MATERIALS AND METHODS.....	38
2.1. Reagents.....	38
2.2. Cell lines	39
2.3. Oncolytic human adenovirus.....	40
2.3.1. dl1520	40
2.3.2. dl1520 propagation	41
2.3.3. dl1520 titration.....	42
2.4. Cell viability assays.....	43
2.4.1. alamarBlue™ assay	43
2.4.2. Neutral red assay	43
2.5. Cell culture	44
2.5.1. Sensitivity of human tumour cell lines to dl1520 chemotherapy ...	44
2.5.2. Differential effects of combined vs. sequential treatment of human tumour cells with dl1520 and chemotherapeutic drugs	45
2.5.3. CAR levels following melphalan treatment.....	51
2.5.4. CAR levels following short 50 µM melphalan treatment	51
2.5.5. Preparation of cultured cell lines to determine the basal CAR levels in 5 human tumour cell lines	52
2.6. CAR mRNA quantification.....	52
2.6.1. Total cellular RNA isolation	52
2.6.2. Reverse transcription of RNA.....	53
2.6.3. Polymerase chain reaction.....	54
2.6.4. DNA gel electrophoresis of PCR products	57
2.7. CAR protein quantification.....	58
2.7.1. Total protein isolation	58
2.7.2. Total protein quantification	58
2.7.3. Electrophoresis and blotting	59
2.8. Cell death assayed using flow cytometry following combined dl1520 and melphalan treatment.....	60
2.9. Adenovirus replication in the presence of melphalan.....	61

2.10. Statistical analyses.....	62
CHAPTER 3: RESULTS.....	64
3.1. Titration assay to determine concentration of active dl1520 virus.....	64
3.2. Human tumour cell lines as targets for dl1520 therapy.....	67
3.2.1. Basal CAR protein and CAR mRNA levels.....	67
3.3. Sensitivity of human tumour cell lines to dl1520 and chemotherapy ...	75
3.3.1. Concentration-dependent inhibition of proliferation by dl1520.....	75
3.3.2. Concentration-dependent inhibition of proliferation by chemotherapy	78
3.4. Differential effects of continued versus sequential treatment of human tumour cells with dl1520 and chemotherapeutic drugs.....	87
3.4.1. Selecting drug concentrations to use in combination with dl1520	87
3.4.2. Different treatment schedules for treatment of HN-5a cells with dl1520 and chemotherapy	95
3.5. Melphalan-mediated changes in CAR levels	101
3.5.1. Melphalan-mediated changes in CAR mRNA levels	101
3.5.2. Melphalan-mediated changes in CAR protein levels.....	104
3.5.3. CAR mRNA and protein levels following 50 μ M melphalan treatment for 4 h, 8 h, and 12 h.....	104
3.6. Greater-than-additive cell death after combined treatment with dl1520 and melphalan	109
3.7. Replication of dl1520 in the presence of melphalan.....	114
CHAPTER 4: DISCUSSION	118
4.1. Generation and titration of a dl1520 stock.....	119
4.2. Human tumour cell lines as targets for dl1520 therapy.....	121
4.2.1. CAR is a glycosylated protein	121
4.2.2. CAR protein and CAR mRNA levels in human tumour-derived cell lines	123
4.2.3. Sensitivity of human tumour cell lines to dl1520-mediated inhibition of cellular proliferation.....	124
4.3. Combination of dl1520 with conventional chemotherapy for the treatment of human tumours.....	128
4.3.1. Differential effects of combined vs. sequential treatment of human tumour cells with dl1520 and chemotherapeutic drugs	128
4.3.2. Melphalan-mediated changes in the CAR levels in HN-5a cells.	131

4.3.3. Greater-than-additive cell death after combined treatment with dl1520 and melphalan is not the result of enhanced dl1520 replication.	134
4.4. Conclusions and future directions	137
4.4.1. Conclusions.....	137
4.4.2. Future studies	138
CHAPTER 5: REFERENCES	143
VITA	160

LIST OF FIGURES

Figure	Description	Page
1.3.1.3.	Human adenovirus (class C, serotype 5) morphology.	12
1.3.2.1.	Human adenovirus internalization.	15
1.3.2.4.	Human adenovirus genome.	20
2.5.2.1.	Scheduled treatment of various human tumour cell lines with drug and dl1520.	47
2.5.2.2.	Representation of the method used to determine drug-induced changes in dl1520 cytotoxicity, as a function of IC ₅₀ values.	50
3.1.1.	Titration of dl1520 stock.	66
3.2.1.	Basal CAR mRNA levels in 5 human tumour cell lines.	69
3.2.2.	CAR protein glycosylation in human tumour cell lines.	72
3.2.3.	Basal CAR protein levels in 5 human tumour cell lines.	74
3.3.1.	Concentration-dependent growth inhibition of human tumour cells by dl1520.	77
3.3.2.	Sensitivity of HN-5a tumour cells to growth inhibition induced by melphalan, paclitaxel, and cisplatin.	82
3.3.3.	Sensitivity of 3 human tumour cell lines to growth inhibition induced by melphalan.	86
3.4.1.1.	Chemotherapy-mediated changes in sensitivity of dl1520.	89

3.4.1.2.	Chemotherapy-mediated change in sensitivity to dl1520.	91
3.4.2.	Scheduled treatment of HN-5a cells with different chemotherapeutic agents in combination with dl1520.	97
3.4.3.	Scheduled treatment of HT-29, HT-29/carbo-15d-1 and HN-5a/carbo-15a cells with melphalan in combination with dl1520.	100
3.5.1.	CAR mRNA levels in HN-5a cells after 24 h exposure to melphalan.	103
3.5.2.	CAR protein levels in HN-5a cells after 24 h and 48 h exposure to melphalan.	106
3.5.3.	CAR mRNA levels in HN-5a cells after 4 h, 8 h, and 12 h exposure to 50 μ M melphalan.	108
3.5.4.	CAR protein levels in HN-5a cells after 4 h, 8 h, and 12 h exposure to 50 μ M melphalan.	111
3.6.1.	HN-5a cell death following combined treatment with dl1520 and melphalan.	113
3.7.1.	dl1520 replication in the presence of melphalan.	117

LIST OF TABLES

Table	Description	Page
2.6.3.	Semi-quantitative RT-PCR primer sequences and conditions.	56
3.3.1.	Sensitivity of 5 human tumour cell lines to growth inhibition by dl1520.	80
3.3.2.	Sensitivity of 4 human tumour cell lines to growth inhibition induced by chemotherapy drugs.	84
3.4.1.	Concentrations of melphalan, paclitaxel, and cisplatin used to investigate how different treatment schedules affect drug-mediated changes in dl1520 sensitivity of 4 human tumour cell lines.	94

LIST OF ABBREVIATIONS

[]	concentration
2-D	two-dimensional
3-D	three-dimensional
5-FU	5-fluorouracil
Å	Ångstrom
A_{260}	absorbance at 260 nanometers
A_{280}	absorbance at 280 nanometers
α -MEM	Eagle's alpha modified minimum essential medium
ANOVA	analysis of variance
bp	base pair
BSA	bovine serum albumin
CaCl ₂	calcium chloride
CAR	coxsackievirus and adenovirus receptor
carboplatin	<i>cis</i> -Diammine-1,1-cyclobutane dicarboxylate platinum II
cDNA	complementary DNA
cisplatin	<i>cis</i> -Diammine-dichloro-platinum II
CO ₂	carbon dioxide

d	day(s)
dATP	deoxyadenosine triphosphate
dCTP	deoxycytidine triphosphate
dGTP	deoxyguanosine triphosphate
DMEM	Dulbecco's modified Eagle's medium
DMSO	dimethyl sulfoxide
DNA	deoxyribonucleic acid
dNTP	deoxyribonucleotide triphosphate
DTT	dithiothreitol
dTTP	deoxythymidine triphosphate
E	early gene
E1B-19	E1B 19 kilodalton protein
E1B-55	E1B 55 kilodalton protein
ECL	enhanced chemiluminescence
EDTA	ethylenediaminetetraacetic acid
FBS	fetal bovine serum
FITC	fluorescein isothiocyanate
g	gravity
GAPDH	glyceraldehydes-3-phosphate dehydrogenase

h	hour(s)
H ₂ O	water
HAdV	human adenovirus
HCl	hydrochloric acid
HEPES	4-(2-hydroxyethyl)-1-piperazineethanesulfonic acid
HRP	horseradish peroxidase
i.a.	intra-arterial
i.p.	intraperitoneal
i.t.	intratumoural
i.v.	intravenous
IC _x	concentration that inhibits proliferation by x%
KCl	potassium chloride
kDa	kilo Dalton
L	late genes
melphalan	L-phenylalanine mustard
MgCl ₂	magnesium chloride
MGMT	O(6)-methylguanine DNA methyltransferase
min	minute(s)
ml	milliliter

mM	millimolar
MMLV-RT	Moloney murine leukemia virus reverse transcriptase
MOI	multiplicity of infection
mRNA	messenger ribonucleic acid
NaCl	sodium chloride
NCI	National Cancer Institute
nm	nanometer
nM	nanomolar
HNSCC	head and neck squamous cell carcinoma
PBS	phosphate buffered saline
PCR	polymerase chain reaction
PFU	plaque forming units
PI	propidium iodide
PNGase F	peptide-N-glycosidase F
pRB	retinoblastoma protein
RGD	arginine-glycine-aspartic acid
RNA	ribonucleic acid
RP	random primers
S1	mammary epithelial cell line

SDS	sodium dodecyl sulphate
sec	second(s)
SFDA	Chinese State Food and Drug Administration
T-25	25-cm ² tissue culture flask
T-75	75-cm ² tissue culture flask
T4-2	transformed mammary epithelial cell line
T _a	annealing temperature
TAE	tris base, acetic acid, ethylenediaminetetraacetic acid
Taq	Thermus aquaticus
TBS	tris-buffered saline
TBS-T	tris-buffered saline tween 20
Tris	tris(hydroxymethyl)-aminomethane hydrochloride
µg	microgram
µl	microliter
µM	micromolar
UV	ultraviolet
V	volt
vs.	versus
WHO	World Health Organization

CHAPTER 1: INTRODUCTION

1.1. Cancer

The vast majority of diseases afflicting human beings originate from the introduction of foreign pathogens into the human body that share little homology with normal human cells. Treatments for such diseases generally afford a high therapeutic efficacy (that is toxicity is highly selective for pathogens while sparing healthy human tissues) because they are tailored to target pathogen-specific molecules and/or pathways. Conversely, cancer poses a unique problem in that it is derived from one's own cells. The result is a disease that shares considerable homology with the surrounding normal human tissues, making it difficult to generate treatments that are selective for cancer cells. As a result, therapies remain sub-optimal due to non-specific toxicities and varying degrees of therapeutic efficacy. Continued efforts are needed to better understand the disease-specific changes that lead a normal cell to become cancerous, which can then be used to develop tumour-specific therapies.

1.1.1. *The disease*

A common misconception about cancer is that it is a single disease. In fact, cancer is a generalized term used to describe a group of over 200 different diseases all exhibiting similar characteristics. Cancer is the result of genetic modifications that lead to deregulation of cellular homeostasis. Both mutations that are hereditary and those that are acquired through exposure to exogenous

mutagens contribute to disease progression. Many, if not all cancers, exhibit distinct cellular changes that lead to malignant growth including: self-sufficiency in growth signaling, insensitivity to growth-inhibitory signals, evasion of programmed cell death, limitless replicative potential, sustained angiogenesis, and tissue invasion [1]. The acquisition of these “hallmarks of cancer” is not due to a single mutation but rather is the result of accumulated genetic damage to a number of genes within the same cell over time [2]. The most common changes include dominant gain-of-function mutations to proto-oncogenes, that is, genes that positively regulate cell cycle progression, or recessive loss-of-function mutations to tumour suppressors, the genes that negatively regulate the cell cycle. The mechanism by which cells acquire each of these hallmarks and the chronological order in which mutations occur is highly variable. As a result, it is not uncommon to identify tumours that are histologically identical yet behave differently in response to therapeutic intervention. This diversity in response to treatment in combination with the fact that tumour-selective treatments are difficult because tumours originate from normal cells make cancer a difficult disease to treat.

1.1.2. *Cancer statistics*

In its most recent study evaluating the global burden of disease in 2004, the World Health Organization (WHO) estimates that approximately 3.3 million females and 4.2 million males died from cancer worldwide, making it the third leading cause of death [3]. In Canada, an estimated 173,800 people will be

diagnosed and 76,200 people will die from cancer in 2010 [4]. Both the WHO and the Canadian Cancer Society predict that cancer incidence and mortality will continue to climb in the near future due to a growing and aging population. Continued improvement of current therapies, in conjunction with the establishment of novel, more efficient treatments, is needed to help combat this growing disease burden.

1.2. Head and neck cancer

This year approximately 600,000 people will be diagnosed with head and neck squamous cell carcinoma (HNSCC) worldwide and more than half will die from it [5]. The Canadian Cancer Society estimates that in 2010, 4,550 Canadians will be diagnosed and 1,650 people will die from the disease [4]. If caught in the early-stage of disease progression, treatments are generally effective, but treatments for advanced disease are less effective. Moreover, current treatments are associated with unfavorable toxicities to the patients. Limited efficacy and unfavorable toxicities highlight the need to develop newer, more effective treatments. The cell line (HN-5a) derived from a patient with HNSCC was used as an *in vitro* model system for head and neck cancer in the present study.

1.2.1. Molecular biology

HNSCC originates from the squamous epithelium lining the upper aerodigestive tract, which includes the nasal cavity, paranasal sinuses, mouth,

pharynx and larynx. Major risk factors found to contribute to the incidence of HNSCC include alcohol and tobacco consumption [6,7].

The disease pathogenesis for HNSCC originates from a single, normal, epithelial progenitor that after the accumulation of mutations gives rise to a preneoplastic lesion, eventually progressing to an invasive cancer [8]. The progression from a normal epithelial progenitor begins with loss of cell cycle control. A normal epithelial cell that loses control of the cell cycle and becomes highly proliferative is termed a hyperplasia, a benign but proliferative preneoplastic lesion. The next step in the development of preneoplastic lesions is the progression from a hyperplasia to a dysplasia, that is cells that are highly proliferative and are morphologically distinguishable from normal epithelium. A mutation to note in the disease progression of HNSCCs is loss of chromosomal region 17p, which is thought to be associated with the absence of a functional p53 stress response and is found in over 50% of all HNSCCs [9,10]. The tumour suppressor p53 has often been referred to as the “guardian of the genome” because of the important role it plays in maintenance of genomic stability by mediating the cell cycle arrest and apoptosis in response to DNA damage [11,12]. The loss of functional p53 often occurs late in the progression from a dysplasia to an *in situ* carcinoma, cancers that have not invaded beyond the site of origin [9]. Thus, the loss of functional p53 likely contributes to genomic instability, increasing the rate of both accumulation of mutations and disease progression. Combined, these changes drive the progression from a preinvasive, often treatable phenotype, to an invasive and deadly neoplasm.

1.2.2. *Diagnosis*

Accurate staging of patients with HNSCC is critical for determining the appropriate therapeutic strategy. To do so, information must be gathered about the primary tumour and the extent of metastasis to both cervical lymph nodes and distant sites. Taken together, this data can be used to group HNSCC into three general clinical categories: 1) early stage disease (stages I/II) where the primary tumour is no larger than 4 cm in diameter with no signs of metastasis, 2) locally advanced disease (stages III) including primary tumours larger than 4 cm with potential spread to lymph nodes, and 3) recurrent/metastatic disease (stage IV) consisting of primary tumours larger than 4 cm with extensive metastasis to lymph nodes and/or presence of distant metastasis [13].

1.2.3. *Treatment*

The primary goal for treatment of patients with HNSCC is complete abolition of tumour tissues while limiting patient morbidity and tumour relapse. Further, preservation of both structure and function of the complex head and neck organs must be taken into consideration in an attempt to preserve the patient's quality of life [14].

There are several well-established treatment modalities for HNSCC consisting of surgery, radiotherapy, and/or chemotherapy. Determining the specific treatment plan varies from patient-to-patient and is dependent on both site and stage of the primary tumour in combination with other patient factors (age, medical condition)[15].

The standard treatment for early-stage (stages I and II) HNSCC is either surgery or radiotherapy [16]. According to the National Cancer Institute (NCI) treatment guidelines for HNSCC, early-stage primary tumours originating in the nasopharynx, oropharynx, and larynx are preferentially treated with radiation therapy, whereas tumours originating in the hypopharynx, oral cavity and paranasal sinuses are preferentially treated with surgery. Taken together, both treatment strategies are quite successful, with over 80% of early-stage HNSCC patients exhibiting a 5-year survival [14].

Treatments for patients presenting with advanced locoregional and/or recurrent metastatic disease (stages III and IV) are less effective. The overall goal of surgical intervention is tumour excision with sufficient surgical margins to ensure complete removal of all malignant tissues. However, these margins are often difficult to achieve due to proximity of tumour tissue to vital organs and/or spread to distant sites that are inoperable. While effective in early-stage HNSCC, conventional radiation therapy as a lone therapeutic treatment for advanced HNSCC is ineffective for locoregional control and does not improve overall 5-year survival [17]. Further, severe acute toxicities associated with radiation therapy may pose a problem for patient compliance [17].

Unfavorable side effects and limited therapeutic efficacy resulting from surgery and radiation therapy for patients with locally advanced HNSCC have led to the progression of chemotherapy from a palliative to a potentially curative treatment. Chemotherapy has been used for HNSCC in a palliative setting for over 50 years [18]. However, its curative potential was not investigated until the

NCI's multi-institutional, prospective randomized trial in 1987, which was one of the first to demonstrate that chemotherapy was a possible adjuvant therapy for patients with advanced HNSCC [19]. A meta-analysis conducted by the Meta-Analyses of Chemotherapy in Head and Neck Cancer Group of 63 clinical trials between 1965 and 1993 demonstrated a 4% 5-year overall survival benefit for patients treated with chemotherapy in conjunction with standard therapy [20]. A follow-up report including an additional 24 trials between 1993 and 2000 confirmed the benefit of chemotherapy [21]. Tumour response to concurrent chemotherapy and radiation treatment is more pronounced using platinum-based regimens than radiation therapy alone [22,23].

The anticancer activity of *cis*-Diammine-dichloro-platinum II (cisplatin) results from the induction of DNA damage [24,25]. The concurrent treatment of cisplatin with radiation, in doses of 100 mg/m² every 3 weeks during the course of the radiotherapy, was shown to be highly effective and has been widely accepted as the standard of care for concurrent chemoradiotherapy of HNSCC [22]. Additional Food and Drug Administration approved usages of cisplatin include ovarian, testicular, cervical, and non-small cell lung cancers [26]. However, common adverse events associated with use of cisplatin include leucopenia, nausea/vomiting, anemia, and muscular fibrosis [22,27,28]. Unfavorable toxicity profiles, combined with marginal patient response with conventional therapy for patients with advanced HNSCC highlights the need for newer, more efficacious yet less toxic therapeutic strategies.

1.3. Establishment of a novel treatment strategy

Viruses are organisms that are capable of transferring foreign genetic information into host cells, which are subsequently 'hijacked' and used for virus replication. Following successful virus replication the host cell is killed, releasing virus progeny able to infect adjacent cells. As the understanding of virus biology grew, so too did the idea that these same disease-causing agents had the potential to be used for therapeutic purposes. Two general strategies have emerged for using viruses as therapeutics. The first utilizes their naturally occurring ability to act as vectors capable of introducing foreign genetic information into cells. Researchers are able to remove essential genes necessary for virus replication, making them replication-deficient vectors that are used to selectively deliver therapeutic payloads to target cells [29]. The second strategy, which is utilized for this project, modifies the virus in a way that limits the range of potential host cells, making them capable of infecting and/or killing only target cells [30].

Oncolytic virus therapy utilizes replication-selective viruses capable of infecting and/or replicating only in tumour cells. Two mechanisms are used for the creation of oncolytic viruses. The first is to put the expression of essential virus genes under the control of tissue-specific promoters [31]. The second mechanism is to delete essential virus genes necessary for virus replication in normal cells but that are complemented by the genetic defects found in various cancer cells [30]. The latter strategy was used to generate a genetically-modified

human adenovirus (HAdV) that was utilized for the project described in this thesis.

1.3.1. Human adenovirus

1.3.1.1. Rationale for use as a therapeutic agent

The HAdV has three attractive features for its use as a platform for an oncolytic virus: first, the HAdV is not associated with any serious disease [32]; second, the molecular biology underlying virus replication is well understood; and third, commercial manufacturing of oncolytic HAdVs is possible because they can be grown in high titers [33]. However, there are several limitations to the use of HAdVs as oncolytic viruses. Most adults have been exposed to these viruses growing up resulting in a relatively high prevalence of circulating anti-HAdV antibodies, thus limiting the efficacy of systemic administration [34,35,36,37]. Secondly, barriers exist which limit the potential spread to adjacent tumour tissues once virus replication occurs. For example, solid tumour tissues are most often heterogeneous in their cellular composition. Oncolytic HAdVs that are cytotoxic to epithelial-derived tumour cells may induce cytotoxicity less effectively in other cell types such as fibroblasts, which make up a portion of the tumour microenvironment [30]. Moreover, additional factors present in the tumour microenvironment, such as the extracellular matrix, can act as physical barriers that prevent efficient virus distribution within the tumour [38]. Despite these limitations, the HAdV remains one of the most investigated viruses for use as an oncolytic virus.

1.3.1.2. Taxonomy

The taxonomic delineation of the HAdV begins with the family *Adenoviridae*, consisting of viruses able to infect a broad range of vertebrates, which is further categorized into the genus *Mastadenovirus*, viruses capable of infecting mammals. The HAdV was first discovered in 1953 by researchers trying to establish cell lines from human adenoidal tissues and was named from the tissue of origin [39]. Since then, 51 distinct serotypes have been identified which fit into 7 subgroups (A-F) based on genetic and biological homology [40]. HAdV from subgroup C (serotypes 1, 2, 5 and 6), which is used in the present study, are associated with 5-10% of all respiratory illnesses in children [32].

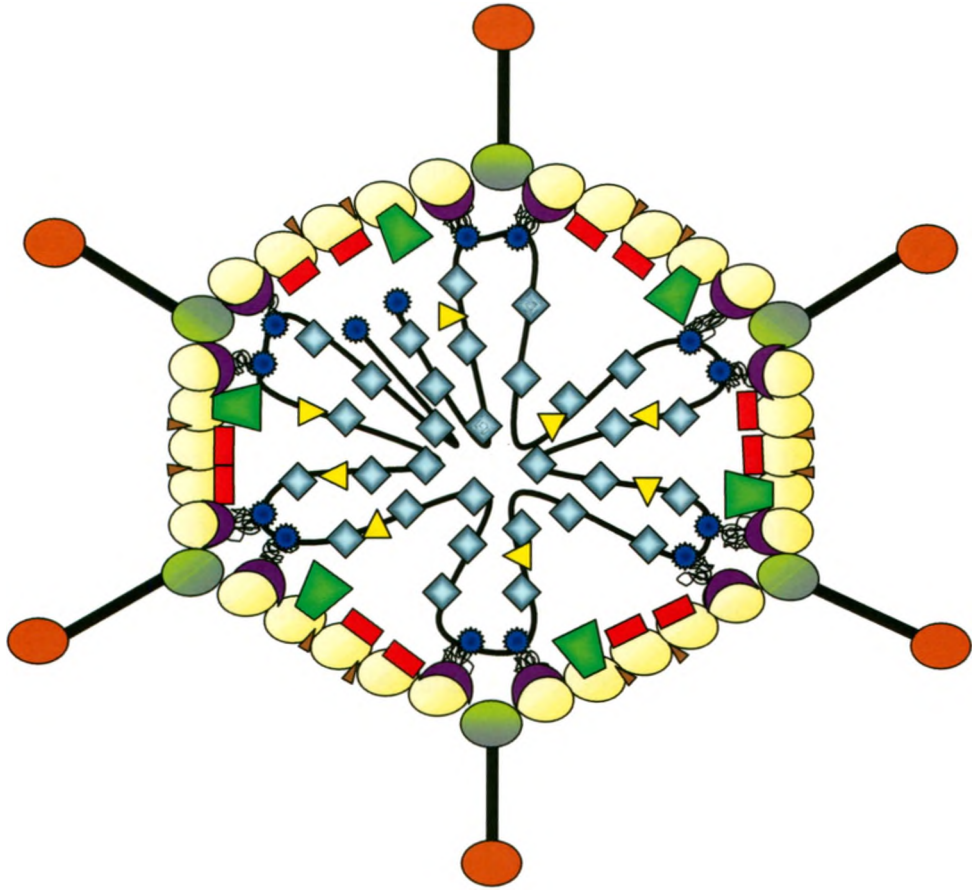
1.3.1.3. Morphology

The HAdV is a non-enveloped virus approximately 90 nm in diameter. The linear, double-stranded DNA genome is encapsulated within an icosahedral protein capsid structure comprised of 9 proteins numbered II-IX in order of their increasing motilities in an SDS-polyacrylamide gel [41].



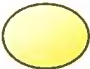
A combination of X-ray crystallography (resolution in the range of 1-10 Å) and electron microscopy (resolution in the range of 25-500 Å) has been used to construct a detailed high-resolution image of the capsid structure of the HAdV [42]. The peptide structures comprising the capsid are categorized as major, minor, and core proteins corresponding to their functions (Figure 1.3.1.3). The major components of the capsid consist of hexons (II), penton base (III), and fiber (IV) proteins [42]. Hexons are the most abundant structural protein. Each capsid

Figure 1.3.1.3. Human adenovirus (class C, serotype 5) morphology.

Capsid proteins are classified according to function. Major capsid proteins (penton, hexon, fiber) form basis of the icosahedral protein capsid. Minor capsid proteins (IIIa, VI, VIII, IX) help to stabilize the major proteins and aid in anchorage of the genome to the capsid. Core proteins (V, VII, Mu) are found associated with HAdV-DNA.



Major Proteins

-  Penton
-  Fiber
-  Hexon

Minor Proteins

-  VIII
-  IIIa
-  VI
-  IX

Core Proteins

-  V
-  Mu
-  VII

consists of 240 homotrimers arranged to form the 20 facets of the icosahedral capsid shape. The 20 facets converge to form 12 vertices from which the penton complex protrudes. The penton complex consists of a pentameric base of peptide III surrounding the proximal portion of the fiber, a trimer of peptide IV, which extends from its center [41,42].

Minor proteins IIIa, VI, VIII and IX are found associated with the hexons and are thought to help cement together and thus stabilize the major capsid proteins [42,43]. The remaining core protein peptides V, VII and Mu are associated with DNA. Anchorage of virus DNA to the capsid is thought to occur through an interaction with DNA-binding protein V and hexon-associated protein VI [44].

1.3.2. Human adenovirus replication process

1.3.2.1. Cellular attachment

Whereas an enveloped virus is able to gain entry to targeted cells simply by fusing with its cell membrane, the entry of a non-enveloped virus is more complex. Typically, these viruses must induce the target cell to actively internalize the virus. The HAdV does this mainly through the cellular process of receptor-mediated endocytosis (Figure 1.3.2.1) [45]. The rate-limiting step in its internalization is the initial binding of the HAdV fiber protein to its primary receptor, the Coxsackievirus and Adenovirus Receptor (CAR) (Figure 1.3.2.1A) [46].

Figure 1.3.2.1. Human adenovirus internalization.

(A) Virus knob of the fiber protein binding to CAR mediates HAdV attachment.

(B) Binding of both $\alpha\beta 3$ and $\alpha\beta 5$ integrins to an RGD sequence on penton base facilitates receptor internalization.

(C) Formation of clathrin-coated pits occurs as the HAdV undergoes receptor-mediated endocytosis.

(D) The decrease in pH associated with the formation of endosome causes detachment of the HAdV fibers and dissociation of $\alpha\beta 3$ but not $\alpha\beta 5$ which remains bound.

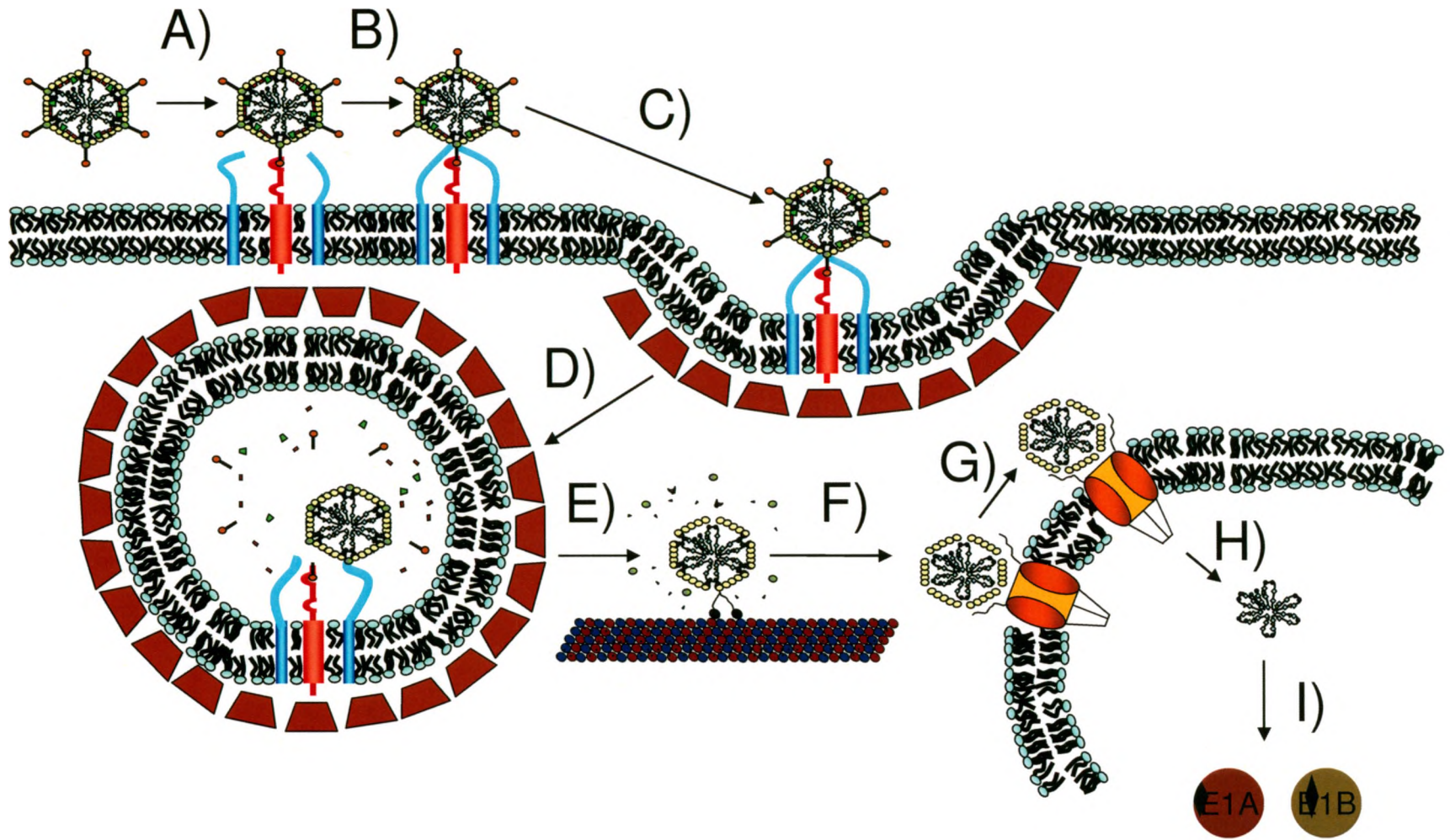
(E) Cytosolic penetrance of the HAdV is still largely unknown. It is believed that $\alpha\beta 5$ binding is associated with endosomal permeabilization.

(F) Nuclear translocation of partially disassembled HAdV capsid.

(G) Association with the nuclear pore complex further mediates capsid disassembly and HAdV genome entry to the nucleus.

(H) HAdV genome gains entry to the nucleus.

(I) Transcription of HAdV genes necessary for HAdV replication.



1.3.2.2. *Coxsackievirus and adenovirus receptor*

The integral membrane cell surface protein CAR consists of 365 amino acids with intracellular, transmembrane, and extracellular domains consisting of 107, 22, and 236 amino acid residues, respectively [47]. This receptor is evolutionarily conserved between humans and mice, which share 91%, 77%, and 95% homology between extracellular, transmembrane, and intracellular domains, respectively [48]. The predicted molecular weight based on the amino acid sequence is 40 kDa [47]. However, N-glycosylation at two amino acid residues, N106 and N201, change the observed molecular weight to 46 kDa as observed by migration using SDS-PAGE [47,49,50].

The extracellular domain of CAR consists of two immunoglobulin-like domains, D1 and D2, corresponding to the distal and proximal regions, respectively [46,47]. The D1 domain is believed to serve as the site for HAdV fiber binding [46]. Deletion of this domain resulted in reduced HAdV infection. The D2 domain was also implicated in HAdV fiber binding by acting as a spacer to allow the D1 domain to be presented [46].

The intracellular domain of CAR is thought to be involved in intracellular signaling [51]. Typically, peptides involved in cell signaling contain conserved multi-molecular protein interaction domains able to modulate peptide-peptide signaling (e.g. SH2, SH3, PDZ). Yeast two-hybrid screening, combined with *in vitro* pull-down experiments demonstrated a direct interaction between the intracellular domain of CAR and several intracellular signaling molecules [51]. This interaction may be due to a sequence similarity between the last four amino

acids on the intracellular c-terminal (DGSIV) tail and known PDZ-binding domains [47].

Epithelial cells are found lining all surfaces of the body. This densely packed layer of cells forms a protective barrier helping to regulate transfer of molecules between the apical and basal surfaces. Epithelial cells associate with each other through junctional complexes formed between cell surface proteins expressed on the lateral plasma membrane. The most apical component of these junctional complexes is known as the tight junction. CAR localizes to tight junctions between epithelial cells where it interacts with extracellular CAR domains on adjacent cells [46,48]. Therefore, putative functions for CAR include cell-cell adhesion and cell signaling.

1.3.2.3. *Internalization*

After binding to CAR, secondary binding of integrins $\alpha\text{v}\beta\text{3}$ and $\alpha\text{v}\beta\text{5}$ to Arginine-Glycine-Aspartic acid (RGD) sequences found on the penton base complex occurs [52,53]. Association of integrins facilitates the formation of early endosomes and subsequent dissociation of the capsid fiber and several minor capsid proteins [54,55]. HAdV penetration of the endosome may involve $\alpha\text{v}\beta\text{5}$ due to the ability of this integrin to remain bound to the penton base under the slightly acidic conditions of the endosome [56,57]. Once in the cytoplasm, additional capsid proteins dissociate, further destabilizing the capsid structure [55]. Partially disassembled HAdV capsids then utilize dynein-tubulin interactions to translocate to the nucleus [58]. The process of HAdV internalization and

subsequent endosomal escape is rapid, with over 80% of HAdV particles found in the cytoplasm or perinuclear space only 20 min after HAdV infection [55]. The nuclear pore complex aids in further capsid disassembly and serves as the gateway for the HAdV genome to enter the nucleus where it is able to initiate HAdV gene transcription [60,61].

1.3.2.4. *Gene expression*

Several studies in the early 1980's collectively helped map the genome of the HAdV subclass C, serotype 5 [62,63,64,65,66,67]. They identified several clusters of gene products responsible for various functions during HAdV replication. Nomenclature of transcribed genes is assigned based on the chronological order relative to HAdV DNA replication. Early genes (E) are transcribed prior to DNA replication, whereas late genes (L) are transcribed following it (Figure 1.3.2.4A).

E(1-4) generate the optimal environment for HAdV replication by inducing cells to enter S-phase of the cell cycle, protection from cellular defense mechanisms, induction of HAdV gene products necessary for replication, and replication of the HAdV genome (Figure 1.3.2.4A).

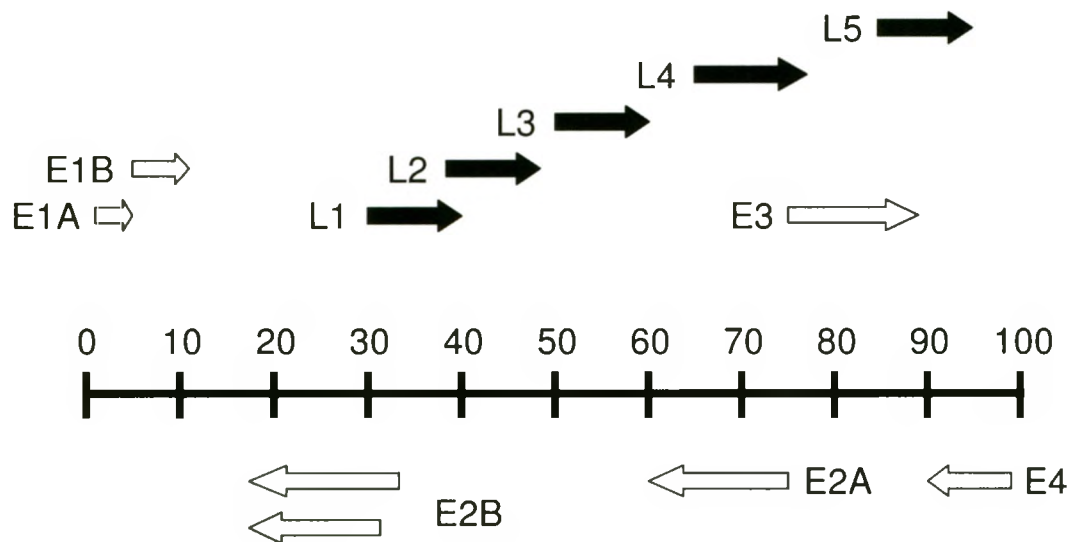
E1A, the first transcribed HAdV gene, protein is able to induce entry into S-phase of the cell cycle by binding to and inactivating the tumour-suppressor retinoblastoma protein (pRB) [68]. In quiescent cells, pRB exists bound to cellular E2F-1 transcription factor, rendering E2F-1 inactive [69]. Binding of E1A to pRB causes the release of E2F-1, which translocates to the nucleus and initiates

Figure 1.3.2.4. Human adenovirus genome.

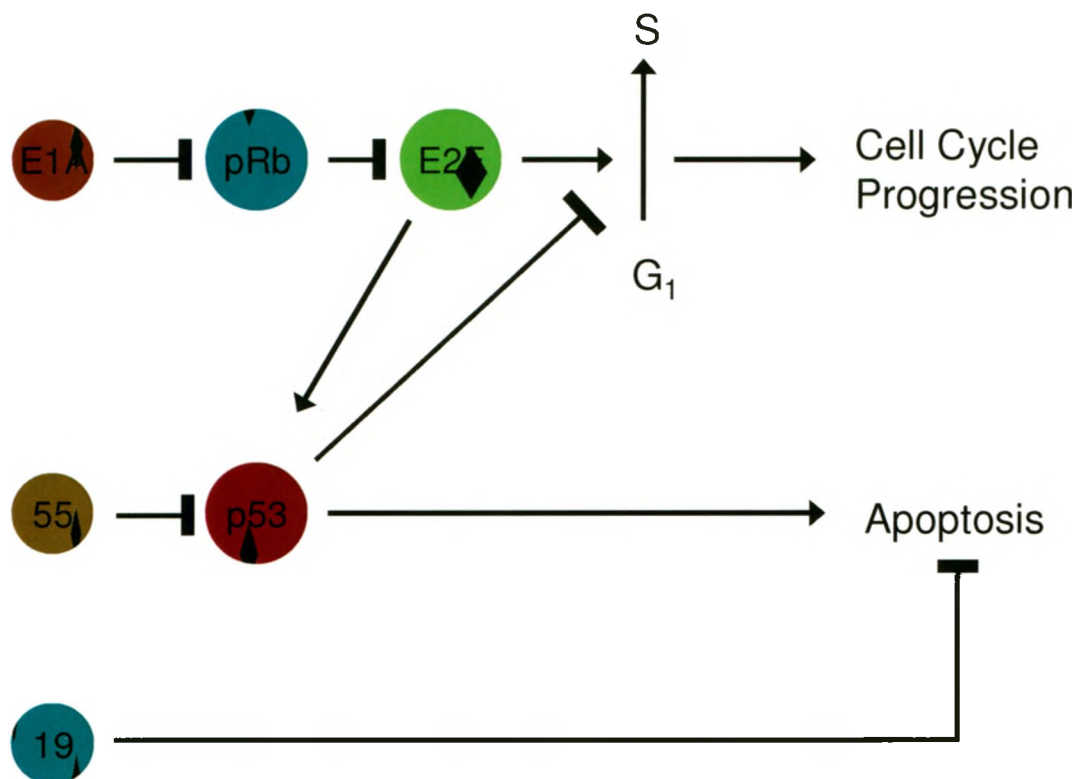
(A) Transcription map of the HAdV genome (modified from [67]). The 36 kb double-stranded DNA genome is broken into 100 map units. Gene products are represented as early (E) or late (L) according to the chronological order in which they are expressed. E1-4 are represented with white arrows, L1-5 are represented with black arrows.

(B) Expression of E1A and E1B gene products drive the cell cycle and inhibit host cell defense mechanisms. E1A induces the cell cycle by liberating cellular transcription factor E2F-1 from inhibitory protein pRB, allowing for transcription of genes that initiate cell cycle progression. However, E1A indirectly activates p53 stress response. E1B-55 and E1B-19 inhibit both p53-dependent and p53-independent apoptosis.

A



B



transcription of genes, the products of which drive the progression of the cell cycle [70,71]. These S-phase-specific gene products help generate the optimal environment for HAdV replication. However, E1A-dependent activation of cell cycle progression indirectly activates a p53-dependent response to protect against aberrant proliferation. This is because one of the genes activated by E2F-1 is p14^{ARF} [72], the product of which is a negative regulator of mdm2, which in turn is a negative regulator of p53 protein. Therefore, the p53 response pathway is inadvertently activated as a result of E1A activity, which would hinder the ability of the HAdV to successfully reproduce [72,73,74]. Thus, to circumvent this problem, the second transcribed HAdV gene product, E1B, inhibits this E1A-induced p53 response.

Four differentially spliced mRNAs (13S, 14S, 14.5S, and 22S) are generated from transcription of the E1B promoter, the two most abundant being the 13S and 22S mRNAs [75]. These mRNAs all contain two open reading frames [67]. Translation from the first open reading frame begins at nucleotide 1711 and proceeds to a stop codon at nucleotide 2236, resulting in a 175 amino acid polypeptide that migrates on SDS polyacrylamide gels with an apparent molecular weight of 19 kDa (E1B-19) [76]. Translation from the second open reading frame begins at nucleotide 2016 and is prematurely stopped on all mRNAs except the 22S product that proceeds uninterrupted to nucleotide 3501, generating a 495 amino acid polypeptide that migrates on SDS polyacrylamide gels with an apparent molecular weight of 55 kDa (E1B-55) [76]. The function of E1B-19 and E1B-55 is to protect the HAdV from the host cell defense

mechanisms. The E1B-55 protein binds to and inactivates p53 protein [77]. Further, E1B-55 has been implicated in p53 protein shuttling from the nucleus to cytoplasm where it then targets p53 protein for poly-ubiquitination and subsequent degradation [78]. Therefore, E1B-55 is responsible for direct inhibition of the p53 stress response. However, in addition to its indirect activation of p53, E1A expression also sensitizes cells to p53-independent cell death, such as TNF-alpha-induced death receptor signaling [79]. The E1B-19 protein shares considerable functional and sequence homology with the cellular anti-apoptotic protein Bcl-2 [80]. E1B-19 binding of proapoptotic proteins (Bak and Bax) prevents mitochondrial pore formation and subsequent apoptosis [81,82].

Transcription of the E2 genes generates proteins necessary for HAdV replication, including the single-stranded DNA-binding protein, DNA polymerase, and the terminal protein precursor [83,84].

Transcription of the E3 region of the HAdV genome yields several immune-modulating proteins that function to protect the HAdV from attack by cytotoxic T-cells by preventing the expression of MHC class I molecules at the cell surface [85], preventing the activation of pro-apoptotic cytokines and also blocking immune-mediated inflammation [86]. Further, transcription from the E3 region is also important for producing a protein necessary for efficient host cell lysis and release of HAdV progeny following HAdV replication [87,88].

The E4 region of the HAdV genome codes for proteins responsible for induction of both early and late HAdV gene transcription, HAdV DNA replication,

shut-off of host mRNA and protein synthesis, and inhibition of host DNA repair mechanisms [89,90].

Transcription of the L1-5 regions is initiated from a single, major late HAdV promoter that is only fully activated during the latter stages of HAdV replication [91]. Transcriptional products from this promoter produce capsid proteins necessary for constructing HAdV progeny [62,63,64,65,66,67].

1.4. Oncolytic human adenovirus dl1520 (ONYX-015, CI-1042)

The ultimate goal in the development of new anticancer treatments is selective activity against tumour cells. Conservative estimates predict that over 50% of all tumours lack functional p53, a tumour suppressor protein able to mediate growth inhibition and/or apoptosis [92]. This difference between normal and cancerous or precancerous cells can be exploited for development of tumour-specific therapies.

In 1996, Dr. Frank McCormick and his team at Onyx Pharmaceuticals were the first to successfully identify a genetically-modified HAdV of serotype 5 capable of selective cytolysis of p53-deficient cells *in vitro* [30]. The HAdV, dl1520 (also known as ONYX-015 and CI-1042) was originally created in an attempt to identify the E1B proteins essential for the process of cellular transformation [93]. The HAdV is genetically modified to contain an 827-base pair (bp) deletion and a point mutation in codon 2022 within the gene coding for E1B. Consequently, a truncated and non-functioning E1B-55 protein is produced without affecting the production of E1B-19 protein [93].

During wild-type HAdV infection, E1B-55 protein binds to and inactivates p53 [77,94]. Further, E1B is able to associate with E4orf6, another early HAdV protein, to export p53 to the cytoplasm and target it for degradation [95,96]. Inhibition of p53 function results in a loss of its growth inhibitory and apoptotic effects thereby allowing for HAdV reproduction to occur [94]. When dl1520 infects a cell expressing functional p53, dl1520 replication is inhibited due to the p53 response. This is because dl1520 does not have functional E1B-55 to inactivate p53. In contrast, p53-deficient cells are unable to induce the p53 response when infected with dl1520 and thus support dl1520 replication and subsequent tumour cell lysis [30]. This preferential replication in p53-deficient cells serves as the basis for the selectivity of dl1520 for cancer.

1.4.1. *In vitro and in vivo studies*

Preferential replication of dl1520 in several p53-deficient cell lines and evidence that non-functional E1B-55 protein (unable to bind and inactivate host p53) produced by dl1520 was responsible for this preferential replication demonstrated the potential for dl1520 to be used as a replication-competent oncolytic virus for the treatment of cancer [30]. In addition, *in vivo* data demonstrated that treatment of p53-deficient but not p53-functional tumour cell xenografts with dl1520 resulted in an 84% reduction in mean tumour volume compared to a UV-inactivated wild-type HAdV control.

Subsequent studies by the same group and others validated these preliminary findings. A panel of tumour cell lines (brain, breast, cervix, colon,

larynx, liver, lung, ovary and pancreas) each with a non-functional p53 were screened *in vitro* and were shown to be sensitive to the cytolysis induced by dl1520 [97]. Further, reducing expression of functional p53 in cell lines resistant to the dl1520-induced cytolysis sensitized them to dl1520 [30,98].

Nonimmortalized, primary human epithelial cells in culture are resistant to the cytolysis induced by dl1520 at concentrations up to 1000x higher than those able to induce complete cytolysis of p53-deficient tumour cell lines [97,99]. This preferential cytolysis of tumour cells while sparing healthy tissues may lead to a relatively high therapeutic index for dl1520 therapy.

In vivo pharmacokinetic studies were conducted in nude mice [97,100,101,102,103,104]. For intratumoural (i.t.) injections, multiple smaller doses were found to be more effective at inhibiting tumour growth than a single dose, possibly due to an increase in dl1520 distribution within the tumour [102]. Maximum tolerated dose for intravenous (i.v.) injection with 100% survival was determined to be 1.7×10^9 plaque forming units (PFU), while the lethal dose, primarily due to liver necrosis, was 5×10^{10} PFU [103]. There is a rapid uptake of dl1520 by the liver and clearance from the blood following i.v. injection [103].

In vivo selectivity was evaluated by administration of dl1520 to mice xenografted with tumour cell lines that were either p53-functional or p53-deficient. An i.t. injection of tumours with 10^8 PFU daily for 5 d resulted in significantly improved survival for mice with tumours deficient in p53 compared to those with functional p53 [97]. Additional *in vivo* studies have demonstrated the ability of dl1520 to reduce tumour growth in both newly injected and established

tumours, suggesting a potential treatment of metastasis [103].

In addition, dl1520 may have potential for treatment of drug-resistant tumours because the mechanism underlying dl1520 cytotoxicity should not, in theory, be blocked by tumour cell strategies that mediate resistance to chemotherapeutic drugs. In fact, acquisition of cisplatin-resistance in an ovarian carcinoma cell line conferred enhanced sensitivity to dl1520 *in vitro* [97, 100,105].

Typical chemotherapeutic regimens rarely consist of a single agent. More often patients receive a treatment consisting of multiple chemotherapeutics in order to enhance therapeutic effect and minimize any side effects. Consequently, combination therapies enhance the potential for positive agent-agent interactions. Therefore, dl1520 should be considered for use as a part of combination therapy.

The potential for conventional chemotherapy and dl1520 to be administered in combination was first evaluated in 1997 [97]. Nude mice were xenografted with HLaC cells, a tumour cell line derived from a human laryngeal carcinoma with a non-functional p53 response. Tumours were then injected with 10^8 PFU dl1520 daily for 5 d and/or intraperitoneal (i.p.) injection of either cisplatin or 5-fluorouracil (5-FU, a chemical inhibitor of thymidylate synthase [106]). Unlike either drug alone, treatment with dl1520 alone enhanced survival times. Further, the median survival was significantly increased by the combination therapy compared to the respective chemotherapy alone treatments: 38 days versus 24 days for 5-FU-treated groups and 44 versus 27 days for the

cisplatin-treated groups, respectively [97]. This study identified a potential additivity between dl1520 and chemotherapy, although they failed to provide evidence to support a greater-than-additive effect. Additional studies investigating treatments consisting of dl1520 and traditional chemotherapeutic drugs have been promising. The *in vitro* and *in vivo* cytotoxicity of dl1520 were augmented when combined with various chemotherapy drugs, including cisplatin, paclitaxel (microtubule-stabilizing anticancer agent [107]), L-phenylalanine mustard (melphalan, a DNA-alkylating agent [108]), and doxorubicin (an inhibitor of topoisomerase II [109]) at concentrations that had minimal cytotoxicity when administered alone [98,99,110]. The combination of dl1520 with radiation therapy did not inhibit dl1520 replication *in vitro*, and the combination treatment resulted in a tumour growth inhibitory effect *in vivo* greater than that achieved with either monotherapy [104]. Taken together, these studies highlight the potential for combined treatment with chemotherapy to potentially improve the therapeutic benefit of dl1520.

1.4.2. Phase I & II clinical trials

Collectively, pre-clinical studies provided promising data for the potential use of dl1520 as a first-line therapy for many human cancers, at least as part of a combination with chemotherapy [97,98,99,103,105]. This pre-clinical success led to the initiation of several small phase I clinical trials by Onyx Pharmaceuticals Inc., the company that, at the time, held the intellectual property rights to the dl1520 in North America and Europe. A broad scope of both primary tumour

origins (head and neck, lung, colorectal, liver and pancreas) and administration routes (i.t., i.v., and intra-arterial [i.a.] injections) were investigated in their trials [34,35,36,111,112,113]. Regardless of route of administration, no dose-limiting toxicities were observed up to and including the maximum administered dose of 2.0×10^{13} PFU [113].

Following both i.v. and i.a. injections of dl1520, HAdV genome was detectable in patient blood samples using a polymerase chain reaction (PCR) for up to 6 h [35,36,113]. One study determined its elimination half-life from the blood to be approximately 20 min [113]. Clearance of dl1520 particles from the blood was likely due to the liver, but dl1520 does not adversely affect liver function [111,112]. Several studies were able to detect a reappearance of dl1520 in blood plasma samples several days after complete clearance of virus particles from the initial treatment [36,113]. This, in combination with detection of dl1520 particles in several tumours but not healthy tissue biopsies, lead to the speculation that the re-emergence of dl1520 particles in the blood was evidence that dl1520 replication and dissemination had occurred from tumour tissues back into systemic circulation [34,36,111,113].

Approximately 50-70% of patients are positive for anti-HAdV-neutralizing antibodies in blood plasma prior to treatment [34,35,36,37]. Following dl1520 treatment, titers were increased and/or became positive for all patients regardless of the virus dose [34,35,36,111,113].

Adverse effects were well documented during the various clinical trials. The most common adverse events were local pain at the site of injection and

mild flu-like symptoms including fever, rigors, myalgias, asthenia and/or chills [34,35,36,111,112,113]. These symptoms presented up to 8 h following administration of dl1520, subsided without therapeutic intervention, and lasted only 24-48 h.

Whereas dl1520 treatment was well tolerated, there were mixed results with regards to therapeutic efficacy. One study reported a significant correlation between the induction of tumour response and the absence of functional p53. However, objective tumour response was observed in only 14% of patients enrolled in the trial with no significant change in time-to-tumour progression [114]. Another trial by the same group evaluated therapeutic efficacy when dl1520 was administered according to the standard i.t. injection schedule (2×10^{11} PFU daily for 5 d) versus a hyperfractionated 4-fold higher dosing schedule (2×10^{11} PFU twice daily for 10 d). There was no difference in the percentage of patients with a tumour response between the two dosing schedules. Further, patient response was similar to their previous trial, with only 14% of patients demonstrating either a partial or complete regression of the injection-treated tumours [115]. Other studies failed to demonstrate objective patient responses, although several trials reported transiently stabilized tumours prior to disease progression and patient death [34,111,113].

While seemingly inefficient as a solo treatment option, the potential for combined therapy of dl1520 with conventional chemotherapeutics has been demonstrated both *in vitro* and *in vivo* [97,98,99,104]. In 2000, phase II clinical trials investigating the combination of dl1520 with cisplatin and 5-FU in patients

with recurrent HNSCC were reported. In one trial, locoregional control was observed [116]. In the second study, patients with multiple tumours were injected with dl1520 into only the largest, most clinically relevant one leaving the others as intra-patient controls [37]. Treatment with concurrent 5-FU or cisplatin induced objective tumour response (greater than or equal to a 50% decrease in size of injected tumour) in 19 of the 37 patients. Of the patients that had tumour responses, no dl1520-injected tumours progressed up to a year after treatment. In patients with multiple tumours, objective response was observed in 9 of 11 dl1520-injected and 3 of 11 non-injected tumours. Further, tumour progression was significantly slowed in dl1520-injected compared to the non-injected tumours. However, a pitfall of this study is they failed to inject the non-injected-dl1520 tumours with a volume of saline to control for the mechanistic act of tumour injections.

1.4.3. Phase III clinical trials

Success both at the preclinical and early phase I and II clinical trials led Onyx Pharmaceuticals to initiate a phase III trial early in 2000, investigating the combination of dl1520 with chemotherapy for the treatment of recurrent head and neck cancer [117]. The proposed trial was to take place at over 40 centers in both the United States and Europe and include over 300 patients. The trial was designed to be a randomized two-arm study comparing intratumoural injection of dl1520 in combination with standard chemotherapy (cisplatin and 5-FU) versus chemotherapy alone.

Unfortunately, in 2000, Onyx Pharmaceuticals lost its financial backing when Pfizer acquired its development partner, Warner-Lambert. At the time, Onyx Pharmaceuticals had two agents that were slated to begin phase III testing: the oncolytic HAdV dl1520 and the small molecule tyrosine kinase inhibitor BAY 43-9006 (now known as Sorafenib). Subsequently, due to loss of financial backing, Onyx Pharmaceuticals suspended the dl1520 project in favor of further development of the BAY 43-9006 [118,119]

At the same time, a similar HAdV was under development in China by Shanghi Sunway Biotech. The HAdV, H101, is almost identical to dl1520 with the only difference being a slightly larger deletion of H101's E3 region [93,120]. In 2000 Sunway Biotech initiated a phase III clinical trial investigating i.t. injection of H101 in combination with cisplatin-based chemotherapy for HNSCC [121]. Patients received i.t. injection of H101 daily for 5 d in combination with or without standard chemotherapy (20 mg/m² cisplatin and 500 mg/m² 5-FU daily for 5 d) followed by 16 d treatment hiatus. Patients received more than 2 but no more than 5 cycles of this treatment regimen. Patients not responding after a single cycle were treated with an alternate chemotherapy (50 mg/m² doxorubicin and 500 mg/m² 5-FU daily for 5 d). Overall patient responses as evaluated according to the WHO criteria were significantly greater when treated with H101 and standard chemotherapy compared to standard therapy alone (78.8% vs. 39.6%, respectively). The main side effects were fever (45.7%), injection site reaction (28.3%) and influenza-like symptoms (9.8%). A major criticism of this study is

that Sunway did not report patient survival due to the fact that many patients lived in isolated rural areas, making patient follow up very difficult [118].

It was on the basis of this trial that the Chinese State Food and Drug Administration (SFDA) approved H101 for the treatment of advanced nasopharyngeal carcinoma in combination with chemotherapy on November 17, 2005 [118]. This legislation marked the first time that any governing body had ever approved an oncolytic virus therapy for cancer.

In 2005, Sunway Biotech Inc. acquired the intellectual property rights to dl1520 from Onyx Pharmaceuticals in hopes to develop use of H101 in North American and European markets [122,123].

1.5. Limitations of oncolytic human adenoviruses

The HAdV is an attractive candidate for generation of oncolytic vectors. However, several obstacles need to be overcome before they are acceptable to be used regularly in the clinic.

1.5.1. CAR levels in tumour tissues

Oncolytic HAdVs are reliant on gaining entry to the target cell before they are able to elicit a therapeutic effect. Association of the HAdV with CAR serves as the primary and rate-limiting step in virus internalization [46,47]. However, there is a complex relationship between CAR level and cancer progression. Both CAR mRNA and CAR protein levels have been shown to be elevated in breast tumour tissues with CAR levels correlating to poor overall survival [124]. In

contrast, a reduction in CAR levels was associated with increased human prostate tumour grade [125]. Further, loss of CAR in patients with gastric cancer significantly correlated to reduced survival and an increase in metastases [126]. *In vitro* siRNA-mediated CAR-knockdown in a gastric carcinoma cell line correlated with increased cell proliferation, migration and invasion [126]. Together, these studies indicate that changes in CAR levels may be tumour-specific and that further studies are needed to better understand the complexity of the interaction between CAR and cancer progression.

Tumour cells that express high levels of CAR may serve as potential targets for HAdV-based therapies. However, sub-cellular CAR protein localization may further limit which tumour cells are potential targets. Cells with basolateral localization of CAR protein have reduced HAdV entry [48]. Disruption of epithelial cell polarity causes deregulation of both CAR protein levels and localization, which subsequently alters HAdV infection [127]. CAR levels was measured in a parental mammary epithelial cell line (S1) expressing a normal, non-malignant phenotype and a transformed variant (T4-2) derived from S1 cells grown in culture deficient in epidermal growth factor signaling [127]. Both cell lines had similar CAR levels when grown in a two-dimensional (2-D) plastic tissue culture plates. However, cultures grown on a reconstituted basement membrane simulating a three-dimensional (3-D) growth environment resulted in a significant increase in both CAR mRNA and CAR protein in the T4-2 cell line compared to the S1 parental line. Further, CAR levels appeared to be localized to tight junctions in S1 cells whereas T4-2 cells exhibited a more diffuse cytoplasmic

localization. As expected, the T4-2 cell line cultured in 3-D was more susceptible to infection with HAdV than its parental counterparts, a difference not observed when both were grown in 2-D culture. A better understanding of both sub-cellular localization and cellular expression of CAR is useful for determining suitable candidates for HAdV-mediated therapies.

In addition to basal levels and localization, CAR levels are responsive to various stimuli, which adds additional level of complexity to the understanding of its biology. Treatment of cells *in vitro* with cytokines diminished CAR cell surface protein levels, total cellular CAR protein and CAR mRNA levels [128]. Contrary to this, disruption of the Raf-MEK-ERK pathway by treating with various MEK inhibitors resulted in an up-regulation of both total CAR protein and CAR cell surface levels [129]. Indeed, CAR levels appears to be modifiable upon exposure to both exogenous and endogenous stimuli. A better understanding of how these stimuli affect CAR levels may lead to the identification of new therapeutic drug-dl1520 combinations which are likely to enhance dl1520 therapy through modification of its primary cell surface receptor.

1.6. Thesis rationale, hypothesis, and objectives

1.6.1. Rationale

Cisplatin, a drug frequently used to treat HNSCC [22,130] augmented therapy with dl1520 *in vitro*, *in vivo* [97,98] and in the clinic [37,116,121]. To date, research has focused primarily on the use of dl1520 to treat HNSCC [34,37,97,98,101,102,114,115,116,121]. There has been limited interest in using

dl1520 for the treatment of different tumour types, such as colorectal carcinomas [36]. We chose to study two human tumour cell lines originating from different tissues, a HNSCC (HN-5a) and a human colorectal adenocarcinoma (HT-29) to both identify new, more effective treatments for HNSCC and to investigate colorectal carcinomas as a potential target for dl1520-mediated therapy. Additionally, previous studies have identified that the acquisition of resistance to chemotherapy has the potential to enhance the sensitivity of human tumour cell lines to dl1520-mediated cytotoxicity *in vitro* [97,105]. Treatment with cisplatin remains part of the standard of care for patients with HNSCC [22]. Use of *cis*-Diammine-1,1-cyclobutane dicarboxylate platinum II (carboplatin, a similar platinum-based DNA-damaging agent to cisplatin) has emerged as an alternative to cisplatin therapy because of similar therapeutic efficacy while exhibiting a more favorable toxicity profile [23,131,132]. However, approximately 30% of patients exhibit locoregional recurrence and/or distant metastasis with only 30% of patients surviving past 5 years [23]. Therefore, included in this study were both cisplatin-resistant (HT-29/CP-5c) and carboplatin-resistant (HN-5a/carbo-15a and HT-29/carob-15d-1) variants of our parental cell lines to investigate the use of dl1520 as a therapeutic strategy for management of these drug-resistant phenotypes. The present study investigated the combination of dl1520 with chemotherapy to enhance therapeutic effect. Chemotherapy drugs chosen to be screened in combination with dl1520 included: cisplatin as it is frequently used to treat HNSCC and has been shown to enhance therapy of HNSCC when combined with dl1520 [22,97,98,130], paclitaxel and melphalan as they have

both previously shown to augment the effect of dl1520 *in vitro* [107,110].

Furthermore, the interaction between dl1520 and chemotherapy has been poorly studied. The present study investigates potential chemotherapy-mediated changes to both levels CAR and dl1520 replication as a potential mechanisms for any potential enhanced therapeutic effects observed when chemotherapy was used in combination with dl1520.

1.6.2. Hypotheses

- 1) Melphalan will enhance the capacity of dl1520 to reduce proliferation/kill human tumour cells better than cisplatin or paclitaxel.
- 2) Melphalan-mediated induction of CAR protein and CAR mRNA levels enhances sensitivity to dl1520.
- 3) Melphalan treatment of human tumour cells enhances dl1520 production.

1.6.3. Specific objectives

- 1) To generate dl1520 stocks of defined PFU/ml capable of reducing growth of human tumour cells.
- 2) Measure basal CAR mRNA and CAR protein levels in 5 human tumour cell lines; HN-5a and carboplatin-resistant variant HN-5a/carbo-15a; HT-29 and a cisplatin-resistant (HT-29/CP-5c) and carboplatin-resistant (HT-29/carbo-15d-1) variants to assess their sustainability for treatment with dl1520.
- 3) Measure the sensitivity of all 5 human tumour cell lines to dl1520, melphalan, paclitaxel, and cisplatin agents alone.

4) Measure chemotherapy-mediated (melphalan, paclitaxel, and cisplatin)

sensitization of human tumour cell lines to dl1520 as a function of a reduction in dl1520 IC₅₀.

5) Measure melphalan-induced changes in CAR mRNA and CAR protein in HN-5a cells.

6) Measure cell death induced by combined melphalan and dl1520 treatment.

7) Measure dl1520 production in the presence of melphalan.

CHAPTER 2: MATERIALS AND METHODS

2.1. Reagents

Eagle's alpha modified minimum essential medium (α -MEM), Dulbecco's modified Eagle's medium (DMEM), and trypsin/ethylenediaminetetraacetic acid (EDTA) were all obtained from Wisent Inc. (Mississauga, ON). Fetal bovine serum (FBS) was purchased from GIBCO™ Invitrogen (Grand Island, NY, USA). All tissue culture plastic was purchased from Nunc™ (Roskilde, Denmark). Chemotherapy drugs used in this study including melphalan (in dH₂O) (GlaxoSmithKline, Mississauga, ON, Canada), cisplatin (in dH₂O) (Hospira, Saint-Laurent, Quebec, Canada), carboplatin (in dH₂O) (Teva Novopharm, Toronto, ON, Canada), and paclitaxel (in Cremophor EL, final Cremophor EL concentration <0.001%) (Biolyse, St. Catharines, ON, Canada) were all purchased from the outpatient pharmacy at the London Regional Cancer Program (London, Health Sciences Centre, London, ON). The following were purchased from Invitrogen (Grand Island, NY, USA): Penicillin/streptomycin, alamarBlue™, Trizol® Reagent, RNase-free H₂O, Moloney murine leukemia virus reverse transcriptase (MMLV-RT), dithiothreitol (DTT), deoxyribonucleotide triphosphate (dNTP) mix, random oligodeoxyribonucleotide primers (RP), *Thermus aquaticus* DNA polymerase (Taq Polymerase), 10x Taq PCR reaction buffer, and sequence-specific forward and reverse PCR primers. The following were purchased from BioShop (Burlington, ON): Dimethyl sulfoxide (DMSO), tris(hydroxymethyl)-aminomethane hydrochloride (Tris), agarose, formaldehyde,

acetic acid, aprotinin, leupeptin, isopropanol, EDTA, bovine serum albumin (BSA), polyacrylamide, skim milk, and 4-(2-hydroxyethyl)-1-piperazineethanesulfonic acid (HEPES). The following were purchased from Sigma-Aldrich (St Louis, MO, USA): Calcium chloride (CaCl_2), ethidium bromide, propidium iodide (PI), Peptide-N-glycosidase F (PNGase F), and a rabbit anti-actin polyclonal antibody. Neutral Red and chloroform were purchased from Fisher Scientific (Unionville, ON, Canada). Ethanol was purchased from Commercial Alcohols (Brampton, ON). Sodium chloride (NaCl) and sodium dodecyl sulfate (SDS) was purchased from EMD Chemicals (Gibbston, NJ, USA). Tween 20 and Triton x-100 were purchased from BDH Chemicals (Toronto, ON). The fluoresceine isothiocyanate (FITC)-conjugated AnnexinV antibody was purchased from BD Biosciences Pharmingen (Mississauga, ON). The anti-CAR-H300 polyclonal rabbit antibody, horseradish peroxidase (HRP)-conjugated goat anti-rabbit secondary antibody, and mouse liver extract used as a positive control for CAR protein expression were purchased from Santa Cruz Biotechnology Inc. (Santa Cruz, CA, USA). The enhanced chemiluminescence (ECL) Plus was purchased from GE Healthcare (VWR). Restore Western Blot Stripping Buffer was purchased from Thermo Scientific (VWR).

2.2. Cell lines

The HNSCC cell line HN-5a was established at St. Joseph's Healthcare Center (London, Ontario) from a patient who had not received any prior treatment [133]. A549 (human lung adenocarcinoma) and HT-29 (human colorectal

adenocarcinoma) cell lines were obtained from American Type Culture Collection (Manassas, VA). HEK293 (human embryonic kidney) were a generous donation from Dr. Joe Mymryk (Department of Microbiology and Immunology, the University of Western Ontario, ON, Canada). HT-29/CP-5c (cisplatin-resistant variant) and HT-29/carbo-15d-1 (carboplatin-resistant variant) were selected by culturing HT-29 cells in the presence of 5 μ M cisplatin and 15 μ M carboplatin, respectively. Individual colonies were selected which had propagated from single cells and cloned. The HN-5a/carbo-15a (carboplatin-resistant variant) cell line was established as described above and reported previously [134]. Drug-resistance of these cell lines was maintained by culturing them in their respective drugs in between experiments.

HEK293 cells were cultured in high-glucose DMEM supplemented with 10% FBS. All other cell lines were cultured in α -MEM supplemented with 10% FBS (growth medium) at 37°C in a humidified atmosphere containing 5% CO₂.

2.3. Oncolytic human adenovirus

2.3.1. dl1520

The HAdV dl1520 (ONYX-015, C11042) was a generous donation from Dr. Arnold Berk and Carol Eng (University of California, Los Angeles, CA, USA). This genetically modified HAdV, class C serotype 5, contains a 827-bp deletion and a point mutation in codon 2022 within the gene coding for E1B. Consequently, a truncated and non-functioning E1B-55 protein is produced without affecting the production of E1B-19 protein [93].

2.3.2. *dl1520* propagation

The HEK293 cell line was transformed from a primary culture of human kidney epithelial cells by introducing sheared HAdV serotype 5 DNA [135]. As a result, HEK293 cells express the most left region (approximately 0-17 map units) of the HAdV genome containing the E1 genes (Figure 1.3.2.4A) [135]. Thus, HEK293 cells are used to propagate E1-deficient mutants because of their ability to complement the mutant phenotype. However, reversion of some mutants to the wild-type is possible through homologous recombination with the host cell genome, although the frequency of these recombinant events is rare, with over 15 consecutive passages in HEK293 cells needed for the emergence of detectable wild-type HAdV [136]. Our *dl1520* stock was propagated using no more than 2 consecutive passages in HEK293 cells, as previously described [30]. Briefly, HEK293 cells were plated in a 75-cm² tissue culture (T-75) flask and cultured until cell density reached approximately 90%. A single T-75 flask was trypsinized and cells were counted using a Beckman Coulter Particle Counter (Beckman Coulter, Inc., Fullerton, CA, USA). Cells were then infected with *dl1520* at a multiplicity of infection (MOI) of 1 and cultured until there was complete cytolysis. Growth medium containing cell debris was then collected and freeze-thawed (dry ice ethanol bath, water bath at 37°C, vortex for 2 min) 3 times to ensure cell lysis and then used to infect additional HEK293 cells (1/10 to each of 10 T-75 flasks). Cells were cultured until their morphology began to change from adherent to rounded-up as this is an indicator of virus replication. Before cells were allowed to rupture, cells were washed off the plate in their own growth

medium and pelleted using centrifugation (100 x g, 5 min, 4°C). Cell/virus pellets were resuspended in 1% of the initial volume with 10 mM Tris (pH 7.4-7.6) and freeze-thawed 3 times in a dry ice ethanol bath to lyse cells and release virus particles. Cell debris was pelleted using centrifugation (100 x g, 5 min, 4°C), and supernatant containing virus particles was used for titration and subsequent experiments.

2.3.3. *dl1520 titration*

HAdV titration was modified from a previously published protocol [33]. Briefly, A549 cells were used to seed 6-well tissue culture plates at a cell density of 2.0×10^5 cells per well and grown until approximately reaching 95% density. The dl1520 stock was serially diluted in 10-fold increments and used to infect wells in triplicate. After a 4-h infection, growth medium was replaced with soft agar (growth medium, 0.5% agarose, 1% penicillin/streptomycin). Plates were cultured until dl1520-untreated controls began to show signs of death (approximately 10-14 d) at which point plates were treated with the Neutral Red dye (50 µg/ml in growth medium) for 3 h to allow retention of the dye by viable cells. Soft agar pucks were removed and cells were fixed (1% CaCl₂ and 1% formaldehyde solution in H₂O) and washed with phosphate-buffered saline (PBS). Plaques are visualized as clear patches among the viable cell monolayer, which was stained red. Plaques were counted at a dilution that gave between 4 and 40 clearly visible plaques per well. The titer of the dl1520 stock was determined by multiplying the average number of plaques/well by its dilution factor.

2.4. Cell viability assays

2.4.1. *AlamarBlue*TM assay

Proliferation of HN-5a and HN-5a/carbo-15a cell lines was assessed using *AlamarBlue*TM cell viability assays in 96-well tissue culture plates according to a protocol previously used by our laboratory [137]. Briefly, 100 μ l of growth medium was replaced with *AlamarBlue*TM reagent (diluted 1:12 in growth medium) and cultured for 3-4 h. During this time, mitochondrial enzymes of metabolically active cells reduce resazurin, a non-fluorescent dye, to resorufin, which emits red-fluorescence [138]. Wells were then excited using a wavelength of 544 nm and emission was measured at 580 nm using a Wallac Victor² multi-label counter (PerkinElmer, Wallac, Gaithersburg, MD). The resulting fluorescence values reflect viable cell density, which were used as an estimate of cell proliferation. Background values as determined in growth medium without cells, were subtracted from all values for cell-containing wells.

2.4.2. *Neutral red* assay

Proliferation of HT-29, HT-29/CP-5c and HT-29/carbo-15d-1 cell lines was assessed using *Neutral Red* cell viability assays in 96-well tissue culture plates as previously described [139]. Briefly, 100 μ l of growth medium from each well was replaced with a *Neutral Red* dye solution (50 μ g/ml in growth medium). Cells were then cultured for 3 h to allow retention of the dye by viable cells. The *Neutral Red* assay is based on lysosomal incorporation of a red dye into viable, uninjured cells [139]. This weakly charged, positive dye diffuses into cells where

it then binds anionic molecules in the lysosomal matrix, causing it to be retained. Damage to either the plasma or lysosomal membranes results in less dye retention. Cells were washed 3 times with 150 μ l of wash buffer (1% CaCl_2 and 1% formaldehyde solution in H_2O) to remove any unincorporated dye. Two hundred μ l of extraction buffer (1% acetic acid and 50% ethanol in H_2O) was added to plates that were shaken for 10 min to extract bound dye. Absorbance at 590 nm was then determined using a Wallac Victor² multi-label counter. Cellular proliferation was calculated from the resulting absorbance values reflecting viable cell density. Background values as determined in growth medium without cells, were subtracted from all values for cell-containing wells.

2.5. Cell culture

2.5.1. Sensitivity of human tumour cell lines to dl1520 chemotherapy

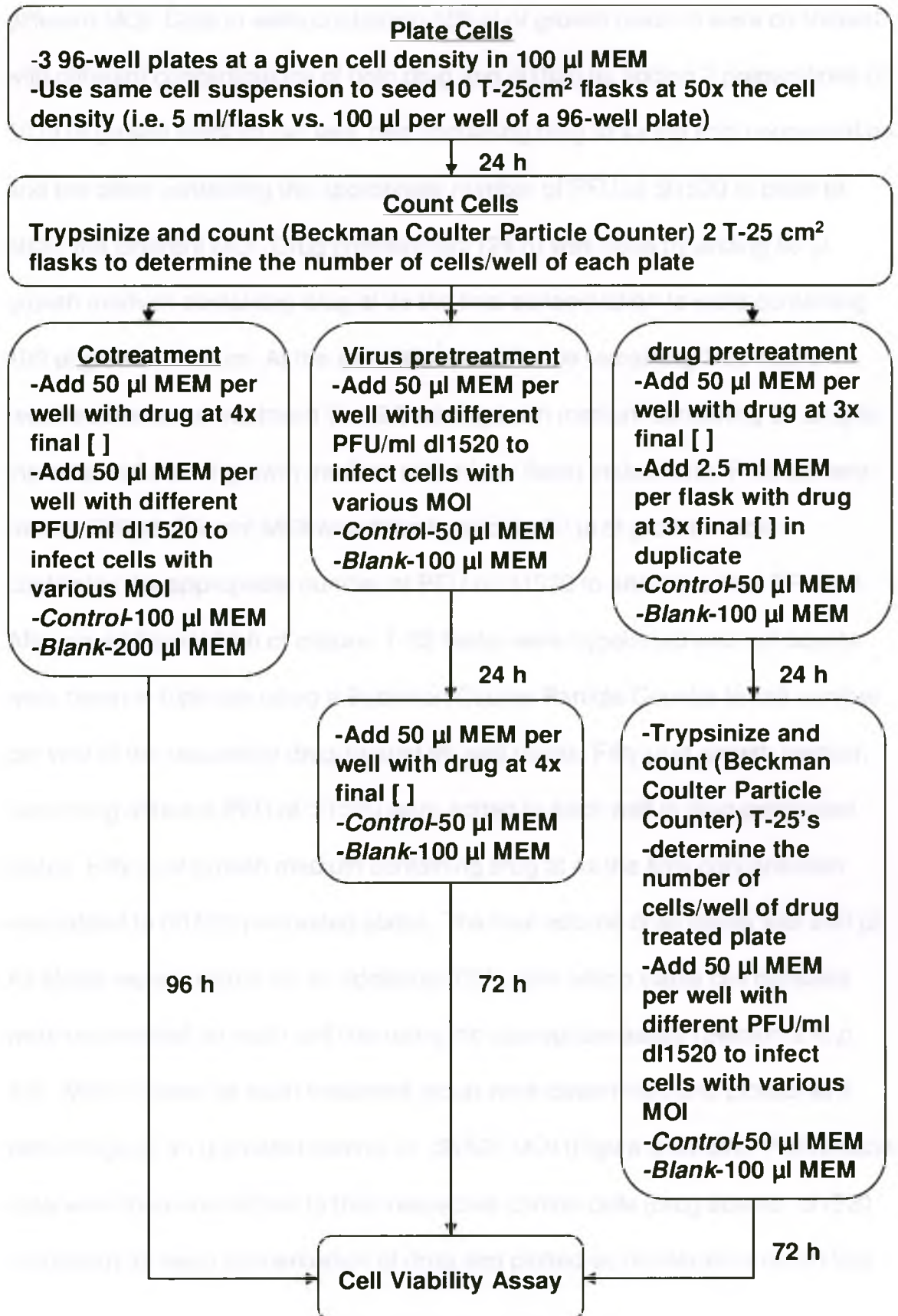
Cell lines were plated on 96-well tissue culture plates in a final volume of 100 μ l. HN-5a and HN-5a/carbo-15a cells were plated at 1.5×10^3 cells/well, and HT-29, HT-29/CP-5c and HT-29/carbo-15d-1 cells were plated at 3.0×10^3 cells/well. At the same time, the same cell suspensions were used to plate a 25- cm^2 tissue culture (T-25) flasks using 50x as many cells (i.e. 100 μ l per well vs. 5 ml per flask) in triplicate. Cells were cultured for 24 h to allow cells to adhere to tissue culture plastic and overcome the lag phase. T-25 flasks were then trypsinized and cells were counted in triplicate using a Beckman Coulter Particle Counter to determine the number of cells per well in the respective 96-well plates. Cells were treated with dl1520 at different MOI by adding to each well 100

μl of growth medium containing the required number of PFU to give the desired MOI. Cells were then cultured for 96 h. For cells being exposed to chemotherapy drugs, 100 μl of growth medium containing chemotherapy drug (melphalan, cisplatin, or paclitaxel) at 2x the final concentration was added to 100 μl of growth medium already in each well and plates were then cultured for 96 h. After incubation, density of viable cells was determined for each cell line using the appropriate assay (*Section 2.4, p. 43*). Mean values for each treatment group were determined and plotted as a percentage of an untreated control. Concentrations of that inhibited proliferation by 70%, 50%, and 20% (IC_{70} , IC_{50} , IC_{20}) were determined by interpolation of the concentration-response curves.

2.5.2. Differential effects of combined vs. sequential treatment of human tumour cells with dl1520 and chemotherapeutic drugs

Cell lines were plated on 96-well tissue culture plates and T-25 flasks as described above (*Section 2.5.1, p. 44*). This experiment evaluated potential the effect that differential treatment schedules have on interactions between various chemotherapy drugs (melphalan, cisplatin, or paclitaxel) and dl1520. Cells received one of three treatments: 96 h combined dl1520 and drug treatment, 24 h drug pretreatment followed by 72 h of combined treatment, or 24 h dl1520 pretreatment followed by 72 h combined treatment (Figure 2.5.2.1). Twenty-four hours after being plated, cell counts were obtained from 2 trypsinized T-25 flasks using Beckman Coulter Particle Counter to determine the number of cells per well for each cell line. These numbers were used to treat cells with dl1520 at

Figure 2.5.2.1. Scheduled treatment of various human tumour cell lines with drug and dl1520.



different MOI. Cells in wells containing 100 μ l of growth medium were co-treated with different concentrations of both drug and dl1520 by adding 2 preparations of 50 μ l of growth medium per well, one containing drug at 4x the final concentration and the other containing the appropriate number of PFU of dl1520 in order to attain the different MOI. Drug pretreatment (24 h) was done by adding 50 μ l growth medium containing drug at 3x the final concentration to wells containing 100 μ l growth medium. At the same time, cells in the remaining T-25 flasks received the same treatment (i.e. 2.5 ml of growth medium containing 3x drug to the initial volume of growth medium of 5 ml per flask) in duplicate. Pretreatment with dl1520 at different MOI was done by adding 50 μ l of growth medium containing the appropriate number of PFU of dl1520 to attain the final PFU/cell. After an additional 24 h of culture, T-25 flasks were trypsinized and cell counts were taken in triplicate using a Beckman Coulter Particle Counter to cell number per well of the respective drug-treated 96-well plates. Fifty μ l of growth medium containing different PFU of dl1520 were added to each well in drug-pretreated plates. Fifty μ l of growth medium containing drug at 4x the final concentration was added to dl1520-pretreated plates. The final volume of all plates was 200 μ l. All plates were cultured for an additional 72 h, after which viable cell densities were determined for each cell line using the appropriate assay (*Section 2.4, p. 43*). Mean values for each treatment group were determined and plotted as a percentage of an untreated control vs. dl1520 MOI (Figure 2.5.2.2A). Proliferation data were then normalized to their respective control cells (drug treated, dl1520 untreated) for each concentration of drug and plotted as proliferation vs. dl1520

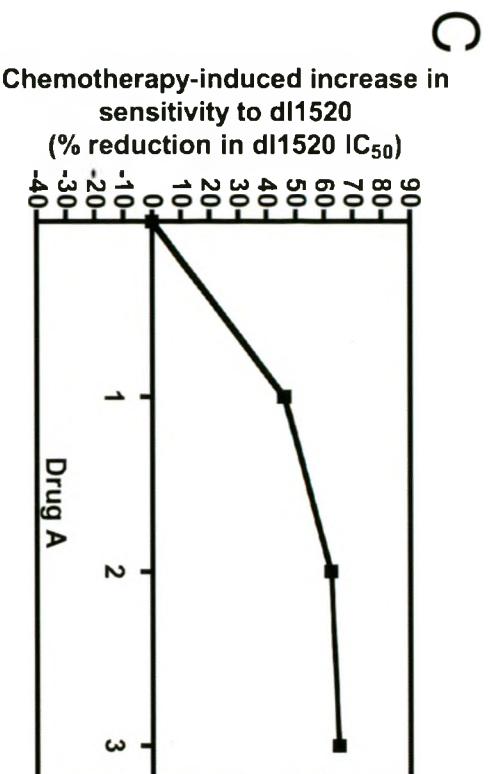
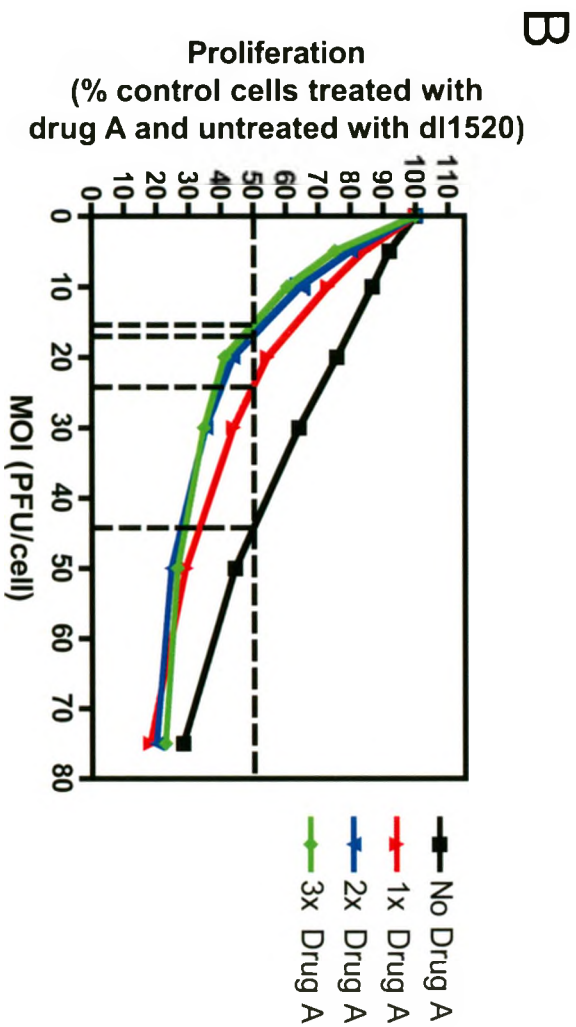
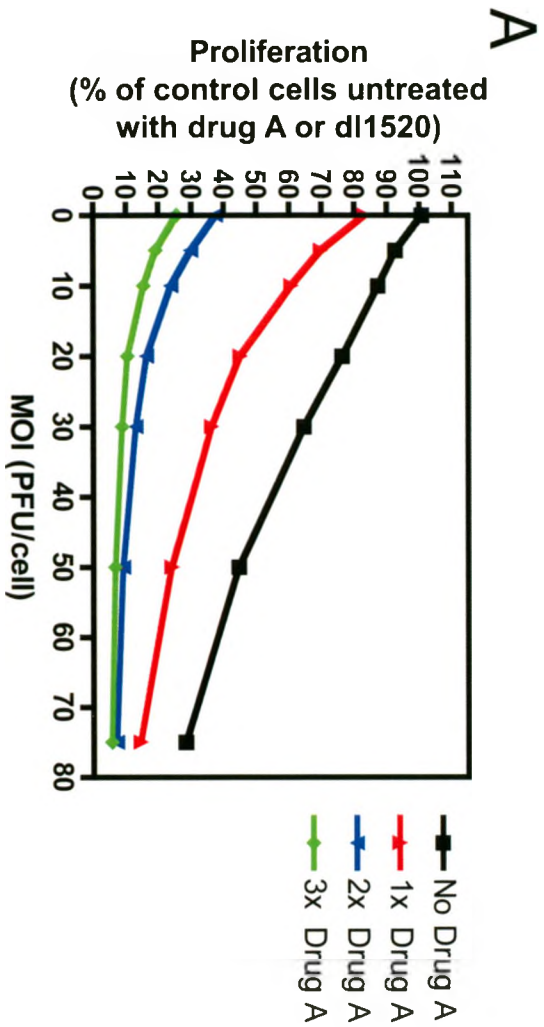
Figure 2.5.2.2. Representation of the method used to determine drug-induced changes dl1520 cytotoxicity, as a function of IC₅₀ value.

A human tumour cell line was treated with dl1520 at different MOI and several concentrations of a chemotherapeutic drug for 96 h.

(A) Proliferation was determined using a colourimetric-based cell viability assay and plotted as a percentage of an untreated control cells vs. dl1520 MOI.

(B) Proliferation data were then normalized to their respective dl1520-untreated controls for each concentration of drug and plotted as proliferation vs. dl1520 MOI. The IC₅₀ values for dl1520 in each concentration of drug were determined by interpolation of plotted data.

(C) The shift in the curve caused by the presence of drug is quantified and plotted as a percent by which the IC₅₀ value is changed against the various concentrations of drug.



MOI (Figure 2.5.2.2B). The IC_{50} values for dl1520 in each concentration of drug were determined by interpolation of plotted data. The shift in the curve caused by the presence of drug was quantified and plotted as the percent of change in the IC_{50} value vs. the concentration of drug (Figure 2.5.2.2C).

2.5.3. CAR levels following melphalan treatment

HN-5a cells were plated on both T-75 and T-25 flasks at 6.0×10^5 and 2.0×10^5 cells/flask, respectively, and cultured for 24 h to allow for cell adherence to tissue culture plastic. Cells were treated with various concentrations of melphalan. After 24 h of culture, cells from T-25 flasks were collected for quantification of CAR mRNA (Section 2.6, p. 52). After 48 h of culture, cells from T-75 flasks were collected for quantification of CAR protein (Section 2.7, p. 58).

2.5.4. CAR levels following short 50 μ M melphalan treatment

HN-5a cells were plated into both T-75 (4.5×10^5 cells for drug-untreated and 7.5×10^5 cells for drug treated) and T-25 (1.5×10^5 for drug-untreated and 2.5×10^5 for drug treated) flasks and cultured for 24 h to allow for cells to adhere to tissue culture plastic. Cells were treated with 50 μ M melphalan. At various times, cells from T-25's were collected for quantification of CAR mRNA (Section 2.6, p. 52) and growth medium from T-75's was replaced with fresh growth medium not containing drug. Cells in T-75's were cultured for a total time of 24 h and 48 h from the time of drug addition, at which time cells were collected for quantification of CAR protein (Section 2.7, p. 58).

2.5.5. Preparation of cultured cell lines to determine the basal CAR levels in 5 human tumour cell lines

For the purpose of growing cells to determine basal CAR mRNA and CAR protein the 5 human tumour cell lines used in this study were used to seed T-75 flasks at different cell densities: HN-5a (7.5×10^5 cells/flask), HN-5a/carbo-15a (6.25×10^5 cells/flask), HT-29 (2.4×10^6 cells/flask), HT-29/CP-5c (2.4×10^6 cells/flask), and HT-29/carbo-15d-1 (2.4×10^6 cells/flask). Cells were cultured for 5 d (or until the cell density reached approximately 70%) and total cellular protein and RNA were harvested for quantification of CAR mRNA (Section 2.6, p. 52) and CAR protein (Section 2.7, p. 58).

2.6. CAR mRNA quantification

2.6.1. Total cellular RNA isolation

Total RNA was harvested from cell lines using the TRIzol[®] extraction protocol as described previously [140]. Briefly, growth medium was aspirated from tissue culture flasks and cells were overlaid with 1 ml of TRIzol[®] Reagent for 5 min. Once cell lysis was complete, the TRIzol[®] cell extract was transferred to 1.5 ml centrifuge tubes and 200 μ l of chloroform was added. Samples were vortexed and spun ($12000 \times g$, 15 min, 4°C) to separate phases. Centrifugation resolved three bands: the lower red chloroform-phenol phase containing both lipids and denatured proteins, the white interphase consisting of DNA, and the upper aqueous phase containing RNA. The aqueous phase was collected and RNA was precipitated by addition of 500 μ l isopropanol. Samples were then

vortexed to promote precipitation, and RNA was pelleted using centrifugation (12000 x g, 15 min, 4°C). RNA pellets were then washed with 1 ml 75% ethanol, vortexed and centrifuged (7500 x g, 5 min, 4°C). Ethanol was removed, and pellets were air dried for 5-10 min and resuspended in 20-40 µl RNase-free H₂O. Samples were incubated for 10 min at 55°C to help dissolve RNA.

Concentration and purity of RNA samples were determined by UV spectroscopy using a NanoDrop 1000 Spectrophotometer (Thermo Scientific, Wilmington, DE, USA). Peak absorbance for nucleic acids and proteins are at 260 (A₂₆₀) and 280 (A₂₈₀) nm respectively, and 1 absorbance unit at 260 nm is equal to 40 µg/ml single-stranded RNA. RNA purity was assessed using the A₂₆₀/A₂₈₀ ratio. Samples with a ratio of 1.6 or higher were considered pure and were used for reverse transcription. Samples were stored at 4°C for short-term storage (shorter than 1 d) and -20°C for long-term storage (longer than 1 d).

2.6.2. Reverse transcription of RNA

RNA was reverse-transcribed to complementary DNA (cDNA) using MMLV-RT as previously shown in our laboratory [137,141]. A volume of RNase-free H₂O was added to 1 µg total RNA to bring the final volume to 10 µl. Ten µl reverse transcription master mix was prepared by adding 4 µl 5x First-Strand Buffer (250 mM Tris-HCl, pH 8.3; 375 mM KCl; 15 mM MgCl₂), 2 µl 0.1 M DTT, 2 µl dNTP mix (containing equal parts dATP, dTTP, dCTP, and dGTP), 1 µl RP (100 pmoles/µl), and 1 µl MMLV-RT (200 units/µl). Volumes of RNA and master mix were combined to prepare a single 20-µl reaction consisting of 1:1 RNA to

reverse transcription master mix. Reactions were vortexed to mix and spun using centrifugation (12,000 x g, 10 s, 21°C) to ensure samples were mixed and collected at the bottom of the tube. An Eppendorf Mastercycler Gradient (Eppendorf, Westbury, NY) thermal cycler was used to incubate reaction tubes at 25°C for 10 min to allow for RPs to anneal to complementary mRNA sequences, 37°C for 60 min to allow MMLV-RT to polymerize cDNA from mRNA transcripts, and 95°C for 5 min to inactivate MMLV-RT and separate cDNA from mRNA templates. Short-term (shorter than 1 d) and long-term (longer than 1 d) storage of samples was at 4°C and -20°C, respectively.

2.6.3. *Polymerase chain reaction*

PCR was used to show the relative levels of our gene of interest, CAR, and the internal control, glyceraldehyde-3-phosphate dehydrogenase (GAPDH). The reverse-transcribed cDNA was amplified using a 25- μ l PCR reaction which was prepared by adding 2.5 μ l 10x Taq PCR Reaction Buffer (200 mM Tris pH 8.4, 500 mM KCl), 1 μ l of 50 mM MgCl₂, 0.5 μ l 10 mM dNTP mix (containing equal parts dATP, dTTP, dCTP, and dGT), 0.25 μ l 50 μ M of both sequence-specific forward and reverse primers (Table 2.6.3), 19.3 μ l H₂O, 0.2 μ l Taq Polymerase, and 1 μ l of cDNA product. Tubes containing PCR reactions were vortexed and spun using centrifugation (12,000 x g, 10 s, 21°C) to ensure samples were mixed and collected at the bottom of the tube. An Eppendorf

Table 2.6.3. Semi-quantitative RT-PCR primer sequences and conditions.

Name	Sequence	Size (bp)	T _a (°C)	# of cycles
CAR	5'-GCTCTAGCGCTCATTGGTCT-3' 5'-GGAACACGGAGAGCACAGAT-3'	390	66	35
GAPDH	5'-TATTGGGCGCCTGGTCACCA-3' 5'-CCACCTTCTTGATGTCATCA-3'	752	58	20

Mastercycler Gradient thermal cycler was used to first incubate tubes at 95°C for 5 min to denature double-stranded DNA. Tubes were then cycled according to the conditions listed elsewhere (Table 2.6.3). The cycles consisted of: denaturation of double stranded DNA at 95°C for 30 s, annealing at specified temperatures for 30 s, and elongation at 72°C for 30 s. Samples were then incubated at 72°C for 10 min to allow complete extension of any semi-polymerized DNA templates. Samples were stored short-term (shorter than 1 d) at 4°C or long-term (longer than 1 d) at -20°C.

2.6.4. DNA gel electrophoresis of PCR products

Ten µl of each PCR reaction (plus 2 µl of orange G dye) was loaded per well of a 1.5% agarose gel (0.5 µg/ml ethidium bromide). DNA fragments amplified from the PCR were separated using DNA gel electrophoresis (50 V, 40 min) in 1 x TAE (40 mM Tris-HCL, 20 mM acetic acid, 1 mM EDTA). Ethidium bromide intercalates with nucleic acids allowing visualization of a fluorescent complex upon UV excitation. DNA fragments were visualized using a Gel Doc™ XS (BioRad, Hercules, CA, USA) and images were captured using PDQuest 7.4.0 (BioRAD). Band intensities of both CAR and GAPDH mRNA were quantified using Alpha-Ease FC software (Alpha Innotech, San Leandro, CA, USA). Relative CAR mRNA levels were determined by dividing CAR densitometric band intensities by those of corresponding GAPDH bands.

2.7. CAR protein quantification

2.7.1. Total protein isolation

Media was aspirated from cells that were washed once with, and scraped in, 5 ml of cold PBS. Cell pellets were generated by centrifugation (100 x g, 5 min, 4°C). Supernatant was aspirated and pellets were resuspended in lysis buffer (147 mM NaCl, 20 mM Tris, 0.1% SDS, 1% Triton x-100, 1 mM EDTA, 10 µg/ml aprotinin, 100 µM leupeptin, pH 7.6) to promote cell lysis followed by 3 freeze-thaw cycles using a dry ice ethanol bath to further disrupt the cellular membranes. To obtain samples for determination of CAR glycosylation, cells were scraped directly into 150 µl lysis buffer and then treated as above. One hundred µg of total protein from lysates was either treated with PNGase F, an N-glycosidase, or H₂O as a negative control according to manufacturer's instructions.

2.7.2. Total protein quantification

Total protein concentration of experimental cell lysates was determined using a BioRad protein assay kit. The main component of the BioRad reagent, Coomassie Brilliant Blue G-250, is red when unbound and blue when bound to aromatic amino acids and arginine residues. Therefore, shifts in absorption from 365 nm to 595 nm following the addition of the BioRad reagent are used as a measure of protein concentration for this assay [142]. A 20 µg/ml stock of BSA in PBS was used to generate a standard protein concentration curve for this assay (2.5 µg/ml to 20 µg/ml). Protein samples were diluted (1:350 or 1:500) in PBS

while the blank consisted of PBS alone. The final volume of all samples for this assay was 700 μ l. Three hundred and fifty μ l of BioRad reagent (diluted 3:2, reagent:PBS) was added to all samples. Three hundred μ l of each sample was loaded in triplicate into a 96-well plate. Absorbance at 595 nm was measured using the Wallac Victor² multi-label counter. Protein concentration for each experimental sample was interpolated from the BSA standard curve.

2.7.3. *Electrophoresis and blotting*

Twenty μ g of total protein was loaded per lane of a 15% SDS-polyacrylamide gel. Fifty μ g of a mouse liver extract was loaded into a single lane and used as a positive control. Proteins were separated based on their size using gel electrophoresis (120 V, 90 min, 21°C) and transferred onto Hybond ECL nitrocellulose membranes (GE Healthcare, Baie-d'Urfé, QC) (30 V, 12 h, 4°C). Prior to probing of membranes with antibodies, non-specific binding of antibodies was reduced by blocking membranes using 5% skim milk in Tris-buffered saline (TBS) (20 mM Tris, 140 mM NaCl in H₂O) containing 0.1% Tween 20 (TBS-T) for 1 h. The anti-CAR H300 polyclonal rabbit antibody was used as the primary antibody to probe for CAR protein. This antibody was diluted 1:1000 using 1% skim milk in TBS-T and membranes were overlaid for 1 h. Membranes were then incubated with HRP-conjugated goat anti-rabbit secondary antibody diluted 1:5000 in 1% skim milk in TBS-T for 1 h. HRP activity was detected by ECL Plus according to manufacturer's instructions. HRP catalyzes the oxidation of acridin substrates, emitting low-intensity light as they decay to a ground state. Bands

were resolved using a Molecular Dynamics Storm 860 Molecular Imager (Molecular Dynamics, Sunnyvale, CA, USA), which uses a 450 nm (blue) laser to excite an ECL Plus fluorescent intermediate, causing signal emission that is then detected by the scanner [143]. Images were captured using ImageQuant v5.1 (Molecular Dynamics, Sunnyvale, CA, USA). Antibodies were stripped from membranes by treating for 15 min with Restore Western Blot Stripping Buffer according to manufacturer's instructions. The blotting procedure was then repeated to probe for actin. The primary antibody for this was a rabbit anti-actin monoclonal antibody diluted 1:2000 in 1% skim milk in TBS-T and overlaid on membranes for 1 h. Densitometric band intensities of both CAR and actin were quantified using Alpha-Ease FC software. Relative CAR levels in protein cell lysates were determined by dividing CAR densitometric band intensities by those of actin.

2.8. Cell death assayed using flow cytometry following combined dl1520 and melphalan treatment

Cell death using AnnexinV/FITC and PI staining was performed as previously described [144]. HN-5a cells were plated in T-75 flasks at 1.5×10^5 cells/flask and cultured for 24 h to allow cells to adhere to tissue culture plastic. Three T-75's were trypsinized and cell counts were taken in triplicate using a Beckman Coulter Particle Counter to determine the number of cells/flask. Cells were then treated with different concentrations of melphalan with or without dl1520 at a MOI of 20. Cells from each experimental condition were collected, in

triplicate, every 24 h for a total of 4 d and assayed for cell death. Growth medium from the various treatments was collected because it may contain cells that had detached from the flask. The adherent population was trypsinized and resuspended in media containing the non-adherent population. Cell counts were then taken in triplicate using a Beckman Coulter Particle Counter. Cells were washed 2x using ice cold wash solution (PBS + 5% BSA) and resuspended in 100 μ l binding buffer (0.14 M NaCl, 2.5 mM CaCl₂, 10 mM HEPES, pH 7.4) at a final concentration of 1×10^6 cells/ml. Cells were stained with both AnnexinV/FITC and PI (2 μ l and 10 μ l of a 50 μ g/ml stock, respectively) for 15 min at room temperature in the dark. Binding buffer was added to dilute cells to a final volume of 500 μ l. FITC and PI fluorescence was determined using a Beckman Coulter Epics XL-MCL Flow Cytometer (Miami, FL, USA) within 1 h of staining. Each sample had 10,000 events measured. Percentage of dead and dying cells are represented as a sum of those that are: AnnexinV(+)
PI(-), AnnexinV(+)
PI(+), and AnnexinV(-)
PI(+).

2.9. Adenovirus replication in the presence of melphalan

Replication of dl1520 in HN-5a cells in the presence of melphalan was assessed using a modification of a previously described HAdV burst assay [29]. Briefly, 1.5×10^5 HN-5a cells were plated on T-75 flasks and cultured for 24 h to allow for cells to adhere to the plate. Three T-75's were trypsinized and cell counts were taken in triplicate using a Beckman Coulter Particle Counter to determine the number of cells per flask. Cells were infected with dl1520 at a MOI

of 20 alone or in combination with 2.5 μM , 5 μM , or 7.5 μM melphalan. Additional flasks of cells were treated with medium alone or medium containing 2.5 μM , 5 μM , or 7.5 μM melphalan in order to generate preconditioned medium. Cells were cultured with virus for 6 h to allow dl1520 attachment and infection to occur. Following incubation, half of the flasks from each dl1520 treatment group were harvested to establish dl1520 attachment while media from the remaining flasks were aspirated to remove any unbound dl1520 and overlaid with their respective preconditioned medium for an additional 66 h (72 h total) to allow for dl1520 replication. Preconditioned medium was used to overlay cells for the duration of their time in culture to simulate as closely as possible the conditions of previous assays where dl1520 was added to cells for the same duration as melphalan. dl1520 were harvested by scraping cells in their own medium, which were then pelleted using centrifugation (100 x g, 5 min, 4°C). Cell pellets were washed 3 times in PBS to remove dl1520 not associated with cells. Cell pellets were then resuspended in 100 μl lysis buffer (10 mM Tris, pH 7.4) and freeze-thawed 3 times using a dry ice ethanol bath to promote cell lysis and release of dl1520. Samples harvested at both 6-h and 72-h time points were titered as described above (*Section 2.3.3, p. 42*). The multiplicity of dl1520 replication was determined by dividing the concentration of dl1520 at 72 h by that at 6 h.

2.10. Statistical analyses

Data are presented as the means from individual experiments (n=3 for each experiment) \pm SEM. Significant differences between two data sets were

determined using a Student's *t*-test. Differences between more than two data sets were determined using a One-Way ANOVA with a post-hoc Tukey's test. Differences between two or more groups of data sets were done using a Two-Way ANOVA with a post-hoc Bonferroni test. Differences were accepted as statistically significant if the *p* value <0.05.

CHAPTER 3: RESULTS

3.1. Titration assay to determine concentration of active dl1520 virus

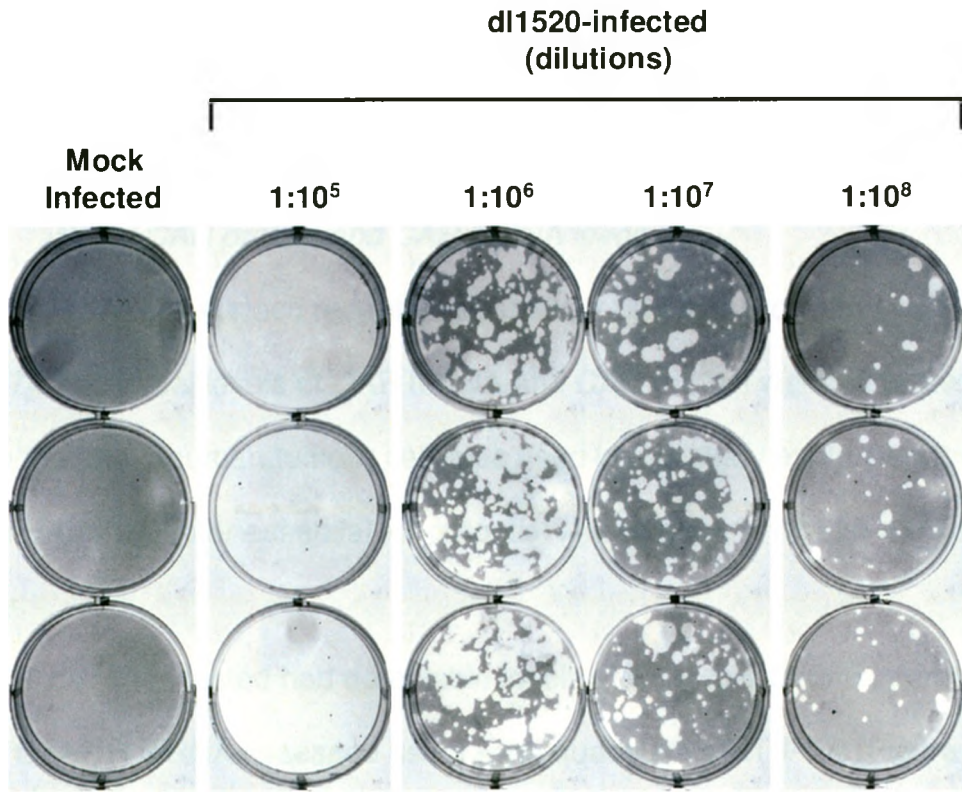
A plaque-forming assay in A549 cells was used to titrate a newly-propagated dl1520 stock solution (Figure 3.1.1A). A confluent monolayer of cells was treated with ten-fold serial dilutions of dl1520 virus particles. There was a marked reduction in dl1520-induced cytolysis when treating cells with increasing dilutions (Figure 3.1.1A). Plaques formed in cell layers treated with dl1520 solution diluted 1:10⁸ (Figure 3.1.1A) were counted and used to determine the concentration of the dl1520 stock solution was approximately 2.0 x 10⁹ PFU/ml. An assay of dl1520 cytotoxicity in HN-5a (head and neck tumour) cells was used to confirm that the dl1520 concentration determined using A549 cells was consistent with dl1520-induced inhibition of proliferation of another cell line. Briefly, HN-5a cells were infected with a range of MOI (0.1, 1, 3, 10, and 30 PFU/cell), cultured for 96 h, and the number of viable cells was assayed using an alamarBlueTM assay. Results were compared to an identical assay performed using dl1520 of a known concentration, as determined by Onyx Pharmaceuticals, the company who originally supplied the virus (Figure 3.1.1B). Treating HN-5a cells with the newly-propagated dl1520 stock at a MOI of 3 and 10 inhibited proliferation by approximately 23% and 56%, respectively (Figure 3.1.1B). Comparable levels of inhibition are observed when treating cells with dl1520 at approximately 3x the MOI from the original stock donated by Onyx

Figure 3.1.1. Titration of dl1520 stock.

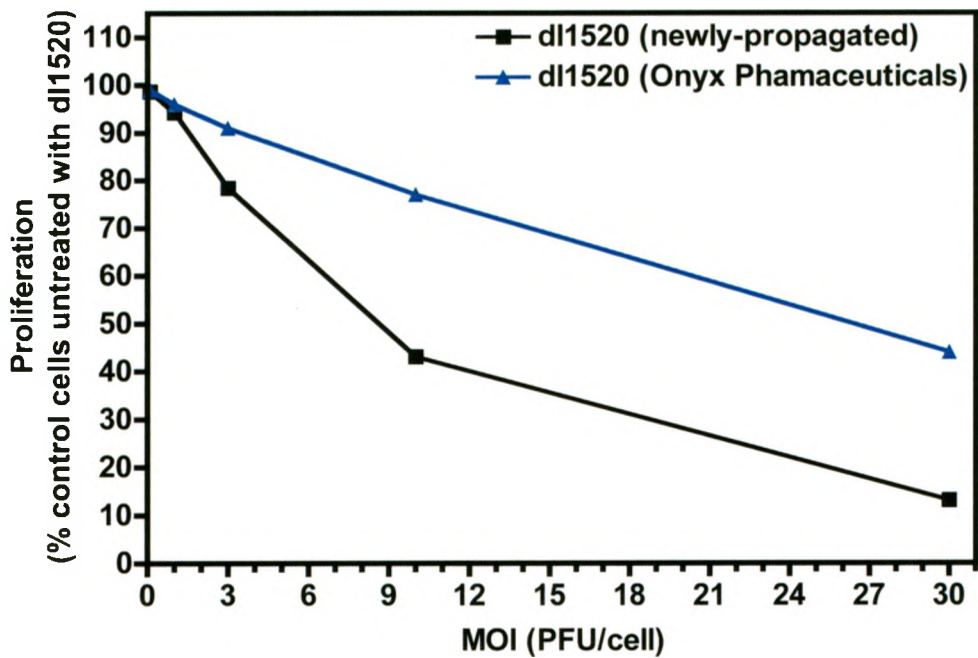
(A) Titration of dl1520 performed using a plaque-forming assay described in *Materials and Methods (Section 2.3.3, p. 42)*. Plaques (*clear*) are visualized in the viable cell monolayer (*grey*). Treatment of cells with dl1520 diluted 1:10⁵ resulted in complete lysis of the cell monolayer. Plaques were counted from the 10⁸ dilution and titer of dl1520 stock solution was determined to be 2.0 x 10⁹ PFU/ml.

(B) A cytotoxicity assay of HN-5a cells treated with dl1520 at different MOI from the stock titered in the present study (A) was compared to data generated using a dl1520 stock of a known concentration donated by Onyx Pharmaceuticals described in *Materials and Methods (Section 2.5.1, p. 44)*. Comparable levels of inhibition of proliferation using the newly-propagated dl1520 stock are observed at an MOI approximately one-third that of a stock of known concentration. This experiment was performed once.

A



B



Pharmaceuticals (Figure 3.1.1B). Based on these observations, it was concluded that the working concentration of our dl1520 stock was 6.0×10^9 PFU/ml.

3.2. Human tumour cell lines as targets for dl1520 therapy

3.2.1. Basal CAR protein and CAR mRNA levels

CAR is a cell surface receptor required for dl1520 association with human cells [47]. The basal levels of CAR mRNA and CAR protein were assessed to confirm that the 5 human tumour cell lines used in this study expressed the cell surface HAdV receptor essential for potential involvement in dl1520-mediated therapy.

All cell lines tested had detectable levels of CAR mRNA and internal control GAPDH mRNA assessed using semi-quantitative RT-PCR (Figure 3.2.1A). Densitometric analysis of RT-PCR-amplified CAR mRNA bands visualized using DNA gel electrophoresis and UV-illumination did not reveal any differences in CAR mRNA levels relative to GAPDH mRNA levels between parental cell lines and their respective drug-resistant variants (Figure 3.2.1B). HN-5a cells had less CAR mRNA than HT-29 and HT-29/carbo-15d-1 cell lines, whereas CAR mRNA levels in HN-5a/carbo-15a were not lower than in any other cell lines except HT-29 (Figure 3.2.1B).

Immunoblots were generated to visualize and quantify CAR protein in the cell lines. A preliminary blot for CAR protein using a commercially available mouse liver extract as a positive control and a protein lysate generated from untreated HN-5a cells was used to confirm the specificity of the primary anti-CAR

Figure 3.2.1. Basal CAR mRNA levels in 5 human tumour cell lines.

Five human tumour cell lines were grown *in vitro* as described in *Materials and Methods* (Sections 2.5.5, p. 52). RNA was isolated from each cell line and both CAR and GAPDH mRNA were PCR-amplified and visualized by gel electrophoresis as described in *Materials and Methods* (Section 2.6, p. 52).

(A) A representative gel illustrating both CAR and GAPDH mRNA from a single experiment.

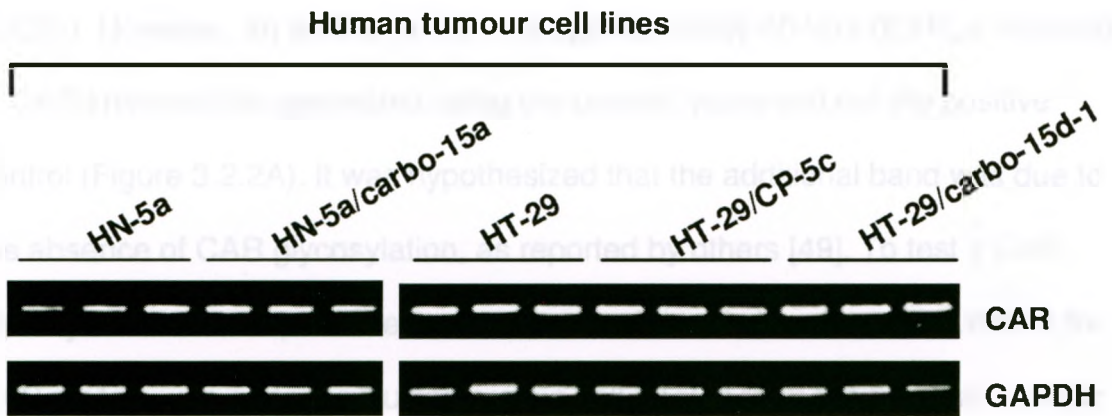
(B) Densitometric quantifications of CAR mRNA were normalized to the GAPDH mRNA control. The means of 3 separate experiments (n=3 for each experiment) \pm SEM are plotted.

^a different from HN-5a (Student's *t*-test, $p < 0.05$).

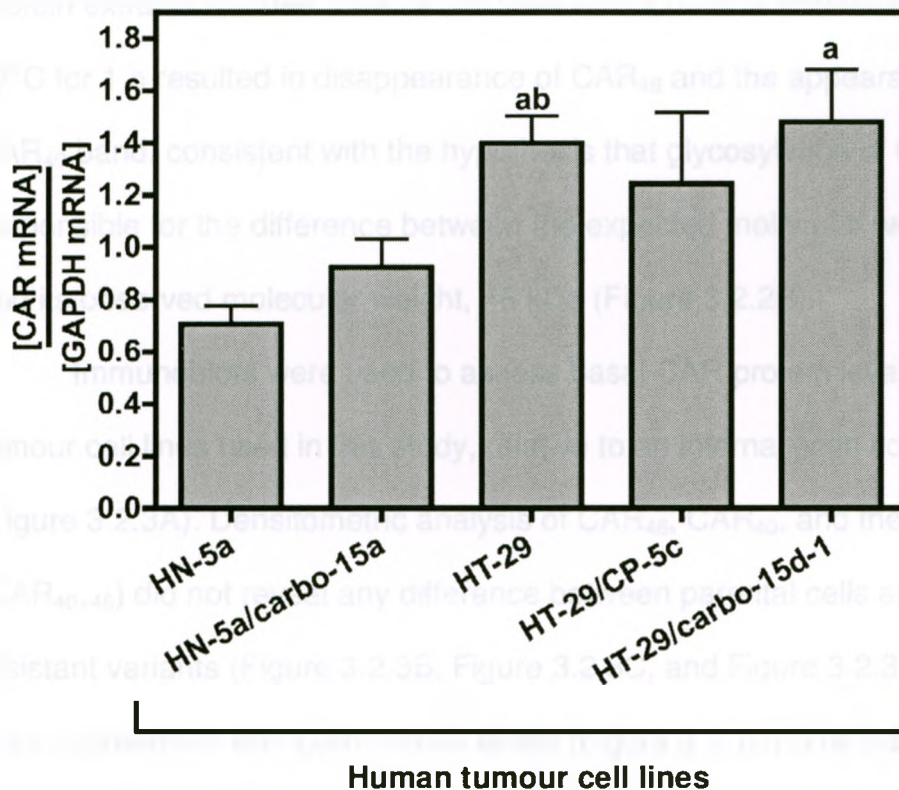
^b different from HN-5a/carbo-15a (Student's *t*-test, $p < 0.05$).

There is no difference in CAR mRNA levels between parental cells and their drug-resistant variants.

A



B



antibody used in the present study (Figure 3.2.2A). As expected, a band resolved at 46 kDa (CAR₄₆) for both the positive control and the protein lysates (Figure 3.2.2A). However, an additional band at approximately 40 kDa (CAR₄₀) resolved in CAR immunoblots generated using the protein lysate and not the positive control (Figure 3.2.2A). It was hypothesized that the additional band was due to the absence of CAR glycosylation, as reported by others [49]. To test if CAR glycosylation was responsible for the observed double band, an immunoblot for CAR protein was performed using protein cell lysates from the 5 human tumour cell lines treated with either PNGase F (an N-glycosidase) or a negative control (distilled water) (Figure 3.2.2B). In the absence of PNGase F, all cell lines resolved strong CAR₄₆ protein (Figure 3.2.2B). A faint second CAR₄₀ band is visible in HT-29 and HT-29/carbo-15d-1 cells (Figure 3.2.2B). Treatment of protein extracts isolated from all cell lines with 2 units of PNGase F enzyme at 37°C for 1 h resulted in disappearance of CAR₄₆ and the appearance of a strong CAR₄₀ band, consistent with the hypothesis that glycosylation of CAR is responsible for the difference between the expected molecular weight, 40 kDa, and its observed molecular weight, 46 kDa (Figure 3.2.2B).

Immunoblots were used to assess basal CAR protein levels in the human tumour cell lines used in this study, relative to an internal actin control protein (Figure 3.2.3A). Densitometric analysis of CAR₄₆, CAR₄₀, and the sum of the two (CAR₄₀₊₄₆) did not reveal any difference between parental cells and their drug-resistant variants (Figure 3.2.3B, Figure 3.2.3C, and Figure 3.2.3D). These data are in agreement with CAR mRNA levels (Figure 3.2.1B). The parental HT-29

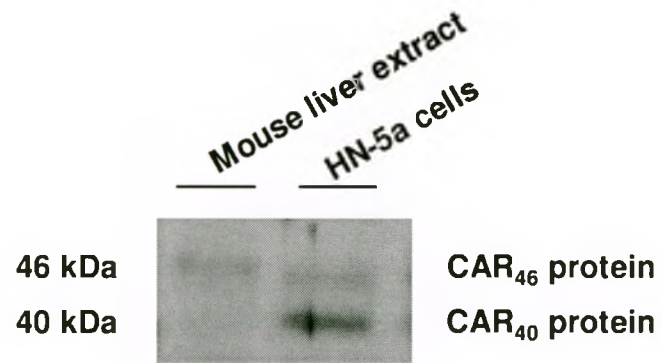
Figure 3.2.2. CAR protein glycosylation in human tumour cell lines.

Five human tumour cell lines were grown *in vitro* as described in *Materials and Methods* (Section 2.5.5, p. 52). Total cellular protein was isolated and CAR protein was visualized by SDS-PAGE and immunoblotting as described in *Materials and Methods* (section 2.7, p. 58).

(A) An immunoblot for CAR protein in a sample isolated from HN-5a cells and a commercially available positive control (mouse liver extract) for CAR protein.

(B) Protein lysates were treated with or without PNGase F and subjected to SDS-PAGE and immunoblotting as described in *Materials and Methods* (Section 2.7.1, p. 58). CAR protein was visualized by exposing the immunoblotted membrane to X-ray film. This experiment was performed once.

A



B

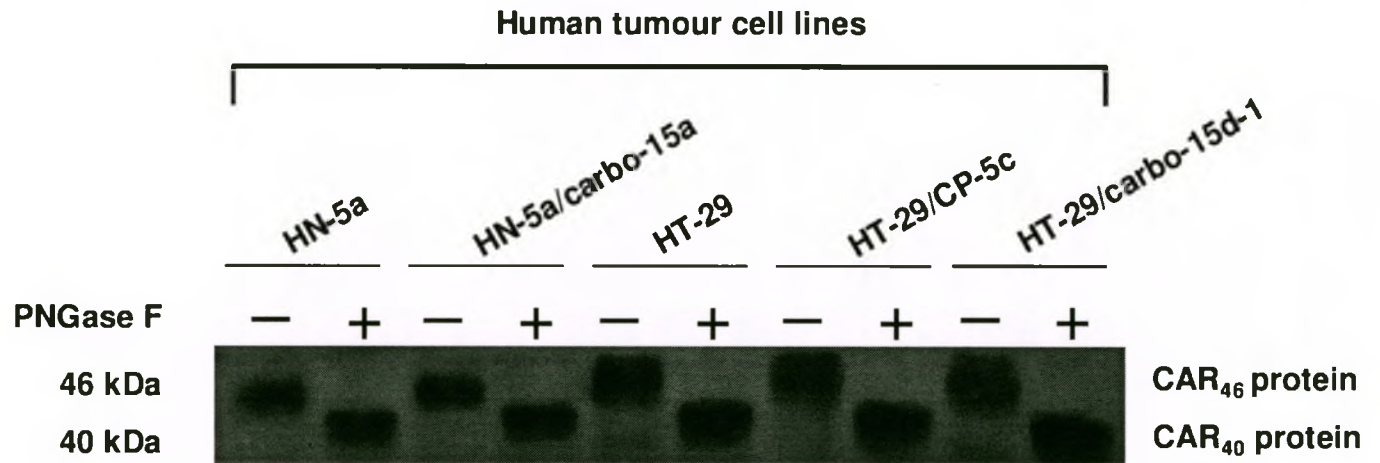


Figure 3.2.3. Basal CAR protein levels in 5 human tumour cell lines.

Five human tumour cell lines were grown *in vitro* as described in *Materials and Methods* (section 2.5.5, p. 52). Total cellular protein was isolated and both CAR and actin protein were visualized by SDS-PAGE and immunoblotting as described in *Materials and Methods* (section 2.7, p. 58).

(A) A representative immunoblot illustrating both CAR and actin protein levels from a single experiment. Cellular levels of:

(B) CAR₄₆,

(C) CAR₄₀, and

(D) CAR₄₀₊₄₆

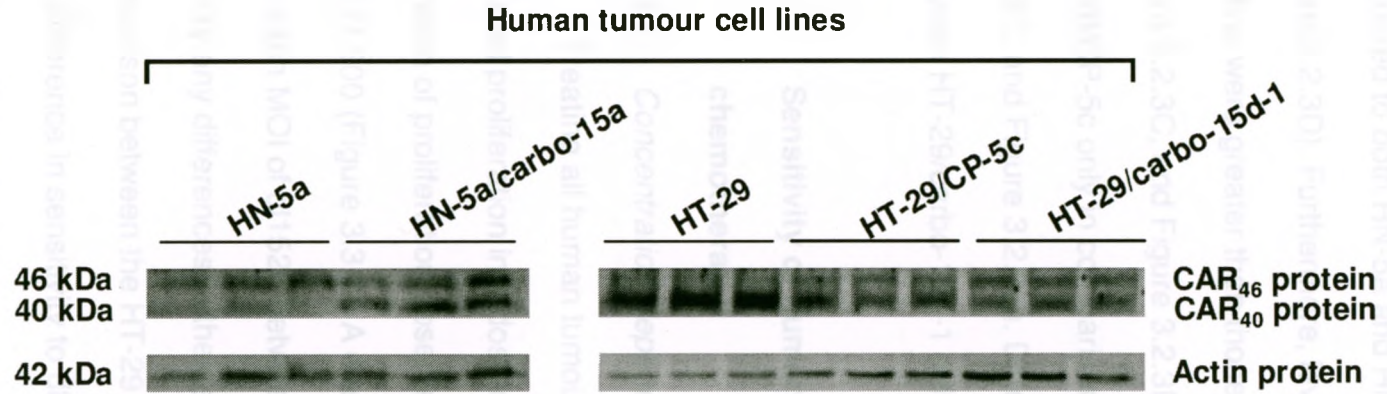
as measured by quantitative densitometry and normalized to their respective actin controls. The means of 3 separate experiments (n=3 for each experiment) ± SEM are plotted.

^a different from HN-5a (Student's *t*-test, p<0.05).

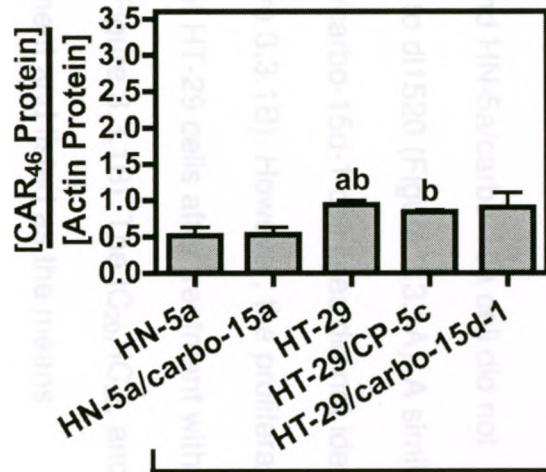
^b different from HN-5a/carbo-15a (Student's *t*-test, p<0.05).

There is no difference in CAR protein levels between parental cells and their drug-resistant variants.

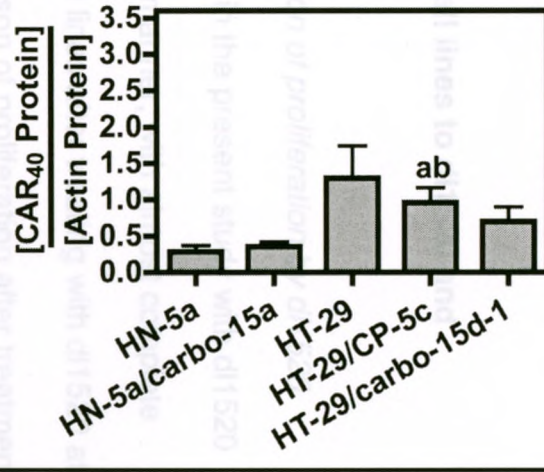
A



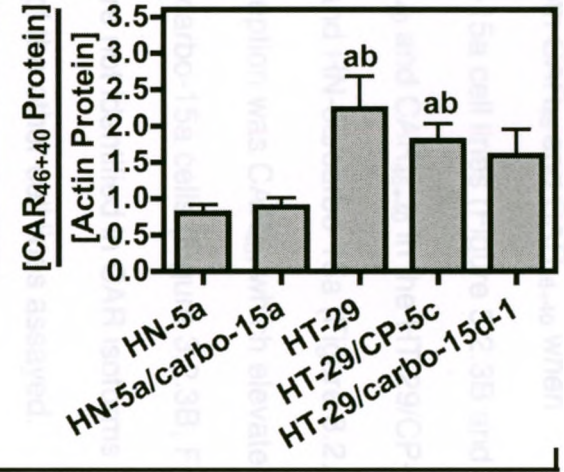
B



C



D



Human tumour cell lines

cell line had significantly higher levels of both CAR₄₆ and CAR₄₆₊₄₀ when compared to both HN-5a and HN-5a/carbo-15a cell lines (Figure 3.2.3B and Figure 3.2.3D). Furthermore, levels of CAR₄₀ and CAR₄₆₊₄₀ in the HT-29/CP-5c cell line were greater than those in HN-5a and HN-5a/carbo-15a (Figure 3.2.3B, Figure 3.2.3C, and Figure 3.2.3D). The exception was CAR₄₆, which elevated in HT-29/CP-5c only in comparison to HN-5a/carbo-15a cells (Figure 3.2.3B, Figure 3.2.3C, and Figure 3.2.3D). Differences were not identified in CAR isoforms between HT-29/carbo-15d-1 cells and any of the other cell lines assayed.

3.3. Sensitivity of human tumour cell lines to dl1520 and chemotherapy

3.3.1. Concentration-dependent inhibition of proliferation by dl1520

Treating all human tumour cell lines in the present study with dl1520 inhibited proliferation in a dose-dependent manner, with almost complete inhibition of proliferation observed in all cell lines after treating with dl1520 at a MOI of 300 (Figure 3.3.1). A direct comparison of proliferation after treatment with each MOI of dl1520 between HN-5a and HN-5a/carbo-15a cell did not identify any differences in their sensitivities to dl1520 (Figure 3.3.1A). A similar comparison between the HT-29 and HT-29/carbo-15d-1 cell lines did not identify any difference in sensitivity to dl1520 (Figure 3.3.1B). However, the proliferation of HT-29/CP-5c cells is different from that of HT-29 cells after treatment with dl1520 at MOIs of 10, 15, 20, 50 and 125 (Figure 3.3.1B). The IC₂₀, IC₅₀, and IC₇₀ values were interpolated from each experiment and listed as the means

Figure 3.3.1. Concentration-dependent growth inhibition of human tumour cells by dl1520.

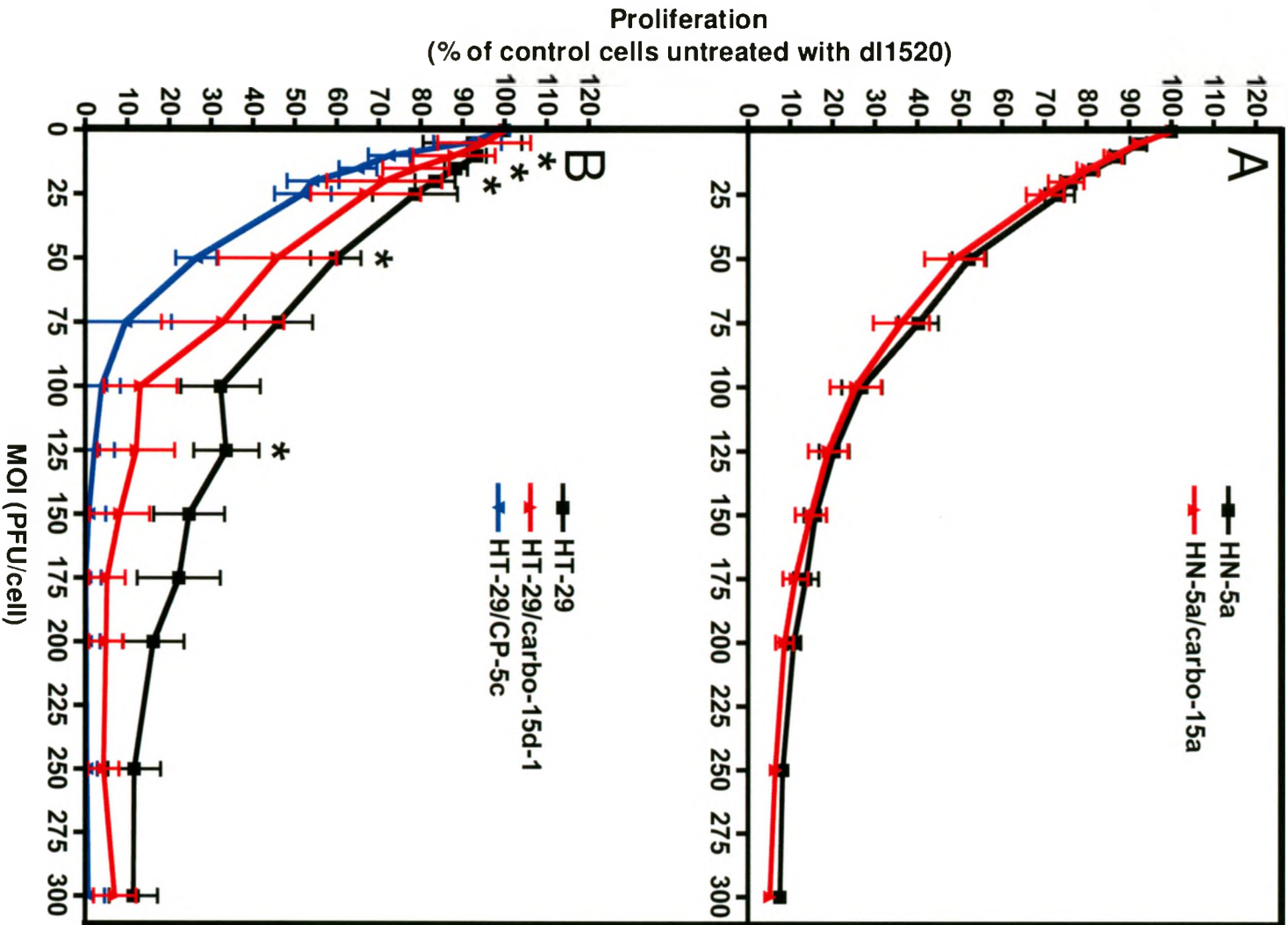
Five human tumour cell lines were treated with different MOIs of dl1520 for 96 h as described in *Materials and Methods* (Section 2.5.1, p. 44). Following treatment, density of viable cells as determined using the appropriate colourimetric-based cell viability assay as described in *Materials and Methods* (Sections 2.4, p. 43). Mean values representing the density of viable cells following dl1520 treatment at each MOI were determined and plotted as a percentage of dl1520-untreated control cells. Means from 3 separate experiments ($n=3$ for each experiment) \pm SEM are plotted.

(A) A comparison of dl1520 sensitivity of HN-5a and HN-5a/carbo-15a cell lines. No differences in sensitivity were detected at any tested MOI of dl1520 (Student's *t*-test, $p<0.05$).

(B) A comparison of dl1520 sensitivity of HT-29 to HT-29/carbo-15d-1 and HT-29/CP-5c cell lines.

* proliferation of HT-29 cells is different from HT-29/CP-5c cell lines at identically-treated MOI of dl1520 (Student's *t*-test, $p<0.05$).

No differences in sensitivity were detected between HT-29 and HT-29/carbo-15d-1 cell lines at any tested MOI of dl1520 (Student's *t*-test, $p<0.05$).



generated from three separate interpolations (one per experiment) \pm SEM (Table 3.3.1). There is no difference in any of the IC values between any of the parental cells and their drug-resistant variants (Table 3.3.1). However, HN-5a and HT-29/CP-5c cell lines were different when comparing IC₂₀, IC₅₀, and IC₇₀ values (Table 3.3.1). Subsequent experiments were designed to investigate chemotherapy-mediated changes in the effects of dl1520 as a function of a reduction in dl1520 IC₅₀. Therefore, the plots in Figure 3.3.1 were used to select the appropriate MOI of dl1520 to ensure that proliferation was inhibited by at least 50% in these experiments.

3.3.2. *Concentration-dependent inhibition of proliferation by chemotherapy*

Treatment of HN-5a cells with the chemotherapeutic drugs melphalan, cisplatin, and paclitaxel inhibits proliferation in a concentration-dependent manner (Figure 3.3.2). Sensitivity of this cell line to the DNA-damaging agents cisplatin and melphalan was in the μ M range (Figure 3.3.2A and Figure 3.3.2C), whereas sensitivity to paclitaxel was in the nM range (Figure 3.3.2B). The corresponding IC₅₀ values for melphalan, paclitaxel, and cisplatin in HN-5a cells are summarized in Table 3.3.2. An additional tumour cell line originating in a different tissue (HT-29) and two carboplatin-resistant variants (HN-5a/carbo15a and HT-29/carbo-15d-1) were sensitive to the anti-proliferative effects of melphalan in a concentration-dependent manner (Figure 3.3.3). Similar to the parental HN-5a cell line, HN-5a/carbo-15a cells were sensitive to melphalan at μ M concentrations (Figure 3.3.3C and Figure 3.3.2A). However, sensitivity to

Table 3.3.1. Sensitivity of 5 human tumour cell lines to growth inhibition induced by dl1520.

The human tumour cell lines were treated as described in the legend of Figure 3.3.1 (p. 76). The MOIs of dl1520 that inhibited proliferation of cell lines by 20%, 50%, and 70 % (IC₂₀, IC₅₀, and IC₇₀, respectively) were interpolated from plotted data from each of three experiments and averaged \pm SEM.

^a different from the corresponding IC value for HN-5a cells (Student's *t*-test, $p < 0.05$).

There were no differences in IC values between parental and their respective drug-resistant variants.

Cell Line	Sensitivity to dl1520 (MOI)		
	IC ₂₀	IC ₅₀	IC ₇₀
HN-5a	16.64 ± 1.41	57.46 ± 8.37	96.31 ± 10.76
HN-5a/carbo-15a	16.56 ± 2.78	52.17 ± 9.68	90.13 ± 14.42
HT-29	26.80 ± 7.82	74.23 ± 18.19	127.20 ± 39.02
HT-29/CP-5c	7.56 ± 1.96 ^a	26.70 ± 5.90 ^a	49.95 ± 9.01 ^a
HT-29/carbo-15d-1	20.13 ± 10.23	48.46 ± 19.03	78.27 ± 25.11

Figure 3.3.2. Sensitivity of HN-5a tumour cells to growth inhibition induced by melphalan, paclitaxel, and cisplatin.

HN-5a cells were grown *in vitro* for 96-h in the presence of the indicated concentrations of:

(A) melphalan,

(B) paclitaxel, or

(C) cisplatin

as described in *Materials and Methods* (Section 2.5.1, p. 44). Following treatment the density of viable cells was determined using an alamarBlue™ cell viability assay as described in *Materials and Methods* (Sections 2.4.1, p. 43). Mean values representing the density of viable cells following treatment with each concentration of drug were determined and plotted as a percentage of drug-untreated control cells. For each drug, the means of 3 separate experiments (n=3 for each experiment) ± SEM are plotted.

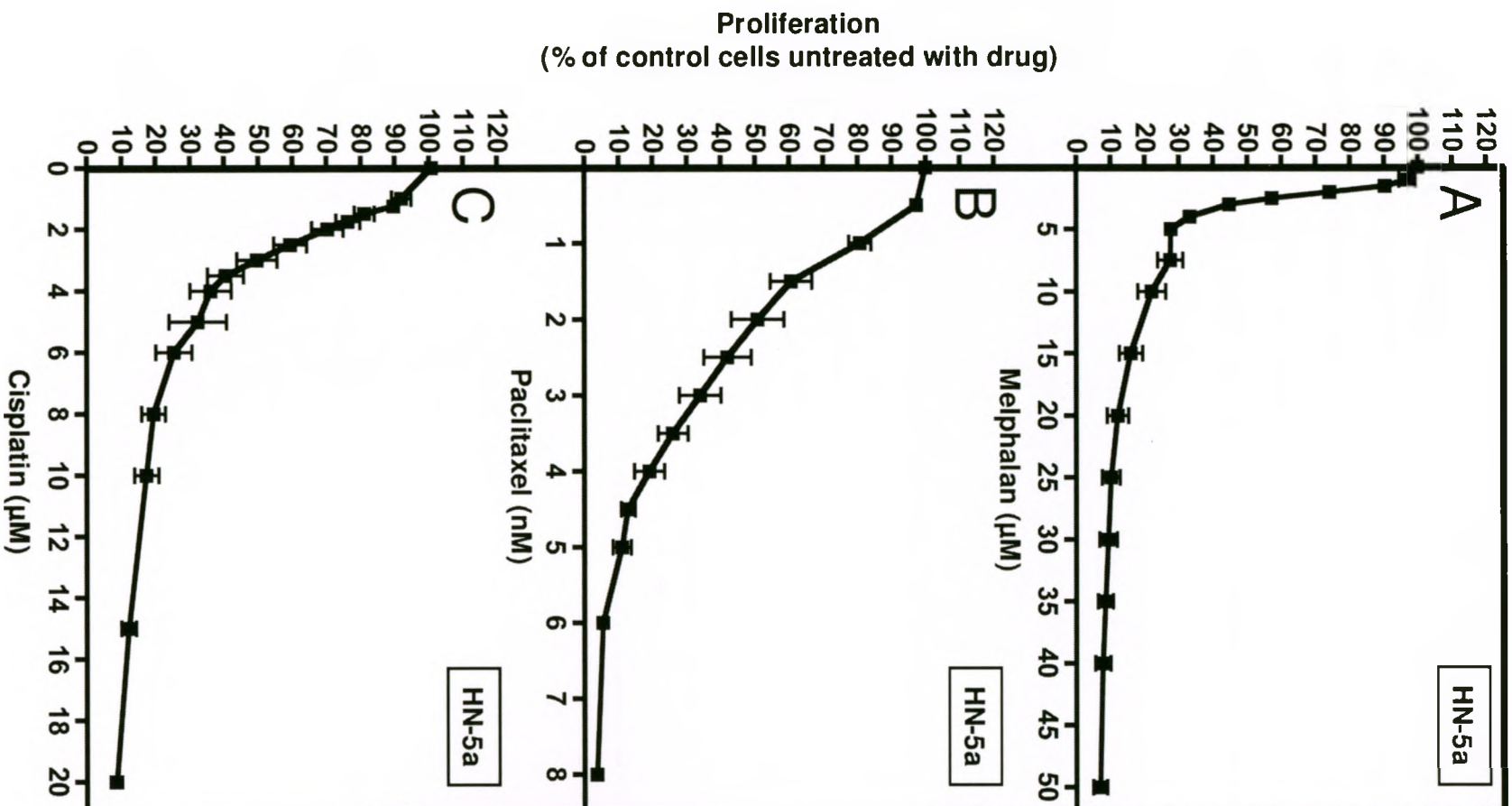


Table 3.3.2. Sensitivity of 4 human tumour cell lines to growth inhibition induced by chemotherapy drugs.

Cell lines were treated as described in the legends of Figures 3.3.2 and 3.3.3 (p. 81 and 85, respectively) Concentrations of chemotherapy drug that inhibited proliferation of the indicated cell lines by 50% (IC_{50}) were interpolated from plotted data from three experiments and averaged \pm SEM.

^a different from the corresponding IC_{50} value for HN-5a cells (Student's *t*-test, $p < 0.05$).

ND are values that were "not determined".

Cell Line	Sensitivity to Chemotherapy (IC ₅₀)		
	Melphalan (μ M)	Paclitaxel (nM)	Cisplatin (μ M)
HN-5a	2.79 \pm 0.04	2.09 \pm 0.35	3.05 \pm 0.29
HN-5a/carbo-15a	6.41 \pm 0.23 ^a	ND	ND
HT-29	27.41 \pm 3.37	ND	ND
HT-29/carbo-15d-1	26.76 \pm 3.80	ND	ND

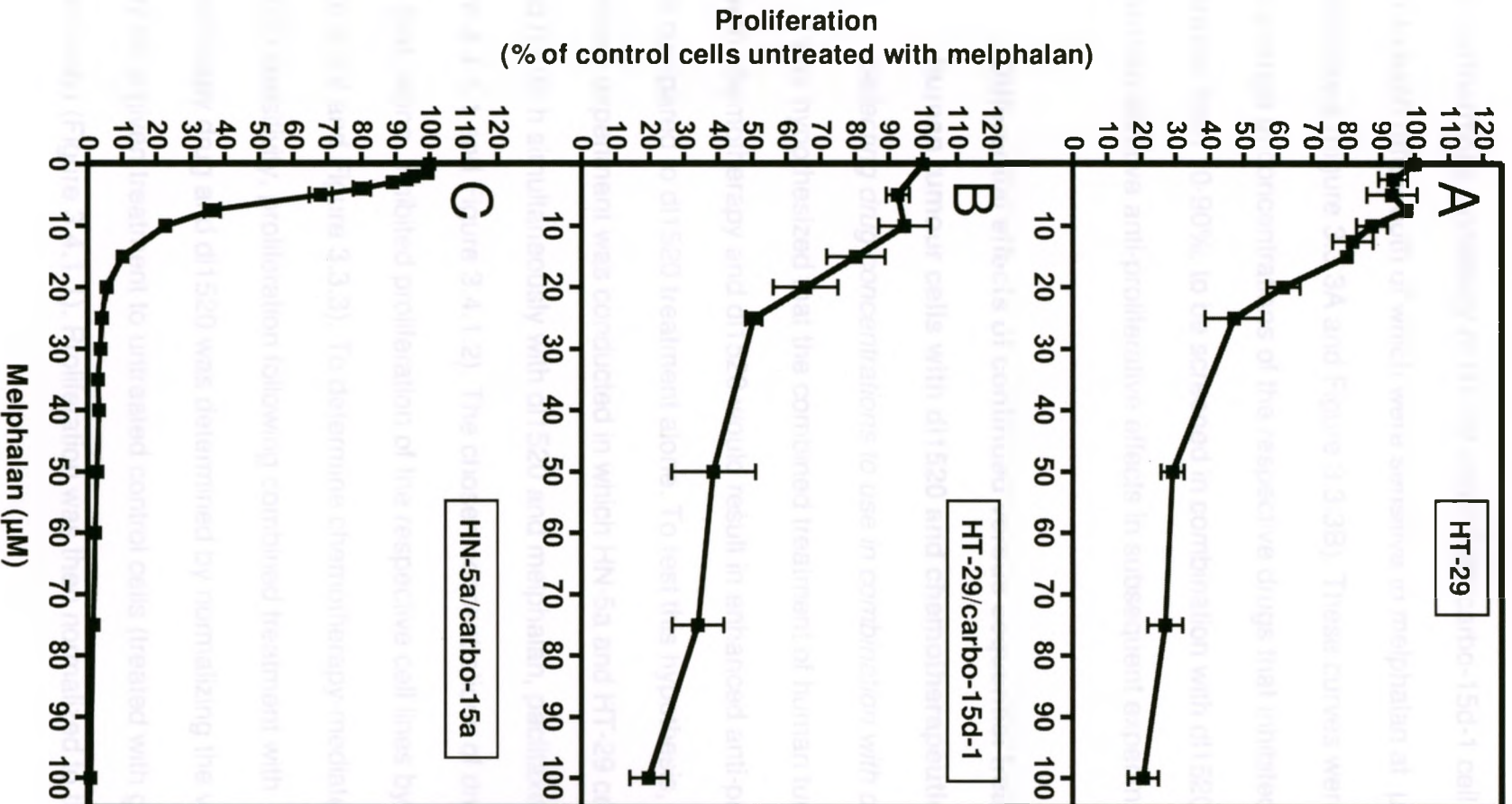
Figure 3.3.3. Sensitivity of 3 human tumour cell lines to growth inhibition induced by melphalan.

(A) HT-29,

(B) HT-29/carbo-15d-1, and

(C) HN-5a/carbo-15a

cell lines were cultured for 96 h with different concentrations of melphalan as described in *Materials and Methods* (Section 2.5.1, p. 44). Following treatment, the density of viable cells was determined using the appropriate colourimetric-based cell viability assay as described in *Materials and Methods* (Sections 2.4, p. 43). Mean values representing density of viable cells following treatment with each melphalan concentration were determined and plotted as a percentage of melphalan-untreated control cells. For each cell line, the means of 3 separate experiments ($n=3$ for each experiment) \pm SEM are plotted.



melphalan was different in HN-5a/carbo-15a cells compared to HN-5a (Table 3.3.2). Furthermore, sensitivity of HT-29 and HT-29/carbo-15d-1 cell lines were similar to each other, both of which were sensitive to melphalan at μM concentrations (Figure 3.3.3A and Figure 3.3.3B). These curves were used to select a range of concentrations of the respective drugs that inhibited proliferation from 10-90%, to be screened in combination with dl1520 for potential greater-than-additive anti-proliferative effects in subsequent experiments.

3.4. Differential effects of continued versus sequential treatment of human tumour cells with dl1520 and chemotherapeutic drugs

3.4.1. Selecting drug concentrations to use in combination with dl1520

It was hypothesized that the combined treatment of human tumour cell lines with chemotherapy and dl1520 would result in enhanced anti-proliferative effects compared to dl1520 treatment alone. To test this hypothesis, a preliminary experiment was conducted in which HN-5a and HT-29 cells were treated for 96 h simultaneously with dl1520 and melphalan, paclitaxel, or cisplatin (Figure 3.4.1.1 and Figure 3.4.1.2). The chosen concentrations of drug were those that, alone, inhibited proliferation of the respective cell lines by up to 75% (Figure 3.3.2 and Figure 3.3.3). To determine chemotherapy-mediated changes in dl1520 sensitivity, proliferation following combined treatment with chemotherapy drug and dl1520 was determined by normalizing the viable cell density for a given treatment to untreated control cells (treated with growth medium only) (Figure 3.4.1.1). Proliferation was then normalized to their

Figure 3.4.1.1. Chemotherapy-mediated changes in sensitivity to dl1520.

HN-5a cells were treated with dl1520 and:

(A) melphalan,

(B) paclitaxel, or

(C) cisplatin

and

(D) HT-29 cells were treated with dl1520 and melphalan

for 96 h as described in *Materials and Methods* (Section 2.5.2, p. 45). Following treatment, the numbers of viable cells were determined using a colourimetric-based cell viability assay as described in *Materials and Methods* (Section 2.4, p. 43). The numbers of viable cells for a given treatment were normalized to untreated control cells (treated with growth medium only) and plotted vs. dl1520 MOI. Proliferation data was then normalized to their respective dl1520-untreated controls (treated with drug at a given concentration in the absence of dl1520) and plotted relative to dl1520 MOI. The IC_{50} values for dl1520 when treating with a given concentration of drug were interpolated from the plotted data.

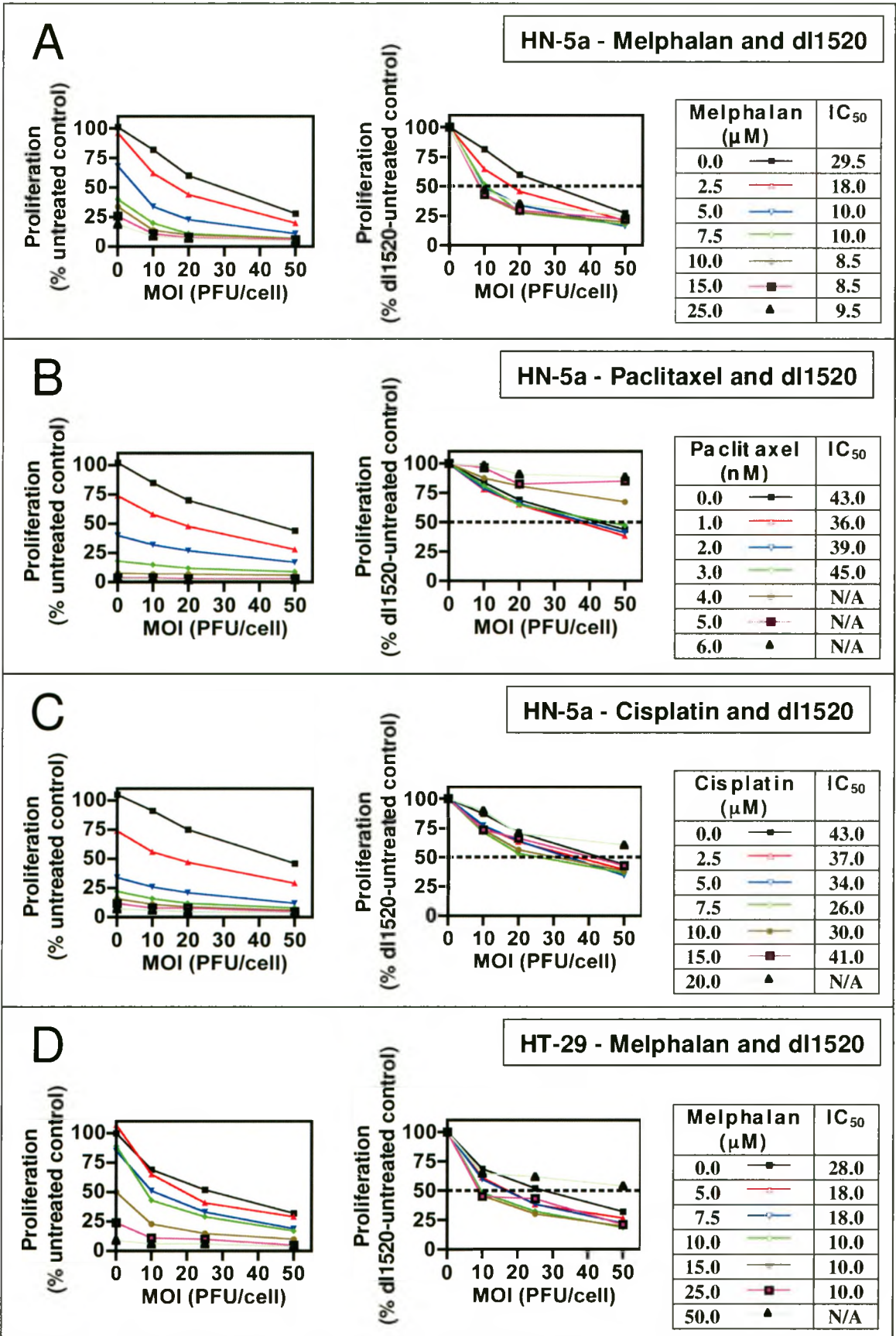
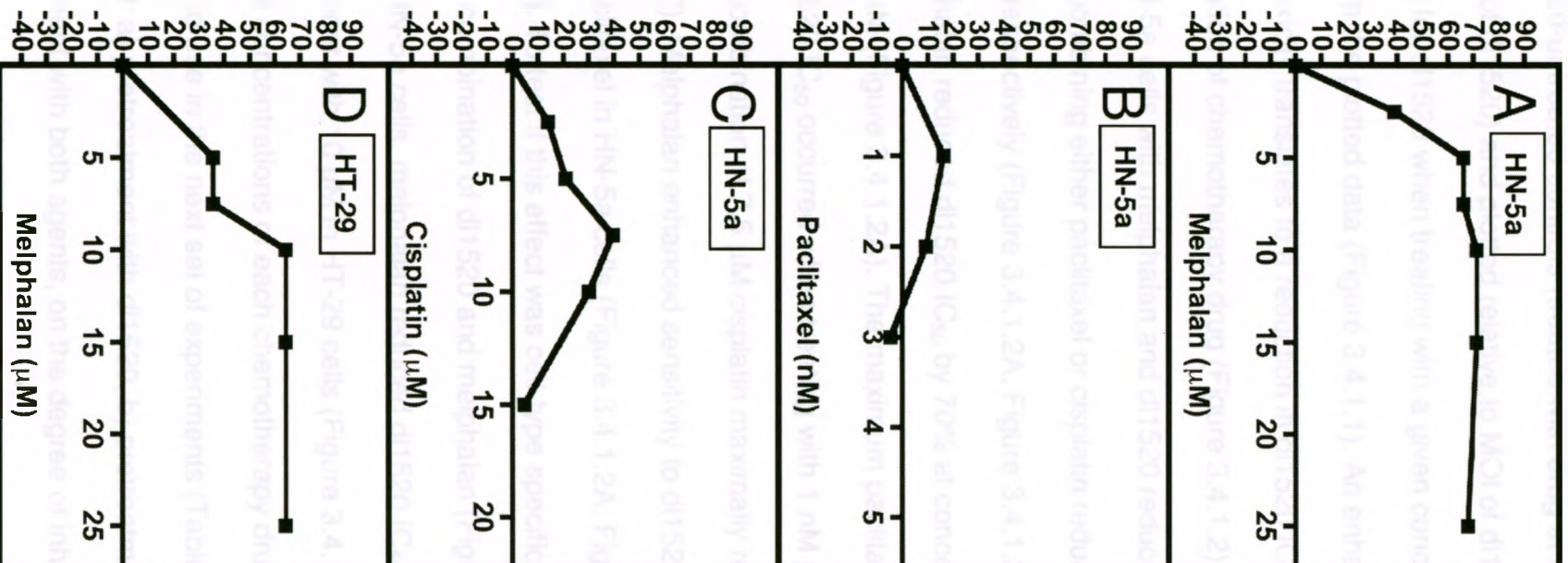


Figure 3.4.1.2. Chemotherapy-mediated change in sensitivity to dl1520.

Cells were treated as described in *Materials and Methods* (Section 2.5.2, p. 45) and analyzed as described in the legend of Figure 3.4.1.2 (p. 88). The chemotherapy-induced percent reduction in the dl1520 IC₅₀ values is plotted vs. drug concentration. This experiment was performed once.

Chemotherapy-induced increase in sensitivity to dl1520
 (% reduction in dl1520 IC₅₀)



respective dl1520-untreated controls (treated with drug at a given concentration in the absence of dl1520) and plotted relative to MOI of dl1520 (Figure 3.4.1.1). The IC_{50} values for dl1520 when treating with a given concentration of drug were interpolated from the plotted data (Figure 3.4.1.1). An enhancement of dl1520-mediated cytotoxicity translates to a reduction in dl1520 IC_{50} when cultured with a given concentration of chemotherapy drug (Figure 3.4.1.2). The combined treatment of HN-5a cells with melphalan and dl1520 reduced dl1520 IC_{50} by up to 70%, whereas combining either paclitaxel or cisplatin reduced dl1520 IC_{50} by 20% and 40%, respectively (Figure 3.4.1.2A, Figure 3.4.1.2B and Figure 3.4.1.2C). Melphalan reduced dl1520 IC_{50} by 70% at concentrations greater than or equal to 7.5 μ M (Figure 3.4.1.2A). The maximum paclitaxel-mediated reduction in dl1520 IC_{50} occurred when treating with 1 nM paclitaxel (Figure 3.4.1.2B). The combination of 7.5 μ M cisplatin maximally reduced the dl1520 IC_{50} (Figure 3.4.1.2C). Melphalan enhanced sensitivity to dl1520 better than both cisplatin and paclitaxel in HN-5a cells (Figure 3.4.1.2A, Figure 3.4.1.2B and Figure 3.4.1.2C). To test if this effect was cell-type specific, HT-29 cells were treated with the combination of dl1520 and melphalan (Figure 3.4.1.2D). Similar to the result in HN-5a cells, melphalan reduced dl1520 IC_{50} by a maximum of 80% after treatment with 10 μ M in HT-29 cells (Figure 3.4.1.2A and Figure 3.4.1.2D). Three concentrations of each chemotherapy drug were chosen from this experiment to use in the next set of experiments (Table 3.4.1) to assess the consequence of: a) pretreatment with dl1520, b) pretreatment with drug, and c) combined treatment with both agents, on the degree of inhibition of proliferation

Table 3.4.1. Concentrations of melphalan, paclitaxel, and cisplatin used to investigate how different treatment schedules affect drug-mediated changes in dl1520 sensitivity of 4 human tumour cell lines.

ND are values that were "not determined".

Cell Line	Chemotherapy drugs		
	Melphalan (μM)	Paclitaxel (nM)	Cisplatin (μM)
HN-5a	2.5, 5, 7.5	1, 2, 3	2.5, 5, 7.5
HN-5a/carbo-15a	2.5, 5, 7.5	ND	ND
HT-29	5, 10, 15	ND	ND
HT-29/carbo-15d-1	5, 10, 15	ND	ND

of human tumour cells. Carboplatin-resistant variants of these cell lines were treated with the same concentrations of drug as their parental cell lines (Table 3.4.1).

3.4.2. *Different treatment schedules for treatment of HN-5a cells with dl1520 and chemotherapy*

To determine how pretreatment of cells with chemotherapy drug followed by dl1520, pretreatment with dl1520 followed by drug, and cotreatment with both agents differ in their capacity to inhibit tumour cell proliferation, cells were treated with: a) 24 h drug pretreatment followed by 72 h of combined treatment, b) 24 h dl1520 pretreatment followed by 72 h combined treatment, and c) 96 h cotreatment. Combining dl1520 with melphalan reduced the dl1520 IC_{50} in HN-5a cells by a maximum of approximately 65% (Figure 3.4.2A). Cotreatment reduced the dl1520 IC_{50} more effectively than dl1520 pretreatment at all concentrations of melphalan (Figure 3.4.2A). Melphalan pretreatment (2.5 μ M) did not decrease dl1520 IC_{50} whereas concentrations greater than or equal to 5 μ M decreased dl1520 IC_{50} to values comparable to those observed after cotreatment (Figure 3.4.2A). Regardless of the treatment schedule, the melphalan-mediated reduction in dl1520 IC_{50} began to plateau at concentrations of melphalan greater than 5 μ M (Figure 3.4.2A). Combined treatment of HN-5a cells with dl1520 and paclitaxel did not reduce the dl1520 IC_{50} at any of the concentrations assayed (Figure 3.4.2B). Moreover, there was no difference in dl1520 IC_{50} induced by paclitaxel between any of the treatment schedules (Figure 3.4.2B). Combining

Figure 3.4.2. Scheduled treatment of HN-5a cells with different chemotherapeutic agents in combination with dl1520.

HN-5a cells were infected with various concentrations of dl1520 and either:

- (A) melphalan,
- (B) paclitaxel, or
- (C) cisplatin

for 96 h as described in *Materials and Methods* (Section 2.5.2, p. 45). Treatments consisted of:

cotreatment: 96 h cotreatment with both drug and dl1520 (—■—)

drug pretreatment: 24 h drug treatment followed by 72 h cotreatment (—◆—)

dl1520 pretreatment: 24 h dl1520 treatment followed by 72 h cotreatment (—▲—)

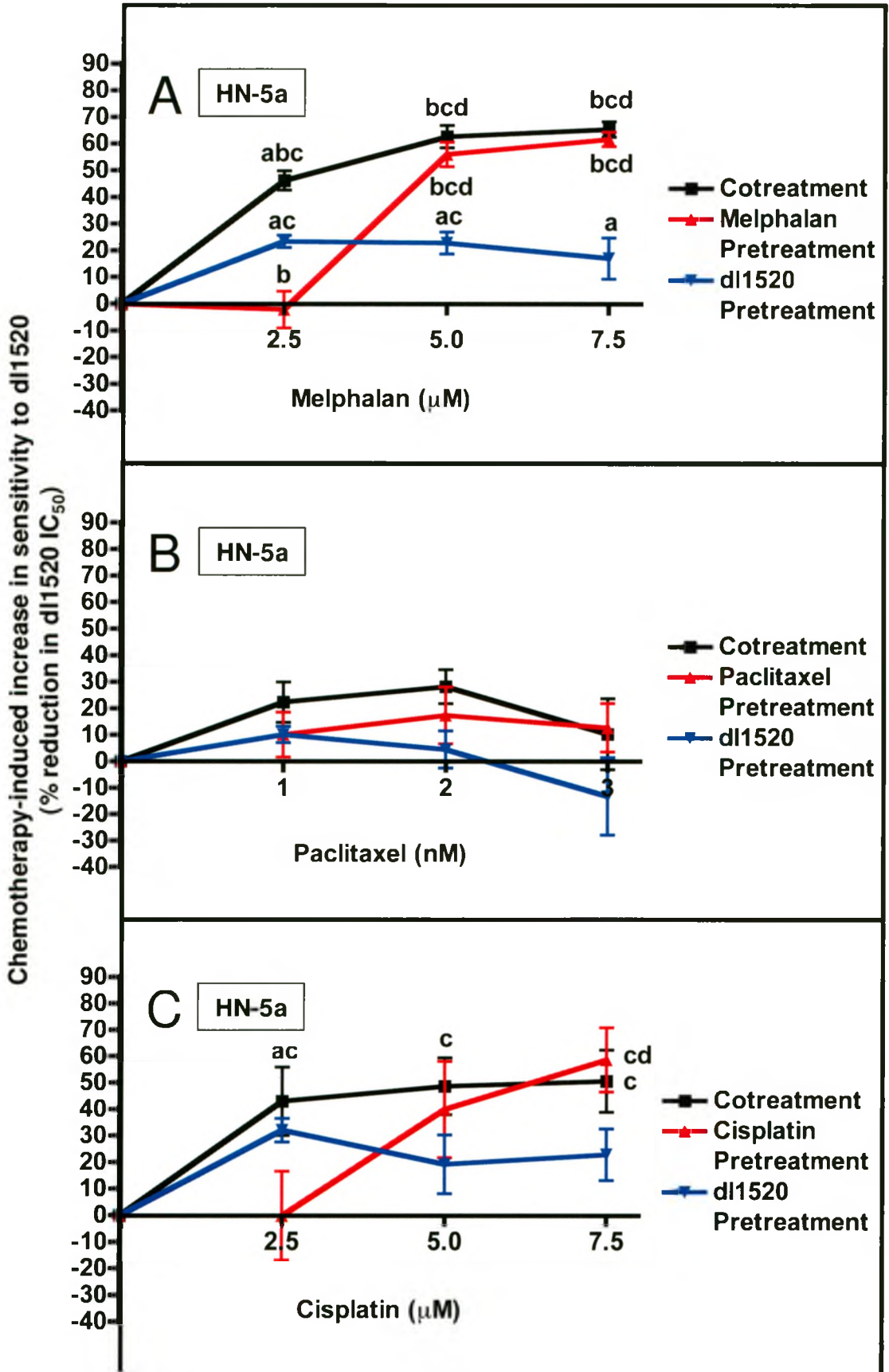
Proliferation after the various treatments was determined using an alamarBlue™ assay as described in *Materials and Methods* (Section 2.4.1, p. 43). Drug-mediated changes in dl1520 sensitivity (% reduction in dl1520 IC₅₀ relative to a drug-untreated dl1520-treated control) are plotted against various concentrations of drug. The means of 4 separate experiments ± SEM are plotted for each drug.

^a different from pretreatment with the same concentration of drug (Two-Way ANOVA, $p < 0.05$).

^b different from pretreatment with dl1520 followed by the same concentration of drug (Two-Way ANOVA, $p < 0.05$).

^c different from zero drug concentration within the same treatment schedule (One-Way ANOVA, $p < 0.05$).

^d different from treatment with the lowest drug concentration within the same treatment schedule (One-Way ANOVA, $p < 0.05$).



dl1520 and cisplatin in HN-5a cells decreased the dl1520 IC_{50} by a maximum of 59% (Figure 3.4.2C). Cotreatment of HN-5a cells with cisplatin (2.5 μ M) and dl1520 was the only treatment schedule that decreased dl1520 IC_{50} more effectively than the 2 alternative treatment schedules that included cisplatin (Figure 3.4.2C). Cotreatment at all cisplatin concentrations decreased dl1520 IC_{50} whereas pretreatment with cisplatin at only one concentration (7.5 μ M) decreased dl1520 IC_{50} (Figure 3.4.2C). Pretreatment with dl1520 did not reduce dl1520 IC_{50} at any concentration of cisplatin (Figure 3.4.2C). In summary, melphalan reduced the dl1520 IC_{50} better than either paclitaxel or cisplatin (Figure 3.4.2).

To determine if melphalan treatment had the same effect in other cell lines, HT-29 and two carboplatin-resistant lines (HN-5a/carbo-15a and HT-29/carbo-15d-1) were assayed for melphalan-mediated changes in dl1520 IC_{50} as described above. Melphalan reduced the dl1520 IC_{50} by a maximum 72% in HT-29 cells (Figure 3.4.3A). Cotreatment of melphalan and dl1520 reduced the dl1520 IC_{50} better than either melphalan pretreatment (all melphalan concentrations) or dl1520 pretreatment (all concentrations of melphalan, with the exception of 2.5 μ M) (Figure 3.4.3A). Pretreatment with dl1520 decreased the dl1520 IC_{50} in HT-29 cells to a greater degree than melphalan pretreatment at concentrations of melphalan below 10 μ M (Figure 3.4.3A). Melphalan pretreatment at 15 μ M decrease the dl1520 IC_{50} (Figure 3.4.3A). Both cotreatment (melphalan and dl1520) and dl1520 pretreatment reduced the dl1520 IC_{50} at all concentrations, although the increase in dl1520-mediated

Figure 3.4.3. Scheduled treatment of HT-29, HT-29/carbo-15d-1 and HN-5a/carbo-15a cells with melphalan in combination with dl1520.

(A) HT-29,

(B) HT-29/carbo-15d-1, or

(C) HN-5a/carbo-15a

for 96 h as described in *Materials and Methods* (Section 2.5.2, p. 45). Treatments consisted of:

cotreatment: 96 h cotreatment with both drug and dl1520 ()

drug pretreatment: 24 h drug treatment followed by 72 h cotreatment ()

dl1520 pretreatment: 24 h dl1520 treatment followed by 72 h cotreatment ()

Proliferation after the various treatments was determined using a colourimetric-based cell viability assay as described in *Materials and Methods* (Section 2.4, p. 43). Drug-mediated changes in dl1520 sensitivity (% reduction in dl1520 IC₅₀ relative to a drug-untreated dl1520-treated control) are plotted against various concentrations of drug. The means of 4 separate experiments \pm SEM are plotted for each drug.

^a different from pretreatment with the same concentration of drug (Two-Way ANOVA, $p < 0.05$).

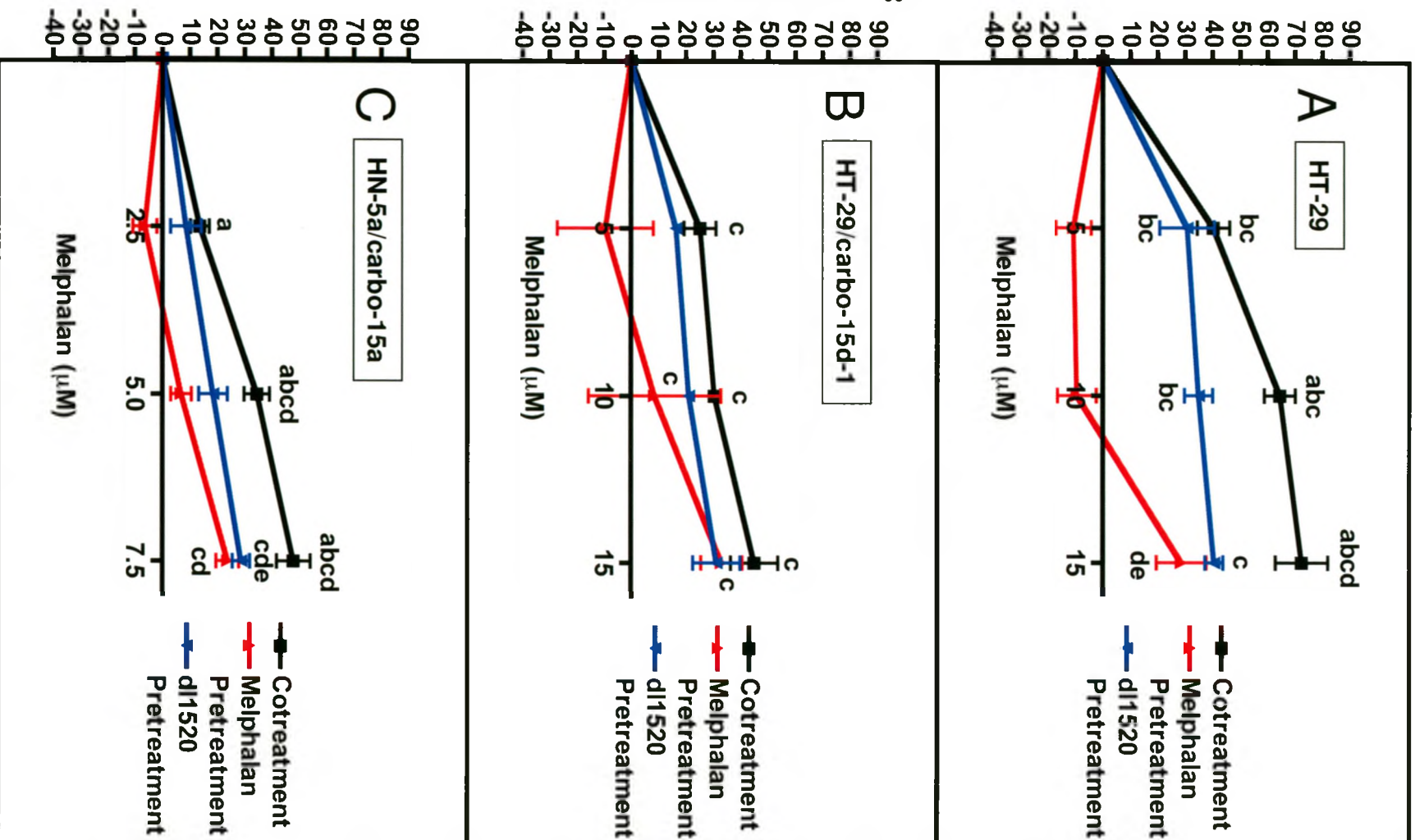
^b different from pretreatment with dl1520 followed by the same concentration of drug (Two-Way ANOVA, $p < 0.05$).

^c different from zero drug concentration within the same treatment schedule (One-Way ANOVA, $p < 0.05$).

^d different than treatment with the lowest drug concentration within the same treatment schedule (One-Way ANOVA, $p < 0.05$).

^e different from intermediate drug concentration within the same treatment schedule (One-Way ANOVA, $p < 0.05$).

Chemotherapy-induced increase in sensitivity to dl1520
 (% reduction in dl1520 IC₅₀)



effects reached a plateau at 10 μM or greater (Figure 3.4.3A). Cotreatment of HT-29/carbo-15d-1 with melphalan and dl1520 reduced dl1520 IC_{50} by a maximum of 45% (Figure 3.4.3B). Cotreatment with all concentrations of melphalan reduced the dl1520 IC_{50} , while dl1520 pretreatment only reduced dl1520 IC_{50} at concentrations of 10 μM or higher (Figure 3.4.3B). Melphalan pretreatment of this cell line did not reduce the dl1520 IC_{50} (Figure 3.4.3B). There was no observed difference between any of the treatment schedules (Figure 3.4.3B). Cotreatment of HN-5a/carbo-15a cells with concentrations of melphalan greater than 5 μM reduced the dl1520 IC_{50} more effectively than after pretreatment with melphalan or pretreatment with dl1520 (Figure 3.4.3C). The maximum reduction in the dl1520 IC_{50} was observed after cotreatment with 5 μM or 7.5 μM melphalan (Figure 3.4.3C).

3.5. Melphalan-mediated changes in CAR levels

The oncolytic virus dl1520 binds CAR as the primary receptor for internalization of target cells [46,47]. It was hypothesized that melphalan enhanced sensitivity of HN-5a cells to dl1520 (Figure 3.4.2A) through an up-regulation of cellular CAR levels.

3.5.1. Melphalan-mediated changes in CAR mRNA levels

CAR mRNA levels in HN-5a cells following a 24-h melphalan treatment were assayed using semi-quantitative RT-PCR (Figure 3.5.1A). Densitometric analysis revealed that CAR mRNA levels were greater after treatment with 50 μM

Figure 3.5.1. CAR mRNA levels in HN-5a cells after 24 h exposure to melphalan.

HN-5a cells were exposed to melphalan at the indicated concentrations for 24 h as described in *Materials and Methods* (Section 2.5.3, p. 51). Following treatment RNA was isolated and both CAR and GAPDH mRNA were amplified and visualized by gel electrophoresis as described in *Materials and Methods* (Section 2.6, p. 52).

(A) A representative gel illustrating both CAR mRNA and GAPDH mRNA from a single experiment.

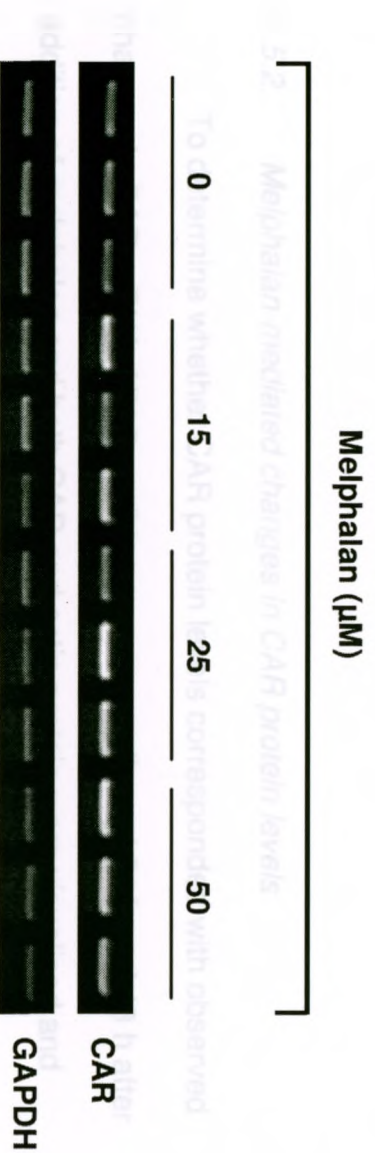
(B) Densitometric quantifications of CAR mRNA were normalized to the GAPDH mRNA control and then plotted relative to the melphalan-untreated control. The means of 3 separate experiments (n=3 for each experiment) \pm SEM are plotted.

^a different from drug-untreated control cells (One-Way ANOVA, $p < 0.05$).

^b different from 15 μ M melphalan (One-Way ANOVA, $p < 0.05$).

A

Analysis for 24 h compared to both a drug-untreated control and 15 μM melphalan treated cells (Figure 2.5.1B).



measured by immunoblotting. There was no change in CAR protein levels.

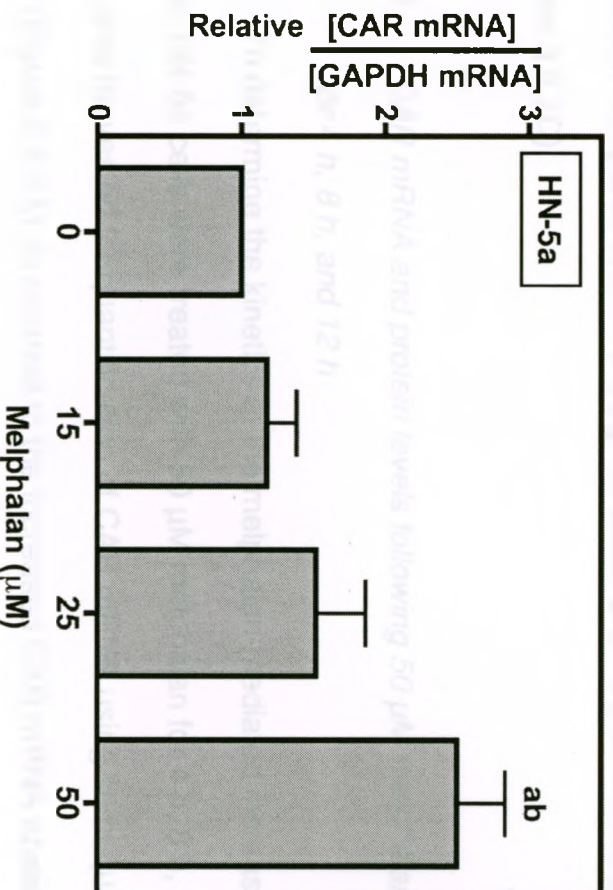
relative to actin control protein, after a 24 h exposure to 15 μM , 25 μM , and 50

μM melphalan in a 24 h treatment course (Figure 2.5.2B). Protein levels were

B

measured by immunoblotting. There was no change in CAR protein levels

relative to GAPDH. CAR protein levels were stable after treatment with 15 μM



melphalan for 24 h compared to both a drug-untreated control and 15 μM melphalan treated cells (Figure 3.5.1B).

3.5.2. *Melphalan-mediated changes in CAR protein levels*

To determine whether CAR protein levels corresponded with observed changes in CAR mRNA, HN-5a cell lysates were collected 24 h and 48 h after addition of melphalan and both CAR and actin protein were visualized and measured by immunoblotting. There was no change in CAR protein levels, relative to actin control protein, after a 24 h exposure to 15 μM , 25 μM , and 50 μM compared to a drug-untreated control (Figure 3.5.2B). However, the 48-h, 50 μM melphalan treatment resulted in elevated CAR protein levels (Figure 3.5.2C). Similar to mRNA, CAR protein levels were greater after treatment with 50 μM melphalan compared to both a drug-untreated and 15 μM melphalan treated cells (Figure 3.5.2D).

3.5.3. *CAR mRNA and protein levels following 50 μM melphalan treatment for 4 h, 8 h, and 12 h*

To determine the kinetics of the melphalan-mediated increase in CAR levels, HN-5a cells were treated with 50 μM melphalan for 4 h, 8 h, and 12 h, and RNA was harvested for quantification of CAR mRNA using semi-quantitative RT-PCR (Figure 3.5.3A). In contrast to the increased CAR mRNA observed at 24 h, there was no change in CAR mRNA levels after treatment with 50 μM melphalan for up to 12 h (Figure 3.5.3B). Following drug treatment (4 h, 8 h,

Figure 3.5.2. CAR protein levels in HN-5a cells after 24 h and 48 h exposure to melphalan.

HN-5a cells were exposed to melphalan at the indicated concentrations for

(A,B) 24 h, or

(C,D) 48 h

as described in *Materials and Methods* (Section 2.5.3, p. 51). Following treatment, total cellular protein was isolated and both CAR and actin protein were visualized by SDS-PAGE and immunoblotting as described in *Materials and Methods* (section 2.7, p. 58).

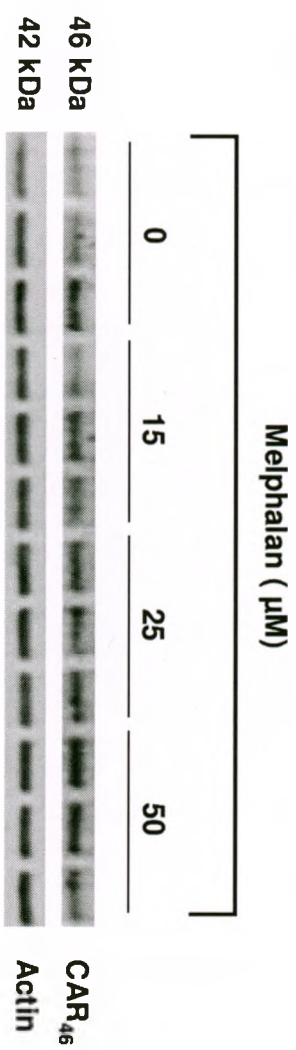
(A,C) A representative immunoblots illustrating both CAR₄₆ and actin protein expression from a single experiment.

(B,D) Densitometric quantifications of CAR₄₆ protein were normalized to their respective actin protein controls and then graphed relative to the melphalan-untreated control. Mean relative CAR protein levels (B: from 4 separate experiments; D: 5 separate experiments; n=3 for each experiment) ± SEM are plotted.

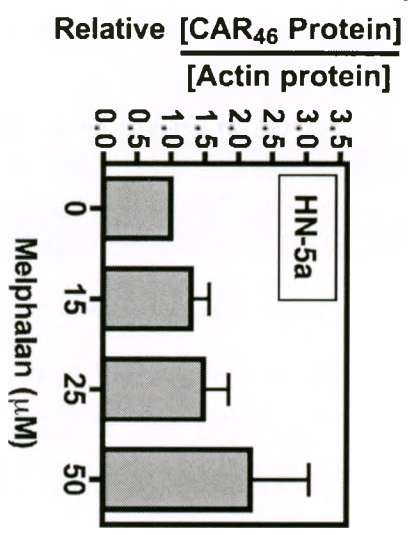
^a different from drug-untreated control cells (One-Way ANOVA, p<0.05).

^b different from 15 μM melphalan (One-Way ANOVA, p<0.05).

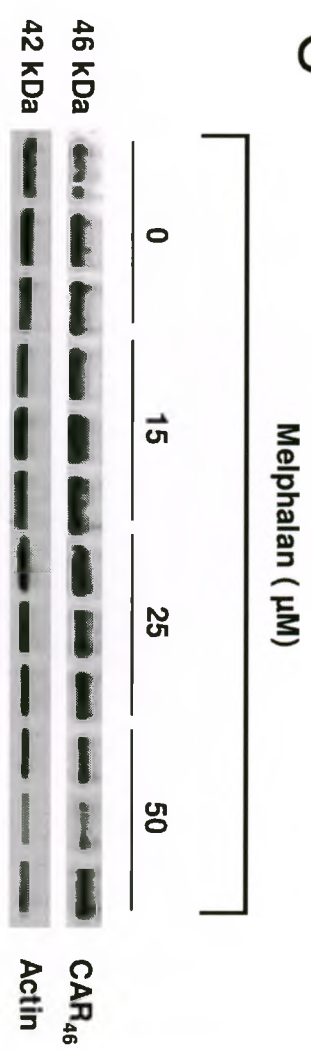
A



B



C



D

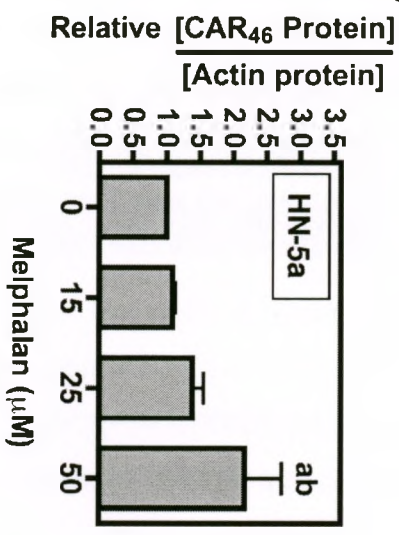


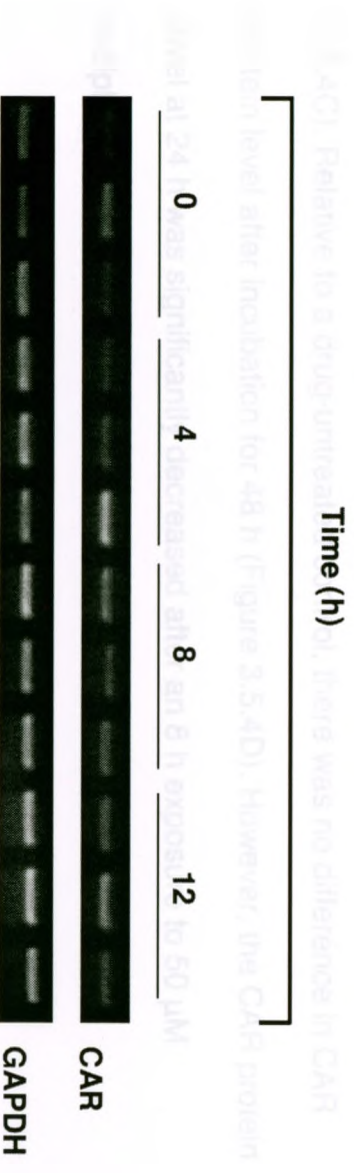
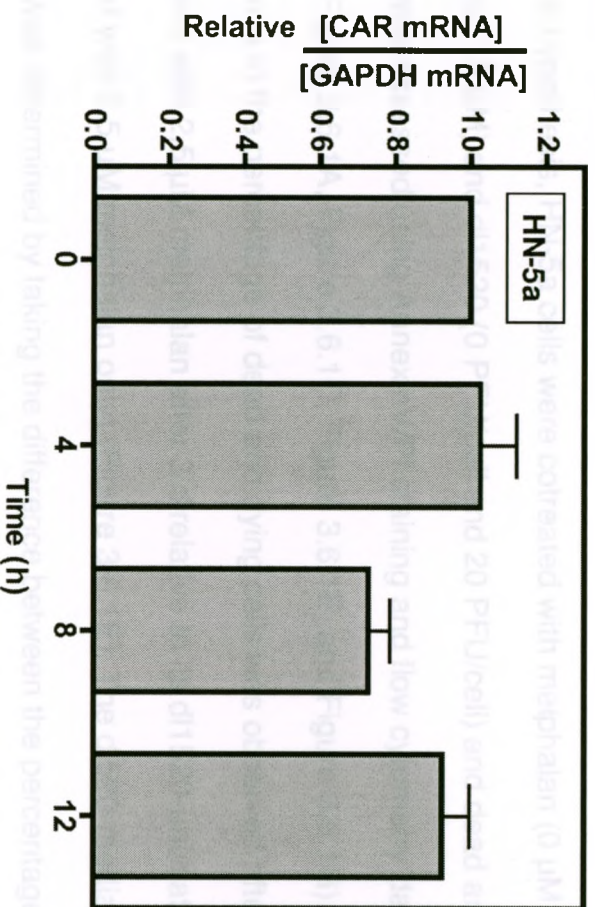
Figure 3.5.3. CAR mRNA levels in HN-5a cells after 4 h, 8 h, and 12 h exposure to 50 μ M melphalan.

HN-5a cells were exposed to 50 μ M melphalan for the indicated times as described in *Materials and Methods* (Section 2.5.4, p. 51). Following treatment RNA was isolated and both CAR and GAPDH mRNA were amplified and visualized by gel electrophoresis as described in *Materials and Methods* (Section 2.6, p. 52).

(A) A representative gel illustrating both CAR mRNA and GAPDH mRNA from a single experiment.

(B) Densitometric quantification of CAR mRNA were normalized to the GAPDH mRNA control and then graphed relative to the melphalan-untreated control. The mean relative CAR mRNA levels from 3 separate experiments (n=3 for each experiment) \pm SEM are plotted.

There were no differences in CAR mRNA expression (One-Way ANOVA, $p < 0.05$).

A**B**

and 12 h) drug was removed and cells were cultured for a total of 24 or 48 h and harvested for immunoblots of CAR protein levels (Figure 3.5.4A and Figure 3.5.4C). Relative to a drug-untreated control, there was no difference in CAR protein level after incubation for 48 h (Figure 3.5.4D). However, the CAR protein level at 24 h was significantly decreased after an 8 h exposure to 50 μ M melphalan (Figure 3.5.4B).

3.6. Greater-than-additive cell death after combined treatment with dl1520 and melphalan

The capacity of melphalan to enhance sensitivity of human tumour cells (Figure 3.4.2A and Figure 3.4.3) to dl1520 was hypothesized to be due to increased cell death after combined treatment with dl1520 and melphalan. To test this hypothesis, HN-5a cells were cotreated with melphalan (0 μ M, 2.5 μ M, 5 μ M, and 7.5 μ M) and dl1520 (0 PFU/cell and 20 PFU/cell) and dead and dying cells were assessed using AnnexinV/PI staining and flow cytometry daily for four days (Figure 3.6.1A, Figure 3.6.1C, Figure 3.6.1E, and Figure 3.6.1G). The only difference in the percentage of dead and dying cells was observed after treatment with 2.5 μ M melphalan after 3 d relative to its dl1520-untreated control (treated with 2.5 μ M melphalan only) (Figure 3.6.1E). The dl1520-mediated cell death was determined by taking the difference between the percentage of dead and dying cells treated with dl1520/melphalan and the percentage of dead and dying cells treated with melphalan-only (Figure 3.6.1B, Figure 3.6.1D, Figure 3.6.1F, and Figure 3.6.1H). There is a reduction the percentage of dl1520-

Figure 3.5.4. CAR protein levels in HN-5a cells after 4 h, 8 h, and 12 h exposure to 50 μ M melphalan.

HN-5a cells were exposed to 50 μ M melphalan for the indicated times as described in *Materials and Methods* (Section 2.5.4, p. 51). Following treatment, total cellular protein was isolated and both CAR and actin protein was visualized by SDS-PAGE and immunoblotting as described in *Materials and Methods* (Section 2.7, p. 58).

(A,C) Representative immunoblots illustrating both CAR₄₆ and actin protein expression 24 h and 48 h following the addition of drug from a single experiment.

(B,D) Densitometric quantification of CAR protein were normalized to their respective actin protein controls and then graphed relative to the melphalan-untreated control. Mean relative CAR protein levels (B: from 4 separate experiments; D: 5 separate experiments; n=3 for each experiment) \pm SEM are plotted.

^a different from drug-untreated control cells (One-Way ANOVA, $p < 0.05$).

^b different from 15 μ M melphalan (One-Way ANOVA, $p < 0.05$).

^c different from 50 μ M melphalan (One-Way ANOVA, $p < 0.05$).

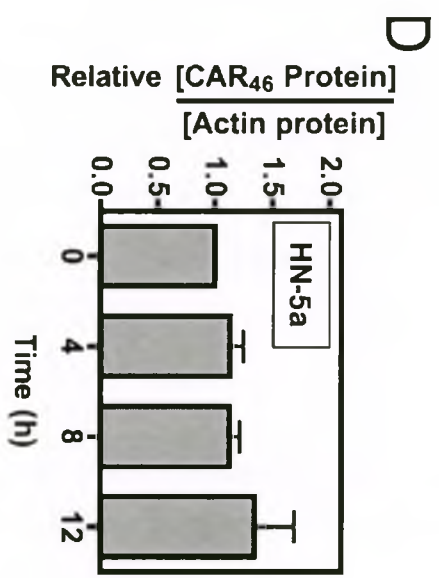
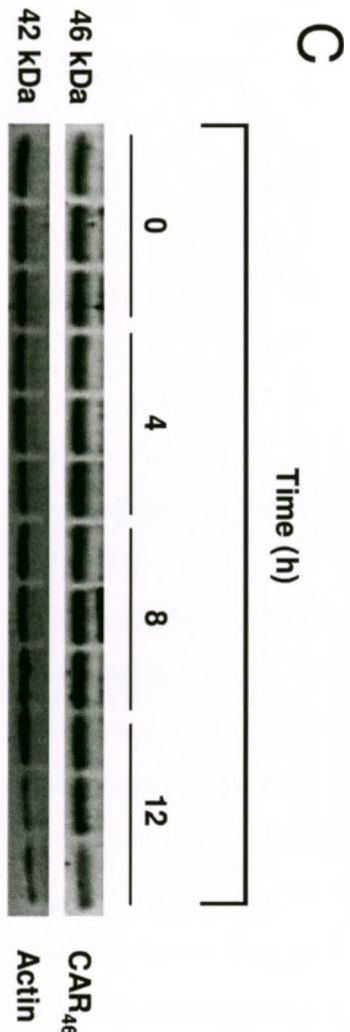
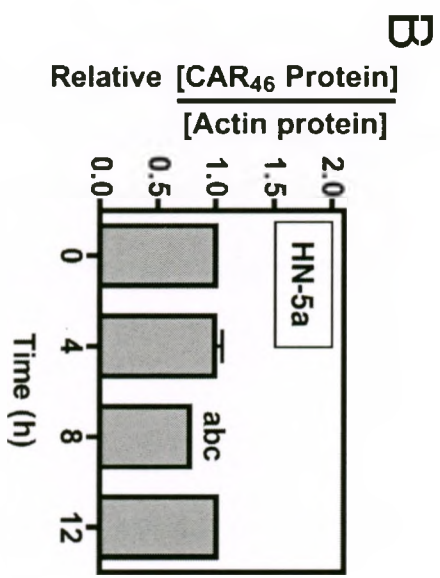
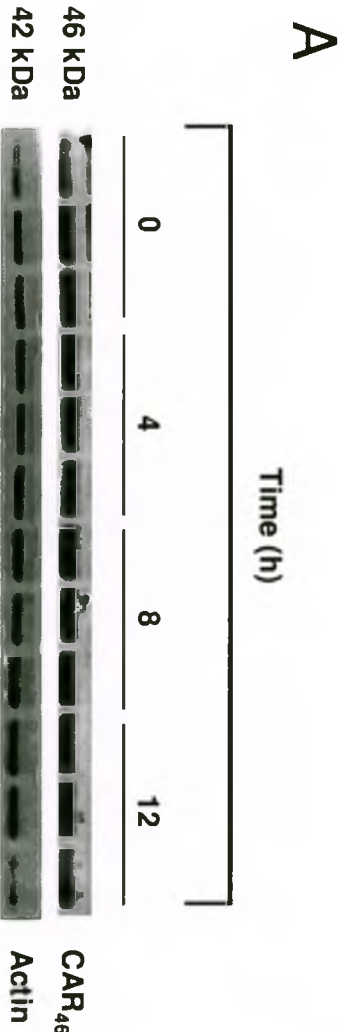


Figure 3.6.1. HN-5a cell death following combined treatment with dl1520 and melphalan.

HN-5a cells were infected with the indicated concentrations of dl1520 and/or melphalan and assayed for cell death at:

(A,B) 1 d,

(C,D) 2 d,

(E,F) 3 d, and

(G,H) 4 d

following treatment as described in *Materials and Methods* (Section 2.8, p. 60).

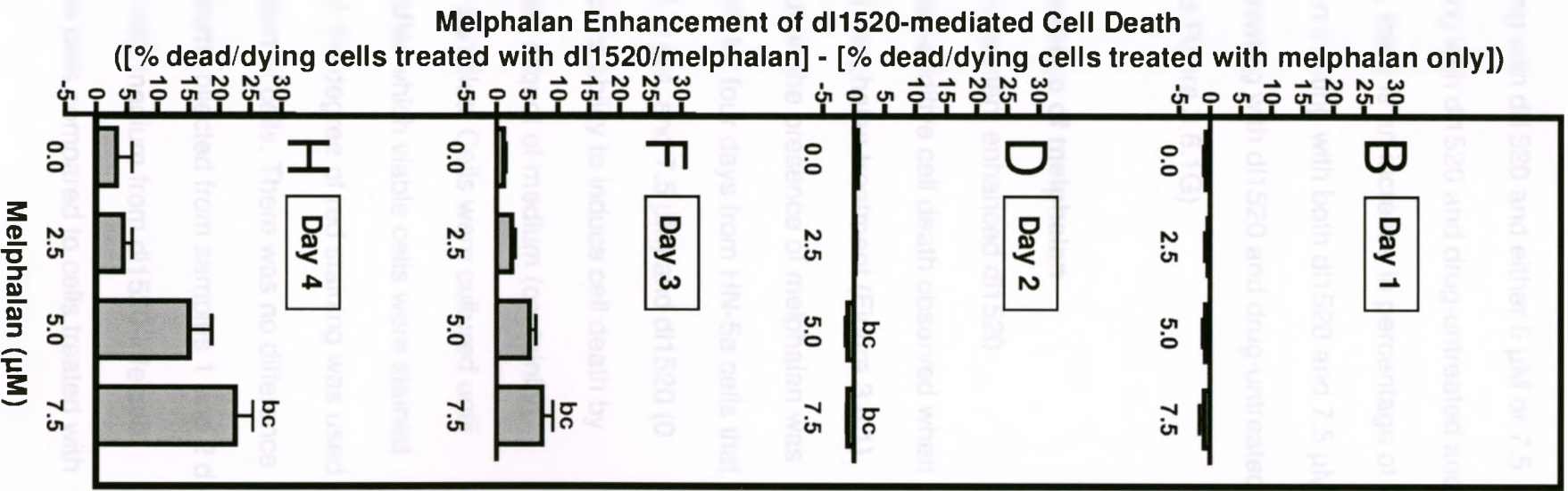
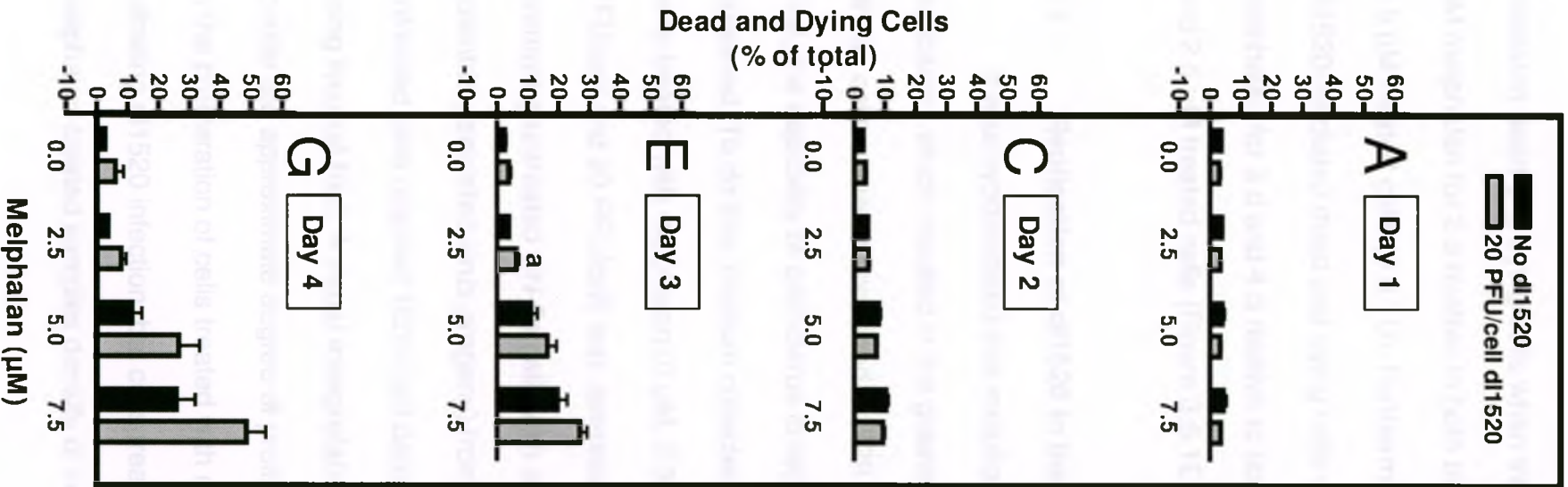
(A,C,E,G) The mean number of dead and dying cells as a percentage of the total cell number is plotted as the means derived from 3 separate experiments (n=3 for each experiment).

^a different from respective dl1520-untreated control (melphalan-treated, dl1520-untreated) (Student's *t*-test, $p < 0.05$).

(B,D,F,H) Melphalan enhancement of dl1520-mediated cell death determined for each concentration of melphalan by subtracting the percentage of dead and dying cells treated with melphalan from cells treated with dl1520 (MOI of 20) and melphalan. The mean differences from 3 separate experiments (n=3 for each experiment), are plotted.

^b different from respective melphalan-untreated cells for a given time point (One-Way ANOVA, $p < 0.05$).

^c different from respective 2.5 μ M melphalan treated cells for a given time point (One-Way ANOVA, $p < 0.05$).



mediated dead and dying cells when treating with dl1520 and either 5 μM or 7.5 μM melphalan for 2 d relative to both treating with dl1520 and drug-untreated and 2.5 μM treated cells (3.6.1D). Furthermore, there is an increase in percentage of dl1520-mediated dead and dying cells when treating with both dl1520 and 7.5 μM melphalan for 3 d and 4 d relative to both treating with dl1520 and drug-untreated and 2.5 μM treated cells (Figure 3.6.1E and Figure 3.6.1G).

3.7. Replication of dl1520 in the presence of melphalan

It was hypothesized that melphalan treatment enhanced dl1520 replication, which resulted in the greater-than-additive cell death observed when HN-5a cells received combined dl1520 and melphalan treatment (Figure 3.6.1). First, the capability of adenovirus to replicate in the presence of melphalan was assessed. To do this, medium collected daily for four days from HN-5a cells that were treated with melphalan (0 μM , 2.5 μM , 5 μM , and 7.5 μM) and dl1520 (0 PFU/cell and 20 PFU/cell) was assessed for its ability to induce cell death by overlaying untreated HN-5a cells with a small aliquot of medium (containing potentially secreted virus progeny) from all samples. Cells were cultured until untreated cells reached 100% cell density after which viable cells were stained using Neutral Red. A visual interpretation of the degree of red staining was used to infer the approximate degree of proliferation of cells. There was no difference in the proliferation of cells treated with medium collected from samples 1 and 2 d following dl1520 infection, but cells treated with medium from dl1520-infected melphalan-treated samples density of viable cells compared to cells treated with

medium harvested from their respective dl1520-untreated controls (melphalan treated only) indicating the potential presence of viable virus (Figure 3.7.1A). A burst assay (described in *Materials and Methods, Section 2.9, p. 61*) was used to identify potential changes in adenovirus replication in the presence of melphalan. There was no difference in the replication of dl1520 in the presence of any of the concentrations of melphalan assessed (2.5 μ M, 5 μ M, and 7.5 μ M) compared to the melphalan-untreated control (treated with dl1520 in the absence of melphalan) (Figure 3.7.1B).

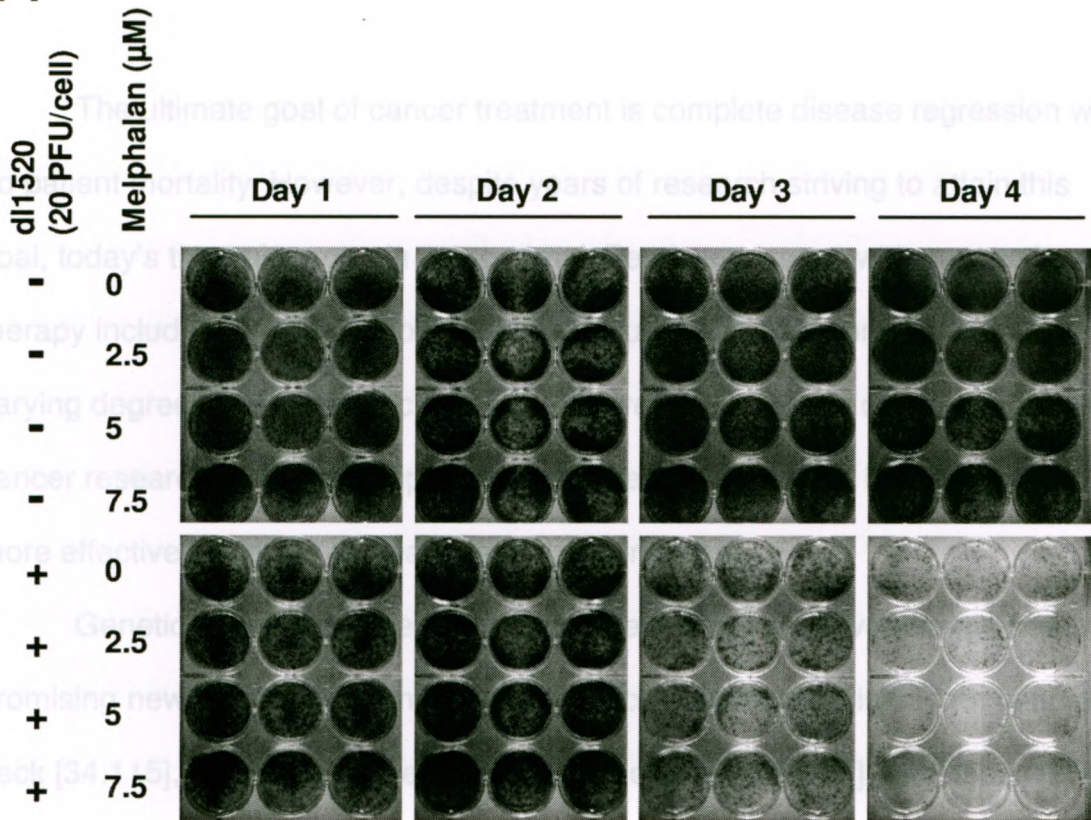
Figure 3.7.1. dl1520 replication in the presence of melphalan.

(A) HN-5a cells were infected with the indicated concentrations of dl1520 and/or melphalan as described in *Materials and Methods* (Section 2.8, p. 60). An aliquot of medium, containing both dead/dying cells and potentially any viral progeny, was removed and used to treat new cells every 24 h for a total of 96 h. These cells were then cultured for 6 d to allow for the control to reach 100% cell density. At the end of 6 days, viable cells were stained with Neutral Red and plates were photographed. This experiment was performed once. Medium from dl1520-infected cells can induce cell death.

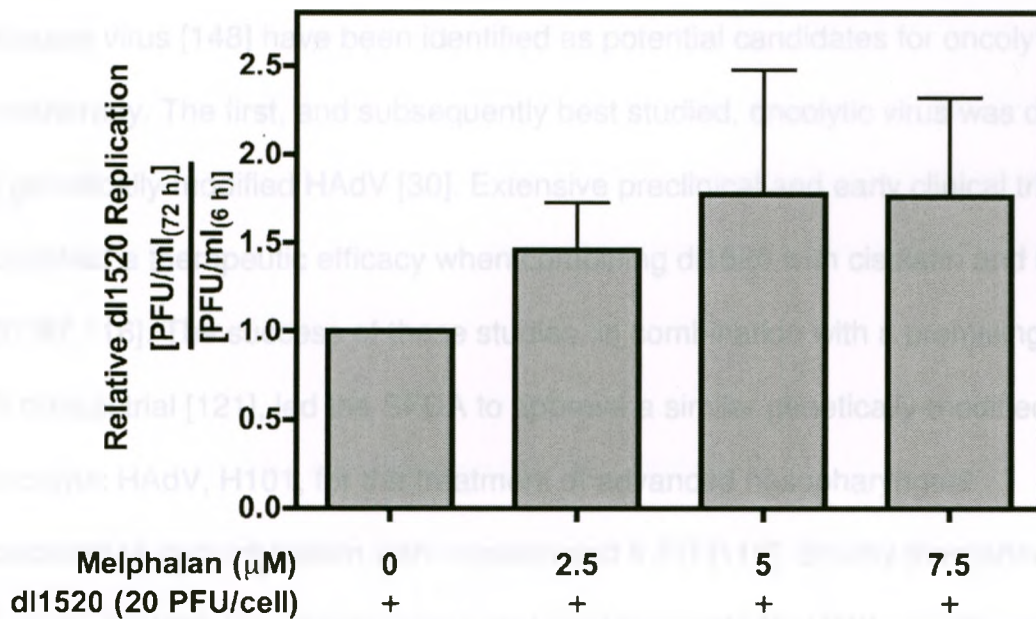
(B) HN-5a cells were infected with the indicated concentrations of dl1520 and/or melphalan and assayed for dl1520 replication as described in *Materials and Methods* (Section 2.9, p. 61). Titration of dl1520 samples isolated after a 72 h infection was normalized to the average titration established from samples at 6 h. The means from 3 experiments (n=3 for each experiment) were normalized to their respective melphalan-untreated controls and plotted \pm SEM.

There were no significant differences in dl1520 replication (One-Way ANOVA, $p < 0.05$).

A



B



CHAPTER 4: DISCUSSION

The ultimate goal of cancer treatment is complete disease regression with no patient mortality. However, despite years of research striving to attain this goal, today's therapies remain sub-optimal. Persistent issues with conventional therapy include non-specific toxicities that influence patient compliance and varying degrees of therapeutic efficacy. As a result, there is a continued effort by cancer researchers to both improve current treatments and to identify novel, more effective therapies to treat this devastating disease.

Genetically-modified, replication-competent viruses have emerged as a promising new treatment for many cancers including, but not limited to, head and neck [34,115], lung [99], colorectal [36,104], cervical [101,102], pancreatic [35], and liver [111] cancers. Several viruses including: HAdV [30], herpes simplex virus type 1 [145], vesicular stomatitis virus [146], reovirus [147], and Newcastle disease virus [148] have been identified as potential candidates for oncolytic virotherapy. The first, and subsequently best studied, oncolytic virus was dl1520, a genetically-modified HAdV [30]. Extensive preclinical and early clinical trials identified a therapeutic efficacy when combining dl1520 with cisplatin and 5-FU [37,97,116]. The success of these studies, in combination with a promising phase III clinical trial [121], led the SFDA to approve a similar genetically-modified oncolytic HAdV, H101, for the treatment of advanced nasopharyngeal carcinomas in combination with cisplatin and 5-FU [118]. Shortly thereafter, Sunway Biotech Inc., the company that held the rights for H101, purchased the

international rights to dl1520 from Onyx Pharmaceuticals Inc., with hopes of pursuing development in other markets [122,123].

Clearly, the therapeutic potential of combining dl1520 with cisplatin and 5-FU has been realized. However, there are several fundamental gaps in our understanding of how treatment with chemotherapy and dl1520 enhanced therapeutic benefit for the patient when combined, including: a) the mechanistic interaction between chemotherapy and dl1520, b) the optimal treatment schedule for administering each agent, and c) the range of chemotherapy drugs that can be used in combination with dl1520. The present study was an *in vitro* investigation of the potential use of novel chemotherapy combinations (melphalan and paclitaxel) with dl1520 in comparison to an established chemotherapy (cisplatin)-dl1520 combination for the treatment of HNSCC (HN-5a), colon cancer (HT-29), and their carboplatin-resistant variants (HN-5a/carbo-15a and HT-29/carbo-15d-1). Furthermore, the optimal schedule for administering each agent and the potential mechanistic interaction between each agent was investigated. The present study supports melphalan as the optimal candidate for combined therapy with dl1520 that, when combined, elicits greater-than-additive anti-tumour effects *in vitro*. Moreover, a potential CAR-melphalan interaction was identified.

4.1. Generation and titration of a dl1520 stock

A plaque-forming assay using A549 (human lung adenocarcinoma) cells titrated the newly-propagated dl1520 stock to be 2.0×10^9 PFU/ml (Figure

3.1.1A). When this titer was used to set up a comparative cytotoxicity assay against a stock of known concentration, the newly-propagated stock exhibited a comparable inhibition of proliferation at approximately a third the apparent dl1520 concentration (Figure 3.1.1B). Standard plaque assays for E1-mutated HAdV are done using HEK293 (human embryonic kidney) cells due to their expression of E1 HAdV genes [93,135]. The original transformation of HEK293 cells was achieved by introducing sheared HAdV serotype 5 DNA [135]. As a result, HEK293 cells express the left-most region (approximately 0-17 map units) of the HAdV genome containing the E1 genes (Figure 1.3.2.4A) and thus complement the E1-mutant HAdV phenotype [135]. In the present study, titration with HEK293 cells was attempted, although unsuccessfully. Continued non-specific toxicities were observed that could not be associated with the type of medium, type of agarose, temperature of the soft agar at the time of addition to cells, cell density at the time of infection, or the mechanistic act of overlaying cells with soft agar. As a substitute, titration in A549 cells was performed. However, dl1520 replication in A549 cells is approximately 30% that of replication in HEK293 cells [149]. The difference in dl1520 replication between A549 and HEK293 cells could account for the observed difference in cytotoxicity induced by the dl1520 stock titrated in the present study and the stock of a known concentration titrated by Onyx Pharmaceuticals Inc. Taken together with results from the comparative cytotoxicity assay, the working concentration of our newly-propagated dl1520 stock was adjusted to be 6.0×10^9 PFU/ml.

4.2. Human tumour cell lines as targets for dl1520 therapy

4.2.1. *CAR is a glycosylated protein*

Immunoblots for CAR protein resolved two distinct bands (CAR₄₆ and CAR₄₀, respectively) in the human tumour-derived cell lines assayed (Figure 3.2.2 and Figure 3.2.3). These data are consistent with a previous study of CAR protein expression in human cervical cancer cells (HeLa), embryonic kidney (293T), and lung cancer (A549) cell lines [49]. Treatment of protein lysates with PNGase F, an N-glycosidase enzyme, resulted in a reduction in the intensity of CAR₄₆ and a strengthening in CAR₄₀ band intensity (Figure 3.2.2B). These results are consistent with a previously published study that demonstrated that the apparent molecular weight of CAR protein, as determined by its ability to migrate through an SDS-polyacrylamide gel, is dependent on glycosylation of its two extracellular immunoglobulin domains [49]. Based on the amino acid sequence of CAR, the predicted molecular weight is expected to be 40 kDa [47,49,50]. However, the extracellular domain contains two amino acid residues, N106 and N201, which are capable of being N-glycosylated [47,50]. The glycosylation of CAR has been studied using site-directed mutagenesis to generate expression vectors harboring CAR mutants unable to be glycosylated at either a single or both immunoglobulin domains. These were then transfected into Chinese hamster ovary (CHO) cells, a cell line with no basal CAR expression [49]. Glycosylation of each site adds approximately 3 kDa to the observed molecular weight of CAR such that when fully glycosylated, CAR protein migrates

through an SDS-polyacrylamide gel with an apparent molecular weight of approximately 46 kDa.

Protein glycosylation is a form of post-translational modification that affects protein stability, folding and trafficking in the endoplasmic reticulum [150]. Therefore, it is possible that CAR₄₀ represents newly-translated CAR protein prior to post-translational modification. The glycosylation status of CAR protein does not affect its cellular localization, but deglycosylation of CAR has been shown to reduce its cell-cell interactions and augment HAdV infection [49]. However, that study did not identify a mechanism for the augmentation of HAdV infection by the deglycosylated isoforms of CAR. Contrary to their initial finding, they showed that deglycosylation of CAR both reduces the levels of HAdV binding and the degree of cooperative binding between a single HAdV capsid fiber protein and cellular CAR receptors [49]. The present study quantified both CAR₄₆ and CAR₄₀ bands from immunoblots for CAR protein due to the possibility that the deglycosylated isoform has different HAdV binding kinetics.

Differences in the banding intensity of both CAR₄₀ protein and CAR₄₆ protein are observed in the same cell line (Figure 3.2.2A and Figure 3.2.2B). The cell surface expression of CAR inversely correlates with cell density [151]. Therefore, it is possible that total cellular CAR protein levels also share a similar inverse correlation with cell density and that differences in the amount of CAR₄₆ protein and CAR₄₀ protein could be due to differences in cell density at the time of protein isolation.

4.2.2. CAR protein and CAR mRNA levels in human tumour-derived cell lines

The capacity of dl1520 to elicit a therapeutic effect is reliant on its ability to gain entry to the target cells. The binding of dl1520 to CAR, its primary receptor, serves as the rate-limiting step in its internalization [46,47]. All cell lines used in the present study had detectable levels of both CAR mRNA and CAR protein (Figure 3.2.1 and Figure 3.2.3). Moreover, relative CAR mRNA levels between cell lines (Figure 3.2.1) were comparable to the relative levels of CAR protein (Figure 3.2.3). This observation is in agreement with several studies that illustrate CAR mRNA correlates with CAR protein levels [126,152]. The CAR expression in healthy tissues is quite diverse, with detectable levels found in pancreas, brain, heart, small intestine, testis, liver, lung, prostate, colorectum, and esophagus [50,153]. In pathology, a down-regulation in CAR levels has been reported in many advanced, poorly differentiated cancers including HNSCC [154], bladder carcinoma [155], gastric cancer [126], prostate cancer [125], liver and pancreatic cancer [153], and both cervical adenocarcinoma and ovarian carcinoma [156]. In contrast, several studies have identified an up-regulation in CAR levels in both *in vitro* models for advanced breast cancer and in samples isolated from patients with advanced breast cancer [124,127]. Taken together, these studies highlight that the tumour response to changes in CAR levels appears to be cell-type-specific. Efficient adenovirus infection positively correlates with CAR protein levels [157,158], and as a result, tumours expressing high levels of CAR represent potential targets for HAdV-mediated therapies. Therefore, the human

tumour cell lines used in the present study represent potential targets for dl1520-mediated therapy.

4.2.3. Sensitivity of human tumour cell lines to dl1520-mediated inhibition of cellular proliferation

All cell lines were sensitive to dl1520-mediated inhibition of proliferation at the concentrations assayed, with close to 90% inhibition of proliferation in all cell lines after treatment with dl1520 at a MOI of 300 (Figure 3.3.1).

High exposure of the oral epithelia to carcinogens through smoking and alcohol consumption has been associated with over 50% of HNSCC tumours containing non-functional p53 [6]. The HT-29 cell line also possesses non-functional p53 [159]. Therefore, the sensitivity of these cell lines to the E1B-deficient dl1520 is expected because its replication is selective for cells with a non-functional p53 [30]. The observed inhibition of proliferation concurs with previously published findings indicating that HT-29 and several HNSCC-derived cell lines are sensitive to dl1520-induced cytotoxicity [97]. Furthermore, both CAR protein and CAR mRNA levels were higher in several HT-29-derived cell lines than HN-5a-derived cell lines (Figure 3.2.1 and Figure 3.2.3) suggesting higher permissiveness to dl1520 infection. However, there was no difference in the dl1520 IC_{50} values between the parental HN-5a and HT-29 cell lines in the present study (57.46 ± 8.37 and 74.23 ± 18.19 PFU/cell, respectively) (Table 3.3.1). These values are in contrast to previously published IC_{50} values for dl1520 in these cell lines of 21 ± 6 and 262 ± 145 PFU/cell, respectively [110].

These differences may be accounted for by the method used to determine the number of cells present at the time of infection. In the previous study, a cell count was taken of the cell suspension used to plate cells and used as an indicator of cell number at the time of infection. The problem with this method is that cell proliferation occurs from the time cells are plated to the time they are infected (24 h later). In the present study, cell counts were taken from a representative T-25 flask at the time of infection to account for this proliferation. Therefore, the determined dl1520 MOI in the present study are more accurate than previously published data.

In the present study there was no difference in the levels of either CAR mRNA or CAR protein between the parental and any of their drug-resistant variants (Figure 3.2.1 and Figure 3.2.3). A strength of the present study is that all cell lines were treated with the same MOIs of dl1520 in triplicate (and the experiment was repeated three times), allowing for a direct statistical comparison of relative proliferation between cell lines at each MOI of dl1520 (Figure 3.3.1). In agreement with CAR mRNA and CAR protein data, there was no difference in sensitivity to dl1520-mediated inhibition of proliferation between the parental cell lines (HN-5a and HT-29) and their respective carboplatin-resistant variants (HN-5a/carbo-15a and HT-29/carbo-15d-1) (Figure 3.3.1 and Table 3.3.1). This is in contrast to a previous study in our laboratory that identified a 15-fold increase in the sensitivity of HN-5a/carbo-15a cells to dl1520-mediated inhibition of proliferation compared to the parental HN-5a cell line [110]. There is the potential that the difference in sensitivity of the HN-5a/carbo-15a cell line to inhibition of

proliferation induced by dl1520 between the present study and the previous study is due to inherent changes that occur to a cell line when cultured *in vitro* over time [135]. The HN-5a/carbo-15a cell line was selected by culturing the parental HN-5a cell line in the presence of carboplatin as described elsewhere [134]. This cell line was cultured in the presence of 15 μ M carboplatin to maintain the drug-resistant phenotype. However, it is possible that a potential reversion to a drug-naïve phenotype may have occurred after consecutive passages *in vitro*, thus accounting for the differences between the past and present study.

A similar comparison of proliferation after treatment with each MOI of dl1520 between HT-29 cells and HT-29/CP-5c identified the cisplatin-resistant variant to be more sensitive to dl1520-induced inhibition of proliferation after treatment with MOIs of 10, 15, 20, 50, and 125 when compared to the parental HT-29 cell line (Figure 3.3.1B). This is in agreement with previous findings from our lab [110]. These results suggest that the acquisition of cisplatin resistance sensitizes cells to dl1520 anti-proliferative effects. The phenomenon of acquired cisplatin resistance conferring enhanced sensitivity of human tumour cells to dl1520-mediated anti-tumour effects has been observed previously in an ovarian cancer cell line model [97,100,105]. An ovarian carcinoma cell line (A2780) selected for resistance to cisplatin (A2780/cp70) is approximately 100-fold more sensitive to dl1520 than the parental cell line [100]. It was proposed that this enhanced sensitivity is the result of enhanced dl1520 replication in the cisplatin-resistant variant compared to the parental cell line [105]. A common mutation associated with resistance to cisplatin is the inactivation of the p53-mediated

stress response [160,161]. A sequence analysis of the p53 gene locus in A2780/cp70 revealed the sequence to be wild-type [162]. However, it is possible for a cell to have a normal p53 gene sequence but to still harbour a non-functional p53 response due to a dysfunction in another component of the response pathway [161,162]. Thus, it has been postulated that the enhanced replication of dl1520 in this cisplatin-resistant variant is accounted for by a mutation in the p53 pathway [105]. In contrast, the HT-29 parental cell line used in the present study has been shown to contain non-functional p53 [159]. Therefore, it would appear that a mutation in p53 is not the cause of this observed sensitization to dl1520. Enhanced HAdV internalization in the HT-29/CP-5c cell line could account for the observed difference in its sensitivity to dl1520 when compared to the parental HT-29 cell line (Figure 3.3.1). However, there is no difference in CAR levels between HT-29 and cisplatin-resistant HT-29/CP-5c cell lines (Figure 3.2.1 and Figure 3.3.3), suggesting that the increase in viral sensitivity is due to an internal cellular mechanism and not a change in viral infection. These results are in accordance with the observation that there is no change in CAR mRNA expression between a drug-naïve laryngeal carcinoma cell line with a cisplatin-resistant variant [163]. Interestingly, the cisplatin-resistant variant in that study demonstrated an enhanced sensitivity to HAdV infection. The authors suggested that a moderate increase in the levels of CAR protein at the cell surface, independent of the CAR mRNA expression level, might be responsible for the difference in HAdV infection [163]. Indeed, several studies identified that CAR protein cell surface expression positively correlated with

adenovirus infectivity of various cell lines [157,163,164]. The present study cannot rule out the fact that total CAR protein levels may not correlate with cell surface expression of CAR protein. Therefore, future studies need to investigate how cell surface expression of CAR protein in the various cell lines affects sensitivity to dl520 infection.

4.3. Combination of dl1520 with conventional chemotherapy for the treatment of human tumours

4.3.1. Differential effects of combined vs. sequential treatment of human tumour cells with dl1520 and chemotherapeutic drugs

Cisplatin and 5-FU are the only two chemotherapy drugs approved for use with dl1520 in the clinic [118]. However, there is evidence that suggests melphalan has potential for combined therapy with dl1520 [110]. The present study compared the anti-proliferative efficacy of an established dl1520-drug combination (cisplatin) with novel dl1520-drug combinations (melphalan or paclitaxel) shown to have potential *in vitro*. In the present study, melphalan enhanced the dl1520-mediated toxicity better than cisplatin or paclitaxel (Figure 3.4.2). Paclitaxel did not enhance sensitivity to dl1520 at any of the concentrations assayed (Figure 3.4.2B), in contrast to previous reports demonstrating that paclitaxel works synergistically with dl1520 *in vitro* [98,99]. Discrepancies between the current and previous studies may be accounted for due to differences in culture conditions, the origins of the cell lines assayed, and the concentrations of paclitaxel assayed.

To identify if the melphalan-mediated reduction in the dl1520 IC_{50} was cell-type-specific, the potential for melphalan to enhance sensitivity to dl1520 using an additional tumour-derived cell line and several carboplatin-resistant variants of the two parental cell lines (Figure 3.4.3). Similar to the results in HN-5a cells, melphalan reduced dl1520 IC_{50} in all cell lines assayed (Figure 3.4.3). This effect was most profound in HT-29 cells, where melphalan reduced the dl1520 IC_{50} by up to 72% at concentrations of drug that had minimal toxicity on their own (Figure 3.4.3A and Figure 3.3.3A). These results are in agreement with previous findings that identified up to an 80% enhancement of dl1520 toxicity by melphalan at concentrations that inhibited proliferation by only 20% [110]. These findings suggest that combining dl1520 with melphalan may be the superior treatment strategy over that of cisplatin and dl1520, which is already approved for use in the clinic.

The conventional *in vitro* method for investigating dl1520-drug combinations has been to co-administer both agents and measure anti-proliferative effects after a given time [98,99]. However, in the clinic, administering two therapeutic agents (i.e. agent A and agent B) can be done in three ways: a) administering agent A and B together, b) administering agent A before B, or c) administering agent B before A. Therefore, the present study took a relatively novel *in vitro* approach and assessed the effects of scheduled administration of dl1520 with melphalan, cisplatin, or paclitaxel to determine which schedule afforded the optimal therapeutic benefit. In general, both cotreatment and drug pretreatment were superior to dl1520 pretreatment (Figure

3.4.2 and Figure 3.4.3). Moreover this phenomenon appeared to be melphalan-specific, as there was no difference in the effects of each treatment schedule for cisplatin and paclitaxel (with the exception of cotreatment with 2.5 μ M cisplatin which reduced dl1520 IC₅₀ better than pretreatment with either cisplatin or dl1520) (Figure 3.4.2). These melphalan-specific effects appeared to be concentration-dependent, as dl1520 pretreatment was better than drug pretreatment when treating with low concentrations of melphalan, whereas melphalan pretreatment was superior to dl1520 pretreatment when treating with moderate to high concentrations of melphalan (Figure 3.4.2A and Figure 3.4.3A). This suggests a melphalan-mediated enhancement of toxicity to dl1520 anti-tumour effects. The present study assessed potential melphalan-mediated changes in CAR levels and dl1520 replication as the cause of this melphalan-mediated enhancement of toxicity to dl1520 (discussed in *Section 4.3.2 p. 131 and Section 4.3.3. p. 134*).

It is important to note that when two therapeutic agents are used together, it is difficult to determine how the agents are interacting. In the present study it was hypothesized that melphalan mediated an enhancement of dl1520 toxicity because of the observed sensitization to dl1520 when pretreatment with melphalan or cotreatment with both agents (Figure 3.4.2A). However, it is entirely possible that dl1520 is enhancing toxicity to melphalan and not vice versa. Indeed, previous studies have identified a schedule-dependent dl1520-mediated enhancement of toxicity to chemotherapy [101,110]. Melphalan toxicity has reportedly been augmented *in vitro* when dl1520 was administered

simultaneously with or 24 h after melphalan but not when dl1520 was administered 24 h prior to melphalan [110]. Additionally, an *in vivo* study assessed scheduled treatment of HLaC (head and neck) tumour cells xenografted into mice treated with chemotherapy (cisplatin and 5-FU) and dl1520 using the identical treatment schedules investigated in the present study [101]. In contrast to results presented here, dl1520 pretreatment was more effective than combined treatment or drug pretreatment [101]. Differences could be accounted for due to the parameters used to assess efficacy of treatment in their study (survival and % complete tumour response) vs. the present study (enhanced cytotoxicity) and the tumour model system studied (*in vivo* in their study vs. *in vitro* in the present study). This highlights the need to validate these preliminary findings using additional tumour model systems.

4.3.2. Melphalan-mediated changes in the CAR levels in HN-5a cells

CAR is frequently down-regulated in many advanced human cancers [125,126,153,154,155,156], and is believed to be involved in cellular growth-inhibition through contact with adjacent cells at tight junctions [51,165]. A negative correlation between CAR protein levels and cell growth, combined with a positive correlation between CAR protein levels and p21 protein levels (negative regulator of the cell cycle) was the first evidence to support the involvement of CAR in growth-inhibition [165]. Loss of CAR-mediated growth-inhibition may help potentiate tumourigenesis, and presents a barrier for successful dl1520-mediated therapies, as CAR is the primary receptor for the

dl1520 attachment [47]. Therefore, chemical induction of CAR protein levels has the potential to enhance dl1520-mediated therapies for cancer.

In the present study, of all the chemotherapy drugs used in combination with dl1520, melphalan had the greatest capacity to sensitize cells to dl1520-mediated anti-proliferative effects (Figure 3.4.2). Moreover, melphalan-mediated reduction in the dl1520 IC_{50} was greatest with either cotreatment (dl1520 and melphalan) or pretreatment (24 h) with melphalan compared to dl1520 pretreatment (24 h) at all concentrations of melphalan assayed (with the exception of pretreatment with 2.5 μ M melphalan which did not sensitize cells to dl1520) (Figure 3.4.2A). It was hypothesized that melphalan treatment up-regulated CAR protein expression resulting in an increased dl1520 infection of HN-5a cells. However, there was no evidence to support this hypothesis when treating HN-5a cells with 15 μ M and 25 μ M melphalan, concentrations at which melphalan reduced dl1520 IC_{50} by approximately 70% (Figure 3.5.2 and Figure 3.4.1.2, respectively). Therefore, melphalan-mediated reduction in dl1520 IC_{50} is likely not the result of a melphalan-mediated up-regulation in CAR. However, treatment of cells with 50 μ M melphalan up-regulated CAR mRNA levels after 24 h (Figure 3.5.1) and CAR protein levels after 48 h (Figure 3.5.2), compared to a melphalan-untreated control. These results agree with previous studies that identified the inducible nature of CAR mRNA [166] and CAR protein cell surface expression by chemotherapy drugs [166,167]. The melphalan-mediated CAR mRNA induction after 24 h (Figure 3.5.1) and CAR protein induction at 48 h but not 24 h (Figure 3.5.2) suggest a potential melphalan-mediated transcriptional

regulation of the CAR gene. Notably, treatment of HN-5a cells with 50 μ M melphalan for 4 h, 8 h, or 12 h did not increase CAR mRNA (Figure 3.5.3) or protein expression (Figure 3.5.4), suggesting that a 24-h incubation with melphalan is necessary to mediate a change in CAR mRNA and CAR protein levels.

The mechanism for the melphalan-mediated up-regulation of CAR expression was not elucidated in the present study. The timeline of the melphalan-induced change in both CAR mRNA (24 h) and CAR protein (48 h) suggest a potential transcriptional regulation of CAR expression by melphalan (Figure 3.5.1 and Figure 3.5.2). DNA methylation is an epigenetic mechanism used to negatively-regulate gene transcription [169]. However, the degree of histone acetylation rather than DNA methylation of the CAR gene plays an important role in regulating CAR gene expression [170]. Histone acetylation reduces the positive charge of the amino terminus of the histones, lowering their affinity for negatively charged DNA, which allows space for transcription factors to bind leading to enhanced gene transcription [171]. In fact, several histone deacetylase inhibitors have been investigated for their ability to positively regulate CAR gene expression [151,170,172,173,174]. Treatment of a human tumour derived cell line with melphalan 50 μ M resulted in an up-regulation in both CAR mRNA and CAR protein levels that may be useful for treatment of human tumours as CAR is frequently down-regulated in many human cancers [125,126,153,154,155,156]. A potentially informative topic of future study would be to investigate the effect of melphalan on histone acetylation in the CAR gene,

and its function on CAR promoter activity to further elucidate the mechanism of melphalan-mediated CAR gene transcription.

4.3.3. *Greater-than-additive cell death after combined treatment with dl1520 and melphalan is not the result of enhanced dl1520 replication*

The combined treatment of HN-5a cells with melphalan and dl1520 enhanced sensitivity of cells to dl1520-mediated inhibition of cellular proliferation as assessed using alamarBlueTM cell viability assays (Figure 3.4.2A). A limitation of this assay is the inability to differentiate between slowed cell growth, enhanced cell death, or a combination of the two. Therefore, the amount of cell death following combined treatment of HN-5a cells with dl1520 and melphalan was assessed using flow cytometry with Annexin V/PI staining (Figure 3.6.1). One day after treatment initiation, all cells treated with dl1520 had less cell death than their respective melphalan-treated controls (Figure 3.6.1B). This is possibly due to HAdV-mediated inhibition of cellular apoptosis, presumably through an E1B-19-dependent mechanism [81,82]. Furthermore, after 2 d, cell death was reduced in cells treated with dl1520 and 5 μ M or 7.5 μ M melphalan compared to cells treated with dl1520 alone or in combination with 2.5 μ M melphalan (Figure 3.6.1D). These results suggest a potential concentration-dependent melphalan-mediated inhibition of dl1520-induced cell death. After 3 d and 4 d, dl1520-induced cell death was increased when cells were treated with 7.5 μ M melphalan compared to the drug-untreated controls (Figure 3.6.1F and Figures 3.6.1H). The timing of this increase in dl1520-mediated cell death is consistent with that of

HAdV replication [175]. Consistent with this, medium collected from cells 3 d and 4 d after treatment with both dl1520 and melphalan inhibited proliferation of a new monolayer of cells, whereas medium collected from 1 d and 2 d post-treatment had no effect (Figure 3.7.1A). Collectively these results suggest that dl1520 replication in the presence of melphalan occurred. Therefore, it was hypothesized that a melphalan-mediated enhancement of dl1520 replication was responsible for the greater-than-additive cell death observed when cells received the cotreatment of dl1520 and 7.5 μ M melphalan (Figure 3.6.1F and Figure 3.6.1H). However, there was no melphalan-mediated increase in dl1520 replication after assessing dl1520 replication using an adenovirus burst assay (Figure 3.7.1B). Drug-mediated changes in HAdV replication have been observed in several studies [101,176,177,178,179]. For example, the anti-cholesterol drug lovastatin and the MEK inhibitor CI1040 enhance HAdV replication [176,177,178]. Contrary to this, the chemotherapy drugs cisplatin, 5-FU, vincristine, and temozolomide do not change HAdV replication [101,178,179]. These observations, combined with the results from the present study, suggest that drug-mediated changes in HAdV replication are drug-specific.

Drug-mediated modulation of cell cycle progression has been postulated as being the cause of drug-mediated changes to HAdV replication. One study identified enhanced adenovirus production from cells that were infected immediately after being released from the G1 phase of the cell cycle [177]. This result could be due to the progression of cells directly into the S-phase of the cell cycle, which has been identified as the optimal cell cycle phase to infect cells in

order to produce the highest virus yield [180]. This is consistent with the finding that HAdV cause the accumulation of cells in the S-phase of the cell cycle up to 12 h post-infection [175,181]. Melphalan induces a G2-M cell cycle arrest in a concentration- and time-dependent manner [168,182]. Consistent with the results from the present study that identified no change in dl1520 replication in the presence of melphalan, it would be hypothesized that melphalan-induced cell cycle arrest in G2 would not hamper dl1520-mediated accumulation of cells in the S-phase of the cell cycle and thus have no effect on HAdV replication. An interesting future study would be to investigate the cell-cycle-specific changes induced by melphalan both alone and in combination with dl1520 using flow cytometry DNA content analysis.

Results from the present study did not implicate melphalan-mediated changes in dl1520 replication as the cause of the greater-than-additive cell death in response to the combined treatment with melphalan and dl1520 (Figure 3.6.1). As described above (*Section 4.3.2, p. 131*), it is important to note that when two therapeutic agents are used together, it is difficult to determine which agent is potentiating the effects of the other agent. Therefore, it is entirely possible that dl1520 is enhancing toxicity to melphalan and not vice versa. For example, the oncolytic HAdV Δ -24-RGD (E1A non-functional for binding pRB, enhanced internalization through integrin binding) enhanced toxicity to the DNA-damaging agent temozolomide [179]. Normal expression of the DNA repair enzyme O(6)-methylguanine DNA methyltransferase (MGMT) was found to render tumours resistant to temozolomide therapy [183]. E1A protein of the HAdV binds to and

inactivates CBP/p300 and in doing so inhibits the MGMT promoter activity [179,184]. This interaction sensitizes cells to temozolomide and is postulated to be the cause of the synergy between temozolomide and Δ -24-RGD [179]. Future studies are needed to elucidate potential dl1520-mediated changes to tumour cell biology (such as inhibition of DNA repair enzymes) that have the potential to sensitize cells to melphalan-mediated toxicities.

4.4. Conclusions and future directions

4.4.1. Conclusions

The present study demonstrates that the combination of melphalan with dl1520 for the treatment of human HNSCC is superior *in vitro* to the clinically approved combination of dl1520 with cisplatin. This study also identified colon cancer, and several drug-resistant variants of both colon and head and neck cancer as potential targets for dl1520-mediated therapy, both alone and in combination with melphalan. Furthermore, potential melphalan-mediated induction of CAR levels in a HNSCC cell line was identified. This suggests melphalan at concentrations of 50 μ M can be used to enhance the efficiency of HAdV-mediated therapies for tumours that have reduced CAR levels. Results from this study are valuable for selecting the optimal tumour type, dl1520-drug combination, and schedule for administration of each agent to maximize the efficacy of treatment of cancer.

4.4.2. *Future studies*

The focus of the work presented in this thesis was to identify novel dl1520-chemotherapy combinations for the treatment of cancer. This study validates preliminary findings from our lab identifying melphalan as a suitable candidate for combination therapy with dl1520. However, there are still gaps in our knowledge that need to be addressed in order to fully understand the interaction between the two.

A pitfall of the present study is that titration of our dl1520 stock was not done using HEK293 cells (the cell line traditionally used to titer E1-deficient HAdV mutants). Therefore, the assumed concentration of the dl1520 stock solution could be potentially incorrect. There are several kit-based assay systems (Clontech, Mountain View, CA, USA) that can be used to further confirm the assumed working concentration of our dl1520 stock including: a) Adeno-XTM rapid titer kit (utilizes an anti-hexon antibody to stain cells positive for adenovirus after infection) or b) Adeno-X qPCR titration kit (utilizes a qPCR based assay of HAdV DNA concentration to titrate the concentration of the newly-propagated stock). Taken together with data from the experiments presented in this thesis, the results from further titrations can be used to correct the indicated MOIs, should the original titration be incorrect. However, all experiments in the present study are done using the same stock at the same assumed concentration of dl1520. Therefore, regardless of the true concentration of the dl1520 stock, the interpretation of results from this study remains the same.

The present study identified several tumour cell lines as potential candidates for dl1520-mediated therapies. While it is known that HT-29 cells possess non-functional p53 [159], the p53 status of the HN-5a cell line and its carboplatin-resistant variant is putatively assumed to be non-functional due to the high frequency of this mutation (50%) due to the consumption of alcohol and tobacco [6]. However, a confirmation of p53 status is needed to verify these cell lines as valid targets for dl1520-mediated therapy. Several techniques can be used to assess p53 status in these cell lines. A direct sequence analysis of the p53 gene can be used to screen cell lines for potential inactivating mutations. Furthermore, the activity of p53 is dependent on its conformation [185]. Therefore, an immunoblot analysis of p53 using conformation-specific antibodies (recognize p53 in a non-functional or functional conformation) and conformation-non-specific antibodies can be used to determine the ratio of inactive p53 relative to the total in a given cell line and can be used as an indicator of p53 functional status [159,161].

The sensitivity of a given cell line to dl1520 infection could not be correlated with the basal levels of CAR mRNA or CAR protein in the present study (Figure 3.2.1, Figure 3.2.3, and Figure 3.3.1). This result is unexpected because CAR protein serves as the primary receptor for HAdV binding to the cell [47]. However, CAR protein cell surface levels rather than total CAR protein levels may be the cause of differential sensitivity to dl1520 [157,163,164]. To investigate cell surface CAR protein levels, flow cytometric and immunofluorescence using a CAR-specific antibody can be used as a

quantitative and qualitative measure, respectively. It has been demonstrated that cell lines expressing higher levels of CAR protein at the cell surface bind and thus internalize more HAdV [157,163,164]. The assessment of differences in adenovirus attachment and internalization can be done in several ways including: a) flow cytometry using HAdV capsid-specific antibodies after cellular infection with a given concentration of dl1520 for a given time, b) immunofluorescence staining HAdV particles using the same antibody described in (a) to visualize HAdV binding, and c) infection of cells with a replication-deficient HAdV containing pCMV- β -galactosidase (β -gal), followed by treatment with X-gal (produces a colourimetric substrate when metabolized by β -gal) after 24h of incubation to allow for production of β -gal, with subsequent quantification of the product. The resultant absorbance can then be used as a measure of HAdV-internalization.

The present study identified melphalan-mediated changes in CAR levels. Moreover, the kinetics of the melphalan-mediated increase in CAR levels suggest a potential transcriptional regulation of CAR by melphalan. To study this, a reporter gene assay can be done as described elsewhere [170,186]. Briefly, cells are transfected with plasmids that contain the luciferase reporter gene under the transcriptional regulation of the putative promoter sequence of the CAR gene. Cells are then treated with melphalan (to putatively induce expression of the CAR promoter and subsequent expression of luciferase protein), followed by luciferin (a luciferase substrate that emits light as a byproduct when metabolized) and the resultant light is measured. This experiment would be able

to show direct activation of the CAR gene promoter by melphalan to further elucidate the mechanism by which melphalan induces levels of CAR mRNA and CAR protein.

The combination of melphalan and dl1520 sensitizes cells to dl1520-mediated inhibition of proliferation. The present study identified that a greater-than-additive cell death from this combination contributes to the observed melphalan-enhanced dl1520-mediated inhibition of proliferation. However, evidence for a greater-than-additive percentage of dead cells could not be determined for all concentrations of melphalan that reduced the dl1520 IC_{50} . Therefore, flow cytometric analysis of DNA content following treatment with melphalan, dl1520, and the combination of the two can be used to elucidate the involvement of growth arrest in the melphalan-mediated reduction in dl1520 IC_{50} . It would be hypothesized that the percentage of cells induced into the S-phase of the cell cycle following combined dl1520 and melphalan treatment would not be different from the percentage induced into S-phase by dl1520 alone as the present study identified no difference in dl1520 replication (Figure 3.7.1).

The present study identified a potential melphalan-mediated sensitization of cells to growth inhibition by dl1520. However, it is entirely possible that the converse is true. A direct assessment of DNA damage could be used to assess potential dl1520-mediated enhancement of DNA damage induced by melphalan. Furthermore, as described earlier in this work (*Section 4.3.3, p. 134*) a potential mechanism for this would be dl1520-mediated inhibition of DNA repair enzymes.

Lastly, following further *in vitro* experiments to validate these findings that melphalan is the superior drug compared to cisplatin to combine with dl1520 treatment, a direct comparison of the two chemotherapy-dl1520 combinations in an *in vivo* mouse model is needed prior to advancing to clinical trials.

1. Nathan, P. F., F. M. Johnson, J. F. and Wilkerson, D. G. (1991) The combination of cisplatin and dl1520: a phase I study. *Journal of Clinical Oncology* 9, 146-52.
2. Nathan, P. F., Johnson, F. M., Foye, J., Ethier, S., Cohen, S., Upp, W., Macintosh, M., May, L., and Lee, M. P. (1992) Cisplatin and dl1520: a phase I study. *Journal of Clinical Oncology* 10, 146-52.
3. Hsiao, J. M., Hsu, Y., Hsu, J., and Pao, C. (1991) Estimating the mean and variance. *Statistics* 20(1), 113-131.
4. Pomeroy, J. C., Pomeroy, C., Rich, A. H., Gardner, J. R., Fisher, R. H., Jay, V. J., Ghossein, M. A., Probst, R. W., and Zimm, B. J. (1991) Cisplatin, dl1520, and melphalan: a phase I study of the combination of cisplatin, dl1520, and melphalan in the treatment of head and neck cancer. *Journal of Clinical Oncology* 9, 146-52.
5. Hsiao, J. M., Hsu, Y., Hsu, J., and Pao, C. (1991) Estimating the mean and variance. *Statistics* 20(1), 113-131.
6. Pomeroy, J. C., Pomeroy, C., Rich, A. H., Gardner, J. R., Fisher, R. H., Jay, V. J., Ghossein, M. A., Probst, R. W., and Zimm, B. J. (1991) Cisplatin, dl1520, and melphalan: a phase I study of the combination of cisplatin, dl1520, and melphalan in the treatment of head and neck cancer. *Journal of Clinical Oncology* 9, 146-52.
7. Pomeroy, J. C., Pomeroy, C., Rich, A. H., Gardner, J. R., Fisher, R. H., Jay, V. J., Ghossein, M. A., Probst, R. W., and Zimm, B. J. (1991) Cisplatin, dl1520, and melphalan: a phase I study of the combination of cisplatin, dl1520, and melphalan in the treatment of head and neck cancer. *Journal of Clinical Oncology* 9, 146-52.
8. Pomeroy, J. C., Pomeroy, C., Rich, A. H., Gardner, J. R., Fisher, R. H., Jay, V. J., Ghossein, M. A., Probst, R. W., and Zimm, B. J. (1991) Cisplatin, dl1520, and melphalan: a phase I study of the combination of cisplatin, dl1520, and melphalan in the treatment of head and neck cancer. *Journal of Clinical Oncology* 9, 146-52.
9. Pomeroy, J. C., Pomeroy, C., Rich, A. H., Gardner, J. R., Fisher, R. H., Jay, V. J., Ghossein, M. A., Probst, R. W., and Zimm, B. J. (1991) Cisplatin, dl1520, and melphalan: a phase I study of the combination of cisplatin, dl1520, and melphalan in the treatment of head and neck cancer. *Journal of Clinical Oncology* 9, 146-52.
10. Pomeroy, J. C., Pomeroy, C., Rich, A. H., Gardner, J. R., Fisher, R. H., Jay, V. J., Ghossein, M. A., Probst, R. W., and Zimm, B. J. (1991) Cisplatin, dl1520, and melphalan: a phase I study of the combination of cisplatin, dl1520, and melphalan in the treatment of head and neck cancer. *Journal of Clinical Oncology* 9, 146-52.
11. Pomeroy, J. C., Pomeroy, C., Rich, A. H., Gardner, J. R., Fisher, R. H., Jay, V. J., Ghossein, M. A., Probst, R. W., and Zimm, B. J. (1991) Cisplatin, dl1520, and melphalan: a phase I study of the combination of cisplatin, dl1520, and melphalan in the treatment of head and neck cancer. *Journal of Clinical Oncology* 9, 146-52.
12. Pomeroy, J. C., Pomeroy, C., Rich, A. H., Gardner, J. R., Fisher, R. H., Jay, V. J., Ghossein, M. A., Probst, R. W., and Zimm, B. J. (1991) Cisplatin, dl1520, and melphalan: a phase I study of the combination of cisplatin, dl1520, and melphalan in the treatment of head and neck cancer. *Journal of Clinical Oncology* 9, 146-52.
13. Pomeroy, J. C., Pomeroy, C., Rich, A. H., Gardner, J. R., Fisher, R. H., Jay, V. J., Ghossein, M. A., Probst, R. W., and Zimm, B. J. (1991) Cisplatin, dl1520, and melphalan: a phase I study of the combination of cisplatin, dl1520, and melphalan in the treatment of head and neck cancer. *Journal of Clinical Oncology* 9, 146-52.
14. Pomeroy, J. C., Pomeroy, C., Rich, A. H., Gardner, J. R., Fisher, R. H., Jay, V. J., Ghossein, M. A., Probst, R. W., and Zimm, B. J. (1991) Cisplatin, dl1520, and melphalan: a phase I study of the combination of cisplatin, dl1520, and melphalan in the treatment of head and neck cancer. *Journal of Clinical Oncology* 9, 146-52.
15. Pomeroy, J. C., Pomeroy, C., Rich, A. H., Gardner, J. R., Fisher, R. H., Jay, V. J., Ghossein, M. A., Probst, R. W., and Zimm, B. J. (1991) Cisplatin, dl1520, and melphalan: a phase I study of the combination of cisplatin, dl1520, and melphalan in the treatment of head and neck cancer. *Journal of Clinical Oncology* 9, 146-52.
16. Pomeroy, J. C., Pomeroy, C., Rich, A. H., Gardner, J. R., Fisher, R. H., Jay, V. J., Ghossein, M. A., Probst, R. W., and Zimm, B. J. (1991) Cisplatin, dl1520, and melphalan: a phase I study of the combination of cisplatin, dl1520, and melphalan in the treatment of head and neck cancer. *Journal of Clinical Oncology* 9, 146-52.
17. Pomeroy, J. C., Pomeroy, C., Rich, A. H., Gardner, J. R., Fisher, R. H., Jay, V. J., Ghossein, M. A., Probst, R. W., and Zimm, B. J. (1991) Cisplatin, dl1520, and melphalan: a phase I study of the combination of cisplatin, dl1520, and melphalan in the treatment of head and neck cancer. *Journal of Clinical Oncology* 9, 146-52.
18. Pomeroy, J. C., Pomeroy, C., Rich, A. H., Gardner, J. R., Fisher, R. H., Jay, V. J., Ghossein, M. A., Probst, R. W., and Zimm, B. J. (1991) Cisplatin, dl1520, and melphalan: a phase I study of the combination of cisplatin, dl1520, and melphalan in the treatment of head and neck cancer. *Journal of Clinical Oncology* 9, 146-52.
19. Pomeroy, J. C., Pomeroy, C., Rich, A. H., Gardner, J. R., Fisher, R. H., Jay, V. J., Ghossein, M. A., Probst, R. W., and Zimm, B. J. (1991) Cisplatin, dl1520, and melphalan: a phase I study of the combination of cisplatin, dl1520, and melphalan in the treatment of head and neck cancer. *Journal of Clinical Oncology* 9, 146-52.
20. Pomeroy, J. C., Pomeroy, C., Rich, A. H., Gardner, J. R., Fisher, R. H., Jay, V. J., Ghossein, M. A., Probst, R. W., and Zimm, B. J. (1991) Cisplatin, dl1520, and melphalan: a phase I study of the combination of cisplatin, dl1520, and melphalan in the treatment of head and neck cancer. *Journal of Clinical Oncology* 9, 146-52.

CHAPTER 5: References

1. Hanahan, D. and Weinberg, R. A., (2000). The hallmarks of cancer. *Cell*, **100**(1): 57-70.
2. Vogelstein, B. and Kinzler, K. W., (2004). Cancer genes and the pathways they control. *Nat Med*, **10**(8): 789-799.
3. Mathers, C., Fat, D. M., Boerma, J. T., and World Health Organization., The global burden of disease : 2004 update. 2008, Geneva, Switzerland: World Health Organization. vii, 146 p.
4. Marrett, L., Chappel, H., De, P., Dryer, D., Ellison, L., Grunfeld, E., Logan, H., MacIntyre, M., Mery, L., and Weir, H. K., Canadian Cancer Statistics 2010. 2010, Canadian Cancer Society.
5. Parkin, D. M., Bray, F., Ferlay, J., and Pisani, P., (2001). Estimating the world cancer burden: Globocan 2000. *Int J Cancer*, **94**(2): 153-156.
6. Brennan, J. A., Boyle, J. O., Koch, W. M., Goodman, S. N., Hruban, R. H., Eby, Y. J., Couch, M. J., Forastiere, A. A., and Sidransky, D., (1995). Association between cigarette smoking and mutation of the p53 gene in squamous-cell carcinoma of the head and neck. *N Engl J Med*, **332**(11): 712-717.
7. Hashibe, M., Brennan, P., Benhamou, S., Castellsague, X., Chen, C., Curado, M. P., Dal Maso, L., Daudt, A. W., Fabianova, E., Fernandez, L., Wunsch-Filho, V., Franceschi, S., Hayes, R. B., Herrero, R., Koifman, S., La Vecchia, C., Lazarus, P., Levi, F., Mates, D., Matos, E., Menezes, A., Muscat, J., Eluf-Neto, J., Olshan, A. F., Rudnai, P., Schwartz, S. M., Smith, E., Sturgis, E. M., Szeszenia-Dabrowska, N., Talamini, R., Wei, Q., Winn, D. M., Zaridze, D., Zatonski, W., Zhang, Z. F., Berthiller, J., and Boffetta, P., (2007). Alcohol drinking in never users of tobacco, cigarette smoking in never drinkers, and the risk of head and neck cancer: pooled analysis in the International Head and Neck Cancer Epidemiology Consortium. *J Natl Cancer Inst*, **99**(10): 777-789.
8. Forastiere, A., Koch, W., Trotti, A., and Sidransky, D., (2001). Head and neck cancer. *N Engl J Med*, **345**(26): 1890-1900.
9. Califano, J., van der Riet, P., Westra, W., Nawroz, H., Clayman, G., Piantadosi, S., Corio, R., Lee, D., Greenberg, B., Koch, W., and Sidransky, D., (1996). Genetic progression model for head and neck cancer: implications for field cancerization. *Cancer Res*, **56**(11): 2488-2492.
10. Somers, K. D., Merrick, M. A., Lopez, M. E., Incognito, L. S., Schechter, G. L., and Casey, G., (1992). Frequent p53 mutations in head and neck cancer. *Cancer Res*, **52**(21): 5997-6000.

11. Diller, L., Kassel, J., Nelson, C. E., Gryka, M. A., Litwak, G., Gebhardt, M., Bressac, B., Ozturk, M., Baker, S. J., Vogelstein, B., and et al., (1990). p53 functions as a cell cycle control protein in osteosarcomas. *Mol Cell Biol*, **10**(11): 5772-5781.
12. Yonish-Rouach, E., Resnitzky, D., Lotem, J., Sachs, L., Kimchi, A., and Oren, M., (1991). Wild-type p53 induces apoptosis of myeloid leukaemic cells that is inhibited by interleukin-6. *Nature*, **352**(6333): 345-347.
13. Page, D., Fleming, I., Fritz, A., Balch, C., Haller, D., and Morrow, M., AJCC Cancer Staging Handbook. 3 ed, ed. F. Greene. 2002, Chicago, IL: American Joing Committee on Cancer.
14. Shah, J. P. and Lydiatt, W., (1995). Treatment of cancer of the head and neck. *CA Cancer J Clin*, **45**(6): 352-368.
15. Shah, J. P. and Gil, Z., (2009). Current concepts in management of oral cancer--surgery. *Oral Oncol*, **45**(4-5): 394-401.
16. National Cancer Institute. Head and Neck Cancer: Treatment. [cited 2010 09/05/2010]; <http://www.cancer.gov/cancertopics/types/head-and-neck/>.
17. Bourhis, J., Lapeyre, M., Tortochaux, J., Rives, M., Aghili, M., Bourdin, S., Lesaunier, F., Benassi, T., Lemanski, C., Geoffrois, L., Lusinchi, A., Verrelle, P., Bardet, E., Julieron, M., Wibault, P., Luboinski, M., and Benhamou, E., (2006). Phase III randomized trial of very accelerated radiation therapy compared with conventional radiation therapy in squamous cell head and neck cancer: a GORTEC trial. *J Clin Oncol*, **24**(18): 2873-2878.
18. Sullivan, R. D., Miller, E., and Sikes, M. P., (1959). Antimetabolite-metabolite combination cancer chemotherapy. Effects of intraarterial methotrexate-intramuscular Citrovorum factor therapy in human cancer. *Cancer*, **12**(1248-1262).
19. (1987). Adjuvant chemotherapy for advanced head and neck squamous carcinoma. Final report of the Head and Neck Contracts Program. *Cancer*, **60**(3): 301-311.
20. Pignon, J. P., Bourhis, J., Domenge, C., and Designe, L., (2000). Chemotherapy added to locoregional treatment for head and neck squamous-cell carcinoma: three meta-analyses of updated individual data. MACH-NC Collaborative Group. Meta-Analysis of Chemotherapy on Head and Neck Cancer. *Lancet*, **355**(9208): 949-955.
21. Pignon, J. P., le Maitre, A., and Bourhis, J., (2007). Meta-Analyses of Chemotherapy in Head and Neck Cancer (MACH-NC): an update. *Int J Radiat Oncol Biol Phys*, **69**(2 Suppl): S112-114.
22. Adelstein, D. J., Li, Y., Adams, G. L., Wagner, H., Jr., Kish, J. A., Ensley, J. F., Schuller, D. E., and Forastiere, A. A., (2003). An intergroup phase III comparison of standard radiation therapy and two schedules of concurrent

- chemoradiotherapy in patients with unresectable squamous cell head and neck cancer. *J Clin Oncol*, **21**(1): 92-98.
23. Jeremic, B., Shibamoto, Y., Stanisavljevic, B., Milojevic, L., Milicic, B., and Nikolic, N., (1997). Radiation therapy alone or with concurrent low-dose daily either cisplatin or carboplatin in locally advanced unresectable squamous cell carcinoma of the head and neck: a prospective randomized trial. *Radiother Oncol*, **43**(1): 29-37.
 24. Brabec, V. and Leng, M., (1993). DNA interstrand cross-links of trans-diamminedichloroplatinum(II) are preferentially formed between guanine and complementary cytosine residues. *Proc Natl Acad Sci U S A*, **90**(11): 5345-5349.
 25. Siddik, Z. H., (2003). Cisplatin: mode of cytotoxic action and molecular basis of resistance. *Oncogene*, **22**(47): 7265-7279.
 26. National Cancer Institute. Cancer Drug Information. [cited 2010 09/05/2010]; <http://www.cancer.gov/cancertopics/druginfo/alphalist>.
 27. Bernier, J., Dometge, C., Ozsahin, M., Matuszewska, K., Lefebvre, J. L., Greiner, R. H., Giralt, J., Maingon, P., Rolland, F., Bolla, M., Cognetti, F., Bourhis, J., Kirkpatrick, A., and van Glabbeke, M., (2004). Postoperative irradiation with or without concomitant chemotherapy for locally advanced head and neck cancer. *N Engl J Med*, **350**(19): 1945-1952.
 28. Forastiere, A. A., Goepfert, H., Maor, M., Pajak, T. F., Weber, R., Morrison, W., Glisson, B., Trotti, A., Ridge, J. A., Chao, C., Peters, G., Lee, D. J., Leaf, A., Ensley, J., and Cooper, J., (2003). Concurrent chemotherapy and radiotherapy for organ preservation in advanced laryngeal cancer. *N Engl J Med*, **349**(22): 2091-2098.
 29. Chamberlain, J. S., Barjot, C., and Scott, J., (2003). Packaging cell lines for generating replication-defective and gutted adenoviral vectors. *Methods Mol Med*, **76**(153-166).
 30. Bischoff, J. R., Kirn, D. H., Williams, A., Heise, C., Horn, S., Muna, M., Ng, L., Nye, J. A., Sampson-Johannes, A., Fattaey, A., and McCormick, F., (1996). An adenovirus mutant that replicates selectively in p53-deficient human tumor cells. *Science*, **274**(5286): 373-376.
 31. Rodriguez, R., Schuur, E. R., Lim, H. Y., Henderson, G. A., Simons, J. W., and Henderson, D. R., (1997). Prostate attenuated replication competent adenovirus (ARCA) CN706: a selective cytotoxic for prostate-specific antigen-positive prostate cancer cells. *Cancer Res*, **57**(13): 2559-2563.
 32. Brandt, C. D., Kim, H. W., Vargosko, A. J., Jeffries, B. C., Arrobio, J. O., Rindge, B., Parrott, R. H., and Chanock, R. M., (1969). Infections in 18,000 infants and children in a controlled study of respiratory tract disease. I. Adenovirus pathogenicity in relation to serologic type and illness syndrome. *Am J Epidemiol*, **90**(6): 484-500.

33. Tollefson, A. E., Kuppaswamy, M., Shashkova, E. V., Doronin, K., and Wold, W. S., (2007). Preparation and titration of CsCl-banded adenovirus stocks. *Methods Mol Med*, **130**(223-235).
34. Ganly, I., Kirn, D., Eckhardt, G., Rodriguez, G. I., Soutar, D. S., Otto, R., Robertson, A. G., Park, O., Gulley, M. L., Heise, C., Von Hoff, D. D., and Kaye, S. B., (2000). A phase I study of Onyx-015, an E1B attenuated adenovirus, administered intratumorally to patients with recurrent head and neck cancer. *Clin Cancer Res*, **6**(3): 798-806.
35. Mulvihill, S., Warren, R., Venook, A., Adler, A., Randlev, B., Heise, C., and Kirn, D., (2001). Safety and feasibility of injection with an E1B-55 kDa gene-deleted, replication-selective adenovirus (ONYX-015) into primary carcinomas of the pancreas: a phase I trial. *Gene Ther*, **8**(4): 308-315.
36. Reid, T., Galanis, E., Abbruzzese, J., Sze, D., Andrews, J., Romel, L., Hatfield, M., Rubin, J., and Kirn, D., (2001). Intra-arterial administration of a replication-selective adenovirus (dl1520) in patients with colorectal carcinoma metastatic to the liver: a phase I trial. *Gene Ther*, **8**(21): 1618-1626.
37. Khuri, F. R., Nemunaitis, J., Ganly, I., Arseneau, J., Tannock, I. F., Romel, L., Gore, M., Ironside, J., MacDougall, R. H., Heise, C., Randlev, B., Gillenwater, A. M., Bruso, P., Kaye, S. B., Hong, W. K., and Kirn, D. H., (2000). a controlled trial of intratumoral ONYX-015, a selectively-replicating adenovirus, in combination with cisplatin and 5-fluorouracil in patients with recurrent head and neck cancer. *Nat Med*, **6**(8): 879-885.
38. Mok, W., Boucher, Y., and Jain, R. K., (2007). Matrix metalloproteinases-1 and -8 improve the distribution and efficacy of an oncolytic virus. *Cancer Res*, **67**(22): 10664-10668.
39. Rowe, W. P., Huebner, R. J., Gilmore, L. K., Parrott, R. H., and Ward, T. G., (1953). Isolation of a cytopathogenic agent from human adenoids undergoing spontaneous degeneration in tissue culture. *Proc Soc Exp Biol Med*, **84**(3): 570-573.
40. Kojaoghlanian, T., Flomenberg, P., and Horwitz, M. S., (2003). The impact of adenovirus infection on the immunocompromised host. *Rev Med Virol*, **13**(3): 155-171.
41. van Oostrum, J. and Burnett, R. M., (1985). Molecular composition of the adenovirus type 2 virion. *J Virol*, **56**(2): 439-448.
42. Stewart, P. L., Fuller, S. D., and Burnett, R. M., (1993). Difference imaging of adenovirus: bridging the resolution gap between X-ray crystallography and electron microscopy. *Embo J*, **12**(7): 2589-2599.
43. Vellinga, J., Van der Heijdt, S., and Hoeben, R. C., (2005). The adenovirus capsid: major progress in minor proteins. *J Gen Virol*, **86**(Pt 6): 1581-1588.

44. Matthews, D. A. and Russell, W. C., (1995). Adenovirus protein-protein interactions: molecular parameters governing the binding of protein VI to hexon and the activation of the adenovirus 23K protease. *J Gen Virol*, **76** (Pt 8)(1959-1969.
45. Varga, M. J., Weibull, C., and Everitt, E., (1991). Infectious entry pathway of adenovirus type 2. *J Virol*, **65**(11): 6061-6070.
46. Excoffon, K. J., Traver, G. L., and Zabner, J., (2005). The role of the extracellular domain in the biology of the coxsackievirus and adenovirus receptor. *Am J Respir Cell Mol Biol*, **32**(6): 498-503.
47. Bergelson, J. M., Cunningham, J. A., Droguett, G., Kurt-Jones, E. A., Krithivas, A., Hong, J. S., Horwitz, M. S., Crowell, R. L., and Finberg, R. W., (1997). Isolation of a common receptor for Coxsackie B viruses and adenoviruses 2 and 5. *Science*, **275**(5304): 1320-1323.
48. Cohen, C. J., Shieh, J. T., Pickles, R. J., Okegawa, T., Hsieh, J. T., and Bergelson, J. M., (2001). The coxsackievirus and adenovirus receptor is a transmembrane component of the tight junction. *Proc Natl Acad Sci U S A*, **98**(26): 15191-15196.
49. Excoffon, K. J., Gansemer, N., Traver, G., and Zabner, J., (2007). Functional effects of coxsackievirus and adenovirus receptor glycosylation on homophilic adhesion and adenoviral infection. *J Virol*, **81**(11): 5573-5578.
50. Tomko, R. P., Xu, R., and Philipson, L., (1997). HCAR and MCAR: the human and mouse cellular receptors for subgroup C adenoviruses and group B coxsackieviruses. *Proc Natl Acad Sci U S A*, **94**(7): 3352-3356.
51. Coyne, C. B., Voelker, T., Pichla, S. L., and Bergelson, J. M., (2004). The coxsackievirus and adenovirus receptor interacts with the multi-PDZ domain protein-1 (MUPP-1) within the tight junction. *J Biol Chem*, **279**(46): 48079-48084.
52. Wickham, T. J., Mathias, P., Cheresch, D. A., and Nemerow, G. R., (1993). Integrins alpha v beta 3 and alpha v beta 5 promote adenovirus internalization but not virus attachment. *Cell*, **73**(2): 309-319.
53. Fabry, C. M., Rosa-Calatrava, M., Conway, J. F., Zubieta, C., Cusack, S., Ruigrok, R. W., and Schoehn, G., (2005). A quasi-atomic model of human adenovirus type 5 capsid. *Embo J*, **24**(9): 1645-1654.
54. Nakano, M. Y., Boucke, K., Suomalainen, M., Stidwill, R. P., and Greber, U. F., (2000). The first step of adenovirus type 2 disassembly occurs at the cell surface, independently of endocytosis and escape to the cytosol. *J Virol*, **74**(15): 7085-7095.
55. Greber, U. F., Willetts, M., Webster, P., and Helenius, A., (1993). Stepwise dismantling of adenovirus 2 during entry into cells. *Cell*, **75**(3): 477-486.

56. Wickham, T. J., Filardo, E. J., Cheresch, D. A., and Nemerow, G. R., (1994). Integrin alpha v beta 5 selectively promotes adenovirus mediated cell membrane permeabilization. *J Cell Biol*, **127**(1): 257-264.
57. Wiethoff, C. M., Wodrich, H., Gerace, L., and Nemerow, G. R., (2005). Adenovirus protein VI mediates membrane disruption following capsid disassembly. *J Virol*, **79**(4): 1992-2000.
58. Bailey, C. J., Crystal, R. G., and Leopold, P. L., (2003). Association of adenovirus with the microtubule organizing center. *J Virol*, **77**(24): 13275-13287.
59. Shiina, M., Lacher, M. D., Christian, C., and Korn, W. M., (2009). RNA interference-mediated knockdown of p21(WAF1) enhances anti-tumor cell activity of oncolytic adenoviruses. *Cancer Gene Ther*, **16**(11): 810-819.
60. Greber, U. F., Suomalainen, M., Stidwill, R. P., Boucke, K., Ebersold, M. W., and Helenius, A., (1997). The role of the nuclear pore complex in adenovirus DNA entry. *Embo J*, **16**(19): 5998-6007.
61. Saphire, A. C., Guan, T., Schirmer, E. C., Nemerow, G. R., and Gerace, L., (2000). Nuclear import of adenovirus DNA in vitro involves the nuclear protein import pathway and hsc70. *J Biol Chem*, **275**(6): 4298-4304.
62. Herisse, J., Courtois, G., and Galibert, F., (1980). Nucleotide sequence of the EcoRI D fragment of adenovirus 2 genome. *Nucleic Acids Res*, **8**(10): 2173-2192.
63. Herisse, J. and Galibert, F., (1981). Nucleotide sequence of the EcoRI E fragment of adenovirus 2 genome. *Nucleic Acids Res*, **9**(5): 1229-1240.
64. Alestrom, P., Akusjarvi, G., Lager, M., Yeh-kai, L., and Pettersson, U., (1984). Genes encoding the core proteins of adenovirus type 2. *J Biol Chem*, **259**(22): 13980-13985.
65. Akusjarvi, G., Alestrom, P., Pettersson, M., Lager, M., Jornvall, H., and Pettersson, U., (1984). The gene for the adenovirus 2 hexon polypeptide. *J Biol Chem*, **259**(22): 13976-13979.
66. Roberts, R. J., O'Neill, K. E., and Yen, C. T., (1984). DNA sequences from the adenovirus 2 genome. *J Biol Chem*, **259**(22): 13968-13975.
67. Gingeras, T. R., Sciaky, D., Gelinas, R. E., Bing-Dong, J., Yen, C. E., Kelly, M. M., Bullock, P. A., Parsons, B. L., O'Neill, K. E., and Roberts, R. J., (1982). Nucleotide sequences from the adenovirus-2 genome. *J Biol Chem*, **257**(22): 13475-13491.
68. Whyte, P., Buchkovich, K. J., Horowitz, J. M., Friend, S. H., Raybuck, M., Weinberg, R. A., and Harlow, E., (1988). Association between an oncogene and an anti-oncogene: the adenovirus E1A proteins bind to the retinoblastoma gene product. *Nature*, **334**(6178): 124-129.

69. Bandara, L. R. and La Thangue, N. B., (1991). Adenovirus E1a prevents the retinoblastoma gene product from complexing with a cellular transcription factor. *Nature*, **351**(6326): 494-497.
70. Chellappan, S., Kraus, V. B., Kroger, B., Munger, K., Howley, P. M., Phelps, W. C., and Nevins, J. R., (1992). Adenovirus E1A, simian virus 40 tumor antigen, and human papillomavirus E7 protein share the capacity to disrupt the interaction between transcription factor E2F and the retinoblastoma gene product. *Proc Natl Acad Sci U S A*, **89**(10): 4549-4553.
71. Hiebert, S. W., Lipp, M., and Nevins, J. R., (1989). E1A-dependent transactivation of the human MYC promoter is mediated by the E2F factor. *Proc Natl Acad Sci U S A*, **86**(10): 3594-3598.
72. Bates, S., Phillips, A. C., Clark, P. A., Stott, F., Peters, G., Ludwig, R. L., and Vousden, K. H., (1998). p14ARF links the tumour suppressors RB and p53. *Nature*, **395**(6698): 124-125.
73. Ries, S. J., Brandts, C. H., Chung, A. S., Biederer, C. H., Hann, B. C., Lipner, E. M., McCormick, F., and Korn, W. M., (2000). Loss of p14ARF in tumor cells facilitates replication of the adenovirus mutant dl1520 (ONYX-015). *Nat Med*, **6**(10): 1128-1133.
74. Honda, R., Tanaka, H., and Yasuda, H., (1997). Oncoprotein MDM2 is a ubiquitin ligase E3 for tumor suppressor p53. *FEBS Lett*, **420**(1): 25-27.
75. Virtanen, A. and Pettersson, U., (1985). Organization of early region 1B of human adenovirus type 2: identification of four differentially spliced mRNAs. *J Virol*, **54**(2): 383-391.
76. Green, M., Brackmann, K. H., Cartas, M. A., and Matsuo, T., (1982). Identification and purification of a protein encoded by the human adenovirus type 2 transforming region. *J Virol*, **42**(1): 30-41.
77. Yew, P. R. and Berk, A. J., (1992). Inhibition of p53 transactivation required for transformation by adenovirus early 1B protein. *Nature*, **357**(6373): 82-85.
78. Woo, J. L. and Berk, A. J., (2007). Adenovirus ubiquitin-protein ligase stimulates viral late mRNA nuclear export. *J Virol*, **81**(2): 575-587.
79. Chen, M. J., Holskin, B., Strickler, J., Gorniak, J., Clark, M. A., Johnson, P. J., Mitcho, M., and Shalloway, D., (1987). Induction by E1A oncogene expression of cellular susceptibility to lysis by TNF. *Nature*, **330**(6148): 581-583.
80. Chiou, S. K., Tseng, C. C., Rao, L., and White, E., (1994). Functional complementation of the adenovirus E1B 19-kilodalton protein with Bcl-2 in the inhibition of apoptosis in infected cells. *J Virol*, **68**(10): 6553-6566.
81. Farrow, S. N., White, J. H., Martinou, I., Raven, T., Pun, K. T., Grinham, C. J., Martinou, J. C., and Brown, R., (1995). Cloning of a bcl-2

- homologue by interaction with adenovirus E1B 19K. *Nature*, **374**(6524): 731-733.
82. Han, J., Sabbatini, P., Perez, D., Rao, L., Modha, D., and White, E., (1996). The E1B 19K protein blocks apoptosis by interacting with and inhibiting the p53-inducible and death-promoting Bax protein. *Genes Dev*, **10**(4): 461-477.
 83. Stillman, B. W., Lewis, J. B., Chow, L. T., Mathews, M. B., and Smart, J. E., (1981). Identification of the gene and mRNA for the adenovirus terminal protein precursor. *Cell*, **23**(2): 497-508.
 84. Roovers, D. J., Young, C. S., Vos, H. L., and Sussenbach, J. S., (1990). Physical mapping of two temperature-sensitive adenovirus mutants affected in the DNA polymerase and DNA binding protein. *Virus Genes*, **4**(1): 53-61.
 85. Burgert, H. G., Maryanski, J. L., and Kvist, S., (1987). "E3/19K" protein of adenovirus type 2 inhibits lysis of cytolytic T lymphocytes by blocking cell-surface expression of histocompatibility class I antigens. *Proc Natl Acad Sci U S A*, **84**(5): 1356-1360.
 86. Gooding, L. R., Sofola, I. O., Tollefson, A. E., Duerksen-Hughes, P., and Wold, W. S., (1990). The adenovirus E3-14.7K protein is a general inhibitor of tumor necrosis factor-mediated cytolysis. *J Immunol*, **145**(9): 3080-3086.
 87. Tollefson, A. E., Ryerse, J. S., Scaria, A., Hermiston, T. W., and Wold, W. S., (1996). The E3-11.6-kDa adenovirus death protein (ADP) is required for efficient cell death: characterization of cells infected with adp mutants. *Virology*, **220**(1): 152-162.
 88. Yun, C. O., Kim, E., Koo, T., Kim, H., Lee, Y. S., and Kim, J. H., (2005). ADP-overexpressing adenovirus elicits enhanced cytopathic effect by induction of apoptosis. *Cancer Gene Ther*, **12**(1): 61-71.
 89. Stracker, T. H., Carson, C. T., and Weitzman, M. D., (2002). Adenovirus oncoproteins inactivate the Mre11-Rad50-NBS1 DNA repair complex. *Nature*, **418**(6895): 348-352.
 90. Halbert, D. N., Cutt, J. R., and Shenk, T., (1985). Adenovirus early region 4 encodes functions required for efficient DNA replication, late gene expression, and host cell shutoff. *J Virol*, **56**(1): 250-257.
 91. Shaw, A. R. and Ziff, E. B., (1980). Transcripts from the adenovirus-2 major late promoter yield a single early family of 3' coterminal mRNAs and five late families. *Cell*, **22**(3): 905-916.
 92. Vogelstein, B., Lane, D., and Levine, A. J., (2000). Surfing the p53 network. *Nature*, **408**(6810): 307-310.

93. Barker, D. D. and Berk, A. J., (1987). Adenovirus proteins from both E1B reading frames are required for transformation of rodent cells by viral infection and DNA transfection. *Virology*, **156**(1): 107-121.
94. Teodoro, J. G. and Branton, P. E., (1997). Regulation of p53-dependent apoptosis, transcriptional repression, and cell transformation by phosphorylation of the 55-kilodalton E1B protein of human adenovirus type 5. *J Virol*, **71**(5): 3620-3627.
95. Moore, M., Horikoshi, N., and Shenk, T., (1996). Oncogenic potential of the adenovirus E4orf6 protein. *Proc Natl Acad Sci U S A*, **93**(21): 11295-11301.
96. Querido, E., Marcellus, R. C., Lai, A., Charbonneau, R., Teodoro, J. G., Ketner, G., and Branton, P. E., (1997). Regulation of p53 levels by the E1B 55-kilodalton protein and E4orf6 in adenovirus-infected cells. *J Virol*, **71**(5): 3788-3798.
97. Heise, C., Sampson-Johannes, A., Williams, A., McCormick, F., Von Hoff, D. D., and Kirn, D. H., (1997). ONYX-015, an E1B gene-attenuated adenovirus, causes tumor-specific cytolysis and antitumoral efficacy that can be augmented by standard chemotherapeutic agents. *Nat Med*, **3**(6): 639-645.
98. Portella, G., Scala, S., Vitagliano, D., Vecchio, G., and Fusco, A., (2002). ONYX-015, an E1B gene-defective adenovirus, induces cell death in human anaplastic thyroid carcinoma cell lines. *J Clin Endocrinol Metab*, **87**(6): 2525-2531.
99. You, L., Yang, C. T., and Jablons, D. M., (2000). ONYX-015 works synergistically with chemotherapy in lung cancer cell lines and primary cultures freshly made from lung cancer patients. *Cancer Res*, **60**(4): 1009-1013.
100. Heise, C., Ganly, I., Kim, Y. T., Sampson-Johannes, A., Brown, R., and Kirn, D., (2000). Efficacy of a replication-selective adenovirus against ovarian carcinomatosis is dependent on tumor burden, viral replication and p53 status. *Gene Ther*, **7**(22): 1925-1929.
101. Heise, C., Lemmon, M., and Kirn, D., (2000). Efficacy with a replication-selective adenovirus plus cisplatin-based chemotherapy: dependence on sequencing but not p53 functional status or route of administration. *Clin Cancer Res*, **6**(12): 4908-4914.
102. Heise, C. C., Williams, A., Olesch, J., and Kirn, D. H., (1999). Efficacy of a replication-competent adenovirus (ONYX-015) following intratumoral injection: intratumoral spread and distribution effects. *Cancer Gene Ther*, **6**(6): 499-504.
103. Heise, C. C., Williams, A. M., Xue, S., Propst, M., and Kirn, D. H., (1999). Intravenous administration of ONYX-015, a selectively replicating adenovirus, induces antitumoral efficacy. *Cancer Res*, **59**(11): 2623-2628.

104. Rogulski, K. R., Freytag, S. O., Zhang, K., Gilbert, J. D., Paielli, D. L., Kim, J. H., Heise, C. C., and Kirn, D. H., (2000). In vivo antitumor activity of ONYX-015 is influenced by p53 status and is augmented by radiotherapy. *Cancer Res*, **60**(5): 1193-1196.
105. Ganly, I., Kim, Y. T., Hann, B., Balmain, A., and Brown, R., (2001). Replication and cytolysis of an E1B-attenuated adenovirus in drug-resistant ovarian tumour cells is associated with reduced apoptosis. *Gene Ther*, **8**(5): 369-375.
106. Longley, D. B., Harkin, D. P., and Johnston, P. G., (2003). 5-fluorouracil: mechanisms of action and clinical strategies. *Nat Rev Cancer*, **3**(5): 330-338.
107. Miller, M. L. and Ojima, I., (2001). Chemistry and chemical biology of taxane anticancer agents. *Chem Rec*, **1**(3): 195-211.
108. Roberts, J. J., Brent, T. P., and Crathorn, A. R., (1971). Evidence for the inactivation and repair of the mammalian DNA template after alkylation by mustard gas and half mustard gas. *Eur J Cancer*, **7**(6): 515-524.
109. Cutts, S. M., Nudelman, A., Rephaeli, A., and Phillips, D. R., (2005). The power and potential of doxorubicin-DNA adducts. *IUBMB Life*, **57**(2): 73-81.
110. Ferguson, P. J., (2004) Synergistic cytotoxicity between melphalan and E1B-deficient adenovirus ONYX-015 in human tumor cell lines and their platinum-resistant variants. *Proc Amer Assoc. Cancer Res*, **45**:510.
111. Habib, N., Salama, H., Abd El Latif Abu Median, A., Isac Anis, I., Abd Al Aziz, R. A., Sarraf, C., Mitry, R., Havlik, R., Seth, P., Hartwigsen, J., Bhushan, R., Nicholls, J., and Jensen, S., (2002). Clinical trial of E1B-deleted adenovirus (dl1520) gene therapy for hepatocellular carcinoma. *Cancer Gene Ther*, **9**(3): 254-259.
112. Habib, N. A., Sarraf, C. E., Mitry, R. R., Havlik, R., Nicholls, J., Kelly, M., Vernon, C. C., Gueret-Wardle, D., El-Masry, R., Salama, H., Ahmed, R., Michail, N., Edward, E., and Jensen, S. L., (2001). E1B-deleted adenovirus (dl1520) gene therapy for patients with primary and secondary liver tumors. *Hum Gene Ther*, **12**(3): 219-226.
113. Nemunaitis, J., Cunningham, C., Buchanan, A., Blackburn, A., Edelman, G., Maples, P., Netto, G., Tong, A., Randlev, B., Olson, S., and Kirn, D., (2001). Intravenous infusion of a replication-selective adenovirus (ONYX-015) in cancer patients: safety, feasibility and biological activity. *Gene Ther*, **8**(10): 746-759.
114. Nemunaitis, J., Ganly, I., Khuri, F., Arseneau, J., Kuhn, J., McCarty, T., Landers, S., Maples, P., Romel, L., Randlev, B., Reid, T., Kaye, S., and Kirn, D., (2000). Selective replication and oncolysis in p53 mutant tumors with ONYX-015, an E1B-55kD gene-deleted adenovirus, in patients with

- advanced head and neck cancer: a phase II trial. *Cancer Res*, **60**(22): 6359-6366.
115. Nemunaitis, J., Khuri, F., Ganly, I., Arseneau, J., Posner, M., Vokes, E., Kuhn, J., McCarty, T., Landers, S., Blackburn, A., Romel, L., Randlev, B., Kaye, S., and Kirn, D., (2001). Phase II trial of intratumoral administration of ONYX-015, a replication-selective adenovirus, in patients with refractory head and neck cancer. *J Clin Oncol*, **19**(2): 289-298.
 116. Lamont, J. P., Nemunaitis, J., Kuhn, J. A., Landers, S. A., and McCarty, T. M., (2000). A prospective phase II trial of ONYX-015 adenovirus and chemotherapy in recurrent squamous cell carcinoma of the head and neck (the Baylor experience). *Ann Surg Oncol*, **7**(8): 588-592.
 117. (1999). Onyx plans phase III trial of ONYX-015 for head & neck cancer. *Oncologist*, **4**(5): 432.
 118. Garber, K., (2006). China approves world's first oncolytic virus therapy for cancer treatment. *J Natl Cancer Inst*, **98**(5): 298-300.
 119. Onyx Pharmaceuticals, Letter to Shareholders. 2002, Onyx Pharmaceuticals: Richmond, CA, USA.
 120. Song, X., Zhou, Y., Jia, R., Xu, X., Wang, H., Hu, J., Ge, S., and Fan, X., Inhibition of retinoblastoma in vitro and in vivo with conditionally replicating oncolytic adenovirus H101. *Invest Ophthalmol Vis Sci*, **51**(5): 2626-2635.
 121. Xia, Z. J., Chang, J. H., Zhang, L., Jiang, W. Q., Guan, Z. Z., Liu, J. W., Zhang, Y., Hu, X. H., Wu, G. H., Wang, H. Q., Chen, Z. C., Chen, J. C., Zhou, Q. H., Lu, J. W., Fan, Q. X., Huang, J. J., and Zheng, X., (2004). [Phase III randomized clinical trial of intratumoral injection of E1B gene-deleted adenovirus (H101) combined with cisplatin-based chemotherapy in treating squamous cell cancer of head and neck or esophagus.]. *Ai Zheng*, **23**(12): 1666-1670.
 122. Jia, H. and Kling, J., (2006). China offers alternative gateway for experimental drugs. *Nat Biotechnol*, **24**(2): 117-118.
 123. Guo, J. and Xin, H., (2006). Chinese gene therapy. Splicing out the West? *Science*, **314**(5803): 1232-1235.
 124. Martin, T. A., Watkins, G., and Jiang, W. G., (2005). The Coxsackie-adenovirus receptor has elevated expression in human breast cancer. *Clin Exp Med*, **5**(3): 122-128.
 125. Rauen, K. A., Sudilovsky, D., Le, J. L., Chew, K. L., Hann, B., Weinberg, V., Schmitt, L. D., and McCormick, F., (2002). Expression of the coxsackie adenovirus receptor in normal prostate and in primary and metastatic prostate carcinoma: potential relevance to gene therapy. *Cancer Res*, **62**(13): 3812-3818.
 126. Anders, M., Vieth, M., Rocken, C., Ebert, M., Pross, M., Gretschel, S., Schlag, P. M., Wiedenmann, B., Kemmner, W., and Hocker, M., (2009).

- Loss of the coxsackie and adenovirus receptor contributes to gastric cancer progression. *Br J Cancer*, **100**(2): 352-359.
127. Anders, M., Hansen, R., Ding, R. X., Rauen, K. A., Bissell, M. J., and Korn, W. M., (2003). Disruption of 3D tissue integrity facilitates adenovirus infection by deregulating the coxsackievirus and adenovirus receptor. *Proc Natl Acad Sci U S A*, **100**(4): 1943-1948.
 128. Vincent, T., Pettersson, R. F., Crystal, R. G., and Leopold, P. L., (2004). Cytokine-mediated downregulation of coxsackievirus-adenovirus receptor in endothelial cells. *J Virol*, **78**(15): 8047-8058.
 129. Anders, M., Christian, C., McMahon, M., McCormick, F., and Korn, W. M., (2003). Inhibition of the Raf/MEK/ERK pathway up-regulates expression of the coxsackievirus and adenovirus receptor in cancer cells. *Cancer Res*, **63**(9): 2088-2095.
 130. Garden, A. S., Harris, J., Vokes, E. E., Forastiere, A. A., Ridge, J. A., Jones, C., Horwitz, E. M., Glisson, B. S., Nabell, L., Cooper, J. S., Demas, W., and Gore, E., (2004). Preliminary results of Radiation Therapy Oncology Group 97-03: a randomized phase ii trial of concurrent radiation and chemotherapy for advanced squamous cell carcinomas of the head and neck. *J Clin Oncol*, **22**(14): 2856-2864.
 131. Ozols, R. F., Bundy, B. N., Greer, B. E., Fowler, J. M., Clarke-Pearson, D., Burger, R. A., Mannel, R. S., DeGeest, K., Hartenbach, E. M., and Baergen, R., (2003). Phase III trial of carboplatin and paclitaxel compared with cisplatin and paclitaxel in patients with optimally resected stage III ovarian cancer: a Gynecologic Oncology Group study. *J Clin Oncol*, **21**(17): 3194-3200.
 132. Wagstaff, A. J., Ward, A., Benfield, P., and Heel, R. C., (1989). Carboplatin. A preliminary review of its pharmacodynamic and pharmacokinetic properties and therapeutic efficacy in the treatment of cancer. *Drugs*, **37**(2): 162-190.
 133. Lapointe, H., Lampe, H., and Banerjee, D., (1992). Head and neck squamous cell carcinoma cell line-induced suppression of in vitro lymphocyte proliferative responses. *Otolaryngol Head Neck Surg*, **106**(2): 149-158.
 134. Ferguson, P. J., Currie, C., and Vincent, M. D., (1999). Enhancement of platinum-drug cytotoxicity in a human head and neck squamous cell carcinoma line and its platinum-resistant variant by liposomal amphotericin B and phospholipase A2-II. *Drug Metab Dispos*, **27**(12): 1399-1405.
 135. Graham, F. L., Smiley, J., Russell, W. C., and Nairn, R., (1977). Characteristics of a human cell line transformed by DNA from human adenovirus type 5. *J Gen Virol*, **36**(1): 59-74.
 136. Lochmuller, H., Jani, A., Huard, J., Prescott, S., Simoneau, M., Massie, B., Karpati, G., and Acsadi, G., (1994). Emergence of early region 1-

- containing replication-competent adenovirus in stocks of replication-defective adenovirus recombinants (delta E1 + delta E3) during multiple passages in 293 cells. *Hum Gene Ther*, **5**(12): 1485-1491.
137. Ferguson, P. J., Collins, O., Dean, N. M., DeMoor, J., Li, C. S., Vincent, M. D., and Koropatnick, J., (1999). Antisense down-regulation of thymidylate synthase to suppress growth and enhance cytotoxicity of 5-FUdR, 5-FU and Tomudex in HeLa cells. *Br J Pharmacol*, **127**(8): 1777-1786.
138. O'Brien, J., Wilson, I., Orton, T., and Pognan, F., (2000). Investigation of the Alamar Blue (resazurin) fluorescent dye for the assessment of mammalian cell cytotoxicity. *Eur J Biochem*, **267**(17): 5421-5426.
139. Babich, H. and Borenfreund, E., (1988). Structure-activity relationships for diorganotins, chlorinated benzenes, and chlorinated anilines established with bluegill sunfish BF-2 cells. *Fundam Appl Toxicol*, **10**(2): 295-301.
140. Peirson, S. N. and Butler, J. N., (2007). RNA extraction from mammalian tissues. *Methods Mol Biol*, **362**(315-327).
141. Berg, R. W., Ferguson, P. J., Vincent, M. D., and Koropatnick, D. J., (2003). A "combination oligonucleotide" antisense strategy to downregulate thymidylate synthase and decrease tumor cell growth and drug resistance. *Cancer Gene Ther*, **10**(4): 278-286.
142. Bradford, M. M., (1976). A rapid and sensitive method for the quantitation of microgram quantities of protein utilizing the principle of protein-dye binding. *Anal Biochem*, **72**(248-254).
143. Dicinson, J. and Fowler, S. J., Quantification of proteins on western blots using ECL. *The Protein Protocols Handbook*, ed. J.M. Walker. 2002: Humana Press. 429-437.
144. Morley, K. L., Investigating the cellular and molecular effects of citrus flavonoids tangeretin and nobiletin in human cancer cells, in *Microbiology and Immunology*. 2007, University of Western Ontario: London, ON. p. 54-55.
145. Lee, C. Y., Rennie, P. S., and Jia, W. W., (2009). MicroRNA regulation of oncolytic herpes simplex virus-1 for selective killing of prostate cancer cells. *Clin Cancer Res*, **15**(16): 5126-5135.
146. Lichty, B. D., Stojdl, D. F., Taylor, R. A., Miller, L., Frenkel, I., Atkins, H., and Bell, J. C., (2004). Vesicular stomatitis virus: a potential therapeutic virus for the treatment of hematologic malignancy. *Hum Gene Ther*, **15**(9): 821-831.
147. Forsyth, P., Roldan, G., George, D., Wallace, C., Palmer, C. A., Morris, D., Cairncross, G., Matthews, M. V., Markert, J., Gillespie, Y., Coffey, M., Thompson, B., and Hamilton, M., (2008). A phase I trial of intratumoral administration of reovirus in patients with histologically confirmed recurrent malignant gliomas. *Mol Ther*, **16**(3): 627-632.

148. Reichard, K. W., Lorence, R. M., Cascino, C. J., Peeples, M. E., Walter, R. J., Fernando, M. B., Reyes, H. M., and Greager, J. A., (1992). Newcastle disease virus selectively kills human tumor cells. *J Surg Res*, **52**(5): 448-453.
149. Harada, J. N. and Berk, A. J., (1999). p53-Independent and -dependent requirements for E1B-55K in adenovirus type 5 replication. *J Virol*, **73**(7): 5333-5344.
150. Wujek, P., Kida, E., Walus, M., Wisniewski, K. E., and Golabek, A. A., (2004). N-glycosylation is crucial for folding, trafficking, and stability of human tripeptidyl-peptidase I. *J Biol Chem*, **279**(13): 12827-12839.
151. Liu, X., Wang, Y., Niu, H., Zhang, X., and Tan, W. S., (2009). The improvement of adenovirus vector production by increased expression of coxsackie adenovirus receptor. *Biotechnol Lett*, **31**(7): 939-944.
152. Abdolazimi, Y., Mojarrad, M., Pedram, M., and Modarressi, M. H., (2007). Analysis of the expression of coxsackievirus and adenovirus receptor in five colon cancer cell lines. *World J Gastroenterol*, **13**(47): 6365-6369.
153. Korn, W. M., Macal, M., Christian, C., Lacher, M. D., McMillan, A., Rauen, K. A., Warren, R. S., and Ferrell, L., (2006). Expression of the coxsackievirus- and adenovirus receptor in gastrointestinal cancer correlates with tumor differentiation. *Cancer Gene Ther*, **13**(8): 792-797.
154. Jee, Y. S., Lee, S. G., Lee, J. C., Kim, M. J., Lee, J. J., Kim, D. Y., Park, S. W., Sung, M. W., and Heo, D. S., (2002). Reduced expression of coxsackievirus and adenovirus receptor (CAR) in tumor tissue compared to normal epithelium in head and neck squamous cell carcinoma patients. *Anticancer Res*, **22**(5): 2629-2634.
155. Sachs, M. D., Rauen, K. A., Ramamurthy, M., Dodson, J. L., De Marzo, A. M., Putzi, M. J., Schoenberg, M. P., and Rodriguez, R., (2002). Integrin alpha(v) and coxsackie adenovirus receptor expression in clinical bladder cancer. *Urology*, **60**(3): 531-536.
156. Bruning, A. and Runnebaum, I. B., (2004). The coxsackie adenovirus receptor inhibits cancer cell migration. *Exp Cell Res*, **298**(2): 624-631.
157. Li, D., Duan, L., Freimuth, P., and O'Malley, B. W., Jr., (1999). Variability of adenovirus receptor density influences gene transfer efficiency and therapeutic response in head and neck cancer. *Clin Cancer Res*, **5**(12): 4175-4181.
158. Li, Y., Pong, R. C., Bergelson, J. M., Hall, M. C., Sagalowsky, A. I., Tseng, C. P., Wang, Z., and Hsieh, J. T., (1999). Loss of adenoviral receptor expression in human bladder cancer cells: a potential impact on the efficacy of gene therapy. *Cancer Res*, **59**(2): 325-330.
159. Rodrigues, N. R., Rowan, A., Smith, M. E., Kerr, I. B., Bodmer, W. F., Gannon, J. V., and Lane, D. P., (1990). p53 mutations in colorectal cancer. *Proc Natl Acad Sci U S A*, **87**(19): 7555-7559.

160. Henriksson, E., Baldetorp, B., Borg, A., Kjellen, E., Akervall, J., Wennerberg, J., and Wahlberg, P., (2006). p53 mutation and cyclin D1 amplification correlate with cisplatin sensitivity in xenografted human squamous cell carcinomas from head and neck. *Acta Oncol*, **45**(3): 300-305.
161. Jones, N. A., Turner, J., McIlwrath, A. J., Brown, R., and Dive, C., (1998). Cisplatin- and paclitaxel-induced apoptosis of ovarian carcinoma cells and the relationship between bax and bak up-regulation and the functional status of p53. *Mol Pharmacol*, **53**(5): 819-826.
162. Brown, R., Clugston, C., Burns, P., Edlin, A., Vasey, P., Vojtesek, B., and Kaye, S. B., (1993). Increased accumulation of p53 protein in cisplatin-resistant ovarian cell lines. *Int J Cancer*, **55**(4): 678-684.
163. Ambriovic-Ristov, A., Gabrilovac, J., Cimbora-Zovko, T., and Osmak, M., (2004). Increased adenoviral transduction efficacy in human laryngeal carcinoma cells resistant to cisplatin is associated with increased expression of integrin alphavbeta3 and coxsackie adenovirus receptor. *Int J Cancer*, **110**(5): 660-667.
164. Kasono, K., Blackwell, J. L., Douglas, J. T., Dmitriev, I., Strong, T. V., Reynolds, P., Kropf, D. A., Carroll, W. R., Peters, G. E., Bucy, R. P., Curiel, D. T., and Krasnykh, V., (1999). Selective gene delivery to head and neck cancer cells via an integrin targeted adenoviral vector. *Clin Cancer Res*, **5**(9): 2571-2579.
165. Okegawa, T., Pong, R. C., Li, Y., Bergelson, J. M., Sagalowsky, A. I., and Hsieh, J. T., (2001). The mechanism of the growth-inhibitory effect of coxsackie and adenovirus receptor (CAR) on human bladder cancer: a functional analysis of car protein structure. *Cancer Res*, **61**(17): 6592-6600.
166. Hemminki, A., Kanerva, A., Liu, B., Wang, M., Alvarez, R. D., Siegal, G. P., and Curiel, D. T., (2003). Modulation of coxsackie-adenovirus receptor expression for increased adenoviral transgene expression. *Cancer Res*, **63**(4): 847-853.
167. Seidman, M. A., Hogan, S. M., Wendland, R. L., Worgall, S., Crystal, R. G., and Leopold, P. L., (2001). Variation in adenovirus receptor expression and adenovirus vector-mediated transgene expression at defined stages of the cell cycle. *Mol Ther*, **4**(1): 13-21.
168. Fernberg, J. O., Lewensohn, R., and Skog, S., (1991). Cell cycle arrest and DNA damage after melphalan treatment of the human myeloma cell line RPMI 8226. *Eur J Haematol*, **47**(3): 161-167.
169. Wu, S. C. and Zhang, Y., Active DNA demethylation: many roads lead to Rome. *Nat Rev Mol Cell Biol*, **11**(9): 607-620.
170. Pong, R. C., Lai, Y. J., Chen, H., Okegawa, T., Frenkel, E., Sagalowsky, A., and Hsieh, J. T., (2003). Epigenetic regulation of coxsackie and

- adenovirus receptor (CAR) gene promoter in urogenital cancer cells. *Cancer Res*, **63**(24): 8680-8686.
171. Grunstein, M., (1997). Histone acetylation in chromatin structure and transcription. *Nature*, **389**(6649): 349-352.
 172. Kuster, K., Grotzinger, C., Koschel, A., Fischer, A., Wiedenmann, B., and Anders, M., Sodium butyrate increases expression of the coxsackie and adenovirus receptor in colon cancer cells. *Cancer Invest*, **28**(3): 268-274.
 173. Pong, R. C., Roark, R., Ou, J. Y., Fan, J., Stanfield, J., Frenkel, E., Sagalowsky, A., and Hsieh, J. T., (2006). Mechanism of increased coxsackie and adenovirus receptor gene expression and adenovirus uptake by phytoestrogen and histone deacetylase inhibitor in human bladder cancer cells and the potential clinical application. *Cancer Res*, **66**(17): 8822-8828.
 174. Zhang, N. H., Song, L. B., Wu, X. J., Li, R. P., Zeng, M. S., Zhu, X. F., Wan, D. S., Liu, Q., Zeng, Y. X., and Zhang, X. S., (2008). Proteasome inhibitor MG-132 modifies coxsackie and adenovirus receptor expression in colon cancer cell line lovo. *Cell Cycle*, **7**(7): 925-933.
 175. O'Shea, C. C., Johnson, L., Bagus, B., Choi, S., Nicholas, C., Shen, A., Boyle, L., Pandey, K., Soria, C., Kunich, J., Shen, Y., Habets, G., Ginzinger, D., and McCormick, F., (2004). Late viral RNA export, rather than p53 inactivation, determines ONYX-015 tumor selectivity. *Cancer Cell*, **6**(6): 611-623.
 176. Libertini, S., Iacuzzo, I., Ferraro, A., Vitale, M., Bifulco, M., Fusco, A., and Portella, G., (2007). Lovastatin enhances the replication of the oncolytic adenovirus dl1520 and its antineoplastic activity against anaplastic thyroid carcinoma cells. *Endocrinology*, **148**(11): 5186-5194.
 177. Shiina, M., Bagheri, N., Lauffenburger, D., and Korn, W. M. Experimentally validated modeling for optimizing therapeutic combinations of oncolytic adenoviruses and MEK inhibitor. in American Association for Cancer Research. 2010. Washington, DC, USA.
 178. AbouEl Hassan, M. A., Braam, S. R., and Kruyt, F. A., (2006). Paclitaxel and vincristine potentiate adenoviral oncolysis that is associated with cell cycle and apoptosis modulation, whereas they differentially affect the viral life cycle in non-small-cell lung cancer cells. *Cancer Gene Ther*, **13**(12): 1105-1114.
 179. Alonso, M. M., Gomez-Manzano, C., Bekele, B. N., Yung, W. K., and Fueyo, J., (2007). Adenovirus-based strategies overcome temozolomide resistance by silencing the O6-methylguanine-DNA methyltransferase promoter. *Cancer Res*, **67**(24): 11499-11504.
 180. Goodrum, F. D. and Ornelles, D. A., (1997). The early region 1B 55-kilodalton oncoprotein of adenovirus relieves growth restrictions imposed on viral replication by the cell cycle. *J Virol*, **71**(1): 548-561.

181. Cherubini, G., Petouchoff, T., Grossi, M., Piersanti, S., Cundari, E., and Saggio, I., (2006). E1B55K-deleted adenovirus (ONYX-015) overrides G1/S and G2/M checkpoints and causes mitotic catastrophe and endoreduplication in p53-proficient normal cells. *Cell Cycle*, **5**(19): 2244-2252.
182. Lupi, M., Cappella, P., Matera, G., Natoli, C., and Ubezio, P., (2006). Interpreting cell cycle effects of drugs: the case of melphalan. *Cancer Chemother Pharmacol*, **57**(4): 443-457.
183. Hegi, M. E., Diserens, A. C., Gorlia, T., Hamou, M. F., de Tribolet, N., Weller, M., Kros, J. M., Hainfellner, J. A., Mason, W., Mariani, L., Bromberg, J. E., Hau, P., Mirimanoff, R. O., Cairncross, J. G., Janzer, R. C., and Stupp, R., (2005). MGMT gene silencing and benefit from temozolomide in glioblastoma. *N Engl J Med*, **352**(10): 997-1003.
184. Bhakat, K. K. and Mitra, S., (2000). Regulation of the human O(6)-methylguanine-DNA methyltransferase gene by transcriptional coactivators cAMP response element-binding protein-binding protein and p300. *J Biol Chem*, **275**(44): 34197-34204.
185. Appella, E. and Anderson, C. W., (2001). Post-translational modifications and activation of p53 by genotoxic stresses. *Eur J Biochem*, **268**(10): 2764-2772.
186. Himes, S. R. and Shannon, M. F., (2000). Assays for transcriptional activity based on the luciferase reporter gene. *Methods Mol Biol*, **130**(165-174).